System Study towards the integration of Indirect Biomass Gasification, Methanol and Power Production

Balaji Sridharan

Technische Universiteit Delft

TU Delft

System Study towards the integration of Indirect Biomass Gasification, Methanol and Power Production

by

Balaji Sridharan

in partial fulfillment of the requirements for the degree of

Master of Science
in Mechanical Engineering

at the Delft University of Technology,
to be defended publicly on Friday September 29, 2017 at 01:30 PM.

Supervisor:	Prof. dr. ir. S. Klein	
	Prof. dr. ir. W. de Jong	
Thesis committee:	Prof. dr. ir. S. Klein,	TU Delft
	Prof. dr. ir. W. de Jong,	TU Delft
	Dr. ir. R.M. Stikkelman,	TU Delft
	M. del Grosso MSc.,	TU Delft

An electronic version of this thesis is available at http://repository.tudelft.nl/.

TU Delft Delft University of Technology

ACKNOWLEDGEMENTS

First and foremost, I would like to thank my family for their belief, allowing me to realize my own potential. Their continual support and wisdom has been and will always be my greatest strength.

I would like to express my gratitude to my supervisors, Prof. Sikke Klein and Prof. Wiebren de Jong, whose dedicated interest and guidance were instrumental to my progress along the course of this thesis. I would like to thank in particular Mara, my daily supervisor and friend, who has helped keeping both me my work within bounds whenever I went adrift. The shape and content of this thesis would have been much different without her support and encouragement. I would also like to thank Dr. Rob Stikkelman for taking the time to read my report and agreeing to be a part of my thesis committee.

I would like to thank my friends at Process & Energy, Lucrezia, Luca, Eliana, Leonie and Roy, who've made working at P&E much enjoyable. And, more importantly, to coffee and those blessed people who've generously lent us their coffee cards during our long days here.

And last but not least, I am indebted to my friends who've helped me make Delft a home away from India, Supriya, Sahil and Sumana.

Balaji Sridharan
Delft, September 15, 2017.

ABSTRACT

The transition from a fossil based economy to a greener, bio-based economy remains challenged by the gap in technological maturity between bio-based processes and conventional fossil energy. Decreasing the price difference between fossil fuels and bio-fuels remains a major constraint. With 98% of the transportation sector now depending on fossil fuels (oil) as the primary fuel, methanol produced from CO_2 and other greener sources is now growing in interest as a more sustainable fuel. This thesis focused on investigating the process biomass gasification, its challenges and its integration with methanol and power production. A number of gasification technologies were studied and the Indirect gasification technology was identified to be technologically advantageous to conventional gasification technologies. The Fast Internally Circulating Fluidised Bed (FICFB) gasification technology of the University of Technology, Vienna was modeled in Aspen Plus®. Different sets of kinetics were studied to improve the accuracy of the developed model in comparison with the data from the 100kW pilot plant at Gussing. The composition of the product gas from the developed model was then validated with the experimental data from the pilot plant if the FICFB gasifier, and found to be accurate up to 3.5%. The principle of Absorption Enhanced Reforming (AER) was then simulated in the developed gasifier by changing the bed material used to dolomite. With dolomite-CO_2 sorption kinetics validated with literature, the AER principle in the gasifier predicted a 4% increase in hydrogen composition in the product gas obtained in addition to a slight increase in the cold gas efficiency of the system.

Different processing steps required to convert biomass to methanol were then identified and modeled in the same Aspen Plus® model. The identified blocks, Gasifier, Gas Cleaning Unit, Methanol Synthesis and the Energy network were optimised by performing a number of sensitivity studies. The now optimised model was then used as a common tool to study the effect of choosing different technologies and parameters within the blocks on the overall process behaviour. Four different case studies were defined, each varying from each other by a difference in technology of one of the blocks. Sankey plots for each of these cases were drawn to visualize the energy losses in such complicated systems. Results of incorporating AER on the end methanol yield and the overall efficiency of the process were studied as one of the cases. Dolomite (AER) although very encouraging as a bed material during gasification, was shown to be detrimental to the methanol synthesis process when used as a common catalyst/bed material for the water gas shift reactor. Two different cases of IGCC (Integrated Gasification Combined Cycle) systems were modeled and studied by varying the gas turbine technology employed. A new technology Inverted Brayton Cycle (IBC) gas turbine was simulated against a standard IGCC system. The Inverted Brayton Cycle system was shown to closely efficient to a standard gas turbine system working on product gas from the gasifier. The scale of biomass gasification was then identified as a significant parameter, which would determine the suitable choice of gas turbine technology to be employed. The thesis concluded by discussing some of the more influential parameters observed during the course of this study and recommending further optimization and mitigation steps corresponding to each of these identified losses. The thesis served its purpose by developing a quantitative tool to compare and validate different technological solutions to improve the process of producing methanol and power from biomass.

CONTENTS

List of Figures

List of Tables

List of Abbreviations

IPCC	Intergovernmental Panel on Climate Change
CDM	Clean Development Mechanism
EPA	Environmental Protection Agency
CFB	Circulating Fluidized Bed
BFB	Bubbling Fluidized Bed
IGCC	Integrated Gasification Combined Cycle
PAH	Poly-Aromatic Hydrocarbons
SNG	Synthetic Natural Gas
FT	Fischer–Tropsch Synthesis
ER	Equivalence ratio
STBR	Steam To Biomass Ratio
GR	Gasification Ratio
FCC	Fluid Catalytic Cracking
ECN	Energy research Centre of the Netherlands
FICFB	Fast internally Circulating Fluidized Bed
SOFC	Solid Oxide Fuel Cell
AER	Absorption Enhanced Reforming
KIT	Karlsruhe Institute of Technology
WGS	Water Gas Shift
GT	Gas Turbine
IGT	Inverted Gas Turbine
CC	Combined Cycle
TIT	Turbine Inlet Temperature
IBC	Inverted Brayton Cycle
NRTL	Non-Random Two Liquid model
UNIQUAC	UNIversal QUAsi-Chemical model
EOS	Equation of State
GCU	Gas Cleaning Unit
CGE	Cold Gas Efficiency

1

INTRODUCTION

Energy crisis and rising CO_2 production rates were the most discussed in the last G8 summit in 2013. The Paris Agreement of 2016 raises the bar set for countries to utilize at least 36% of their energy usage from renewables and also to limit the long term average temperature increase to be with 2°C [1]. In its latest report, the Intergovernmental Panel on Climate Change (IPCC) estimated that to preserve a 50% chance of limiting global warming to 2 °C, the world can support a maximum carbon dioxide (CO_2) emissions "budget" of 3 000 gigatonnes (Gt) (the mid-point in a range of 2 900 Gt to 3 200 Gt) (IPCC), of which an estimated 1 970 Gt had already been emitted before 2014 [2]. To comply with raising threat of climate change and CO2 emissions, harnessing energy from discarded waste heat sources and renewables is the best way to go forward.

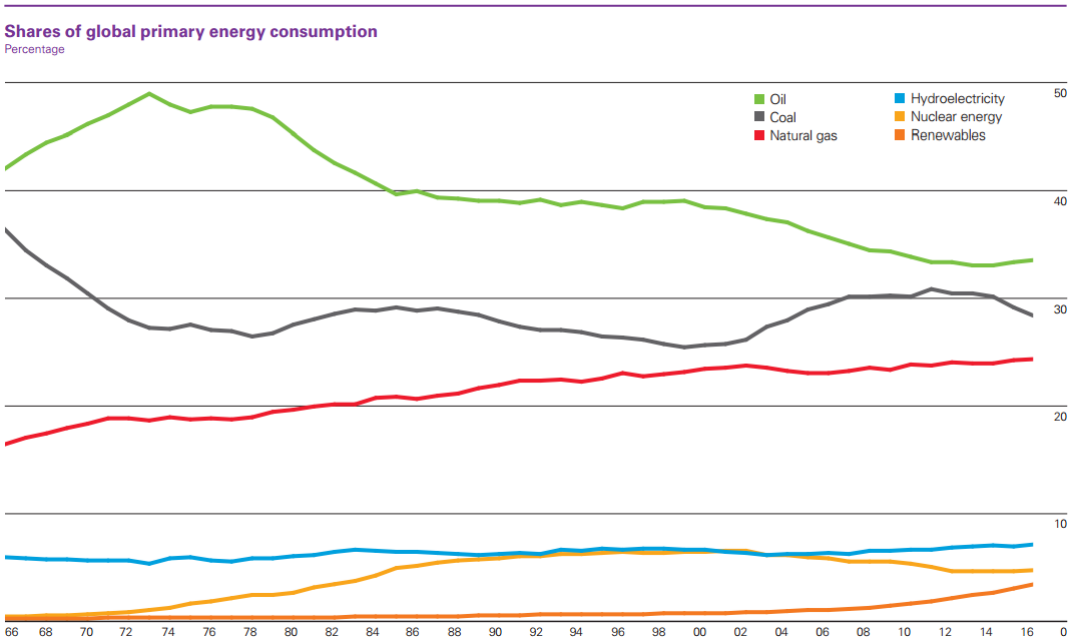

Figure 1.1: Global energy consumption, as reported by BP, in their yearly statistical review of World Energy, 2017 [3]. With time on the X axis (Year), the share of different fuel sources utilized for energy production are studied

This increase in interest in reducing CO_2 emissions can be observed in the recent trend of energy consumption shown in Figure 1.1. A continued decline in oil and coal consumption and a recent increase in energy from renewables indicate the shift in focus towards sustainability. Although the Paris Agreement has brought about an increased attention to reduce emissions ('Mission Innovation', 'International Solar Alliance' and more) and increase energy production from renewables, complete shift to sustainability in energy production still remains a daunting challenge [2].

1.1. BIOMASS BASED ECONOMY

The European Commission describes a bio-based economy as an economy that integrates the full range of natural and renewable biological resources – land and sea resources, biodiversity and biological materials (plant, animal and microbial) – and the processing and consumption of these bio-resources [4]. Hence, a bio-based economy promotes the widespread use of biomass to replace fossil-based resources. Apart from using biomass as a source of energy, comprehensive use of biotechnology to produce chemicals and pharmaceuticals, a economically important step could limit the amount of raw materials needed and could be instrumental in developing a network promoting sustainability.

However, a key challenge with the transition from a fossil based economy to a greener, bio-based economy remains the gap in technological maturity between bio-based processes and conventional fossil energy. Decreasing the price difference between fossil fuels and bio-fuels remains a major constraint. However, the benefits of bio-energy, if properly utlized, can offset the price difference with fossil fuels. The Clean Development Mechanism (CDM) of the Kyoto Protocol offers additional incentives for establishing energy plantations and opportunities for technology transfer. Despite the additional economic incentives and promotion for producing greener bio-fuels to offset the use of fossil fuels, the economics of bio-fuel production needs to be improved as a technology. The subject of this thesis is hence aimed to help bridge this maturity gap between bio-fuel and fossil fuel production.

1.2. METHANOL AS A SUSTAINABLE LINK

The 2015 report on CO_2 emissions in the US recorded by the Environmental Protection Agency (EPA) showed a significant and increasing trend in CO_2 emissions in the transportation sector, as shown in Figure 1.2 [5]. Worldwide, the transportation sector currently depends on oil for roughly 98% of its operations [6]. These fossil based fuels contribute significantly to the level of emissions, NO_x and other greenhouse gases in the atmosphere. Methanol produced from waste sources, has been widely accepted to be more sustainable and energy efficient to be used as an alternative to the currently used fossil fuels. The application of methanol as a fuel in either a fuel cell or as a one-to-one alternative to conventional liquid fuels in Internal Combustion (IC) engines could promote the shift from fossil fuels to a more sustainable methanol. Despite its documented toxicity, methanol handling measures are well established as methanol is now used as a part substitute fuel in IC engines in certain countries around the world.

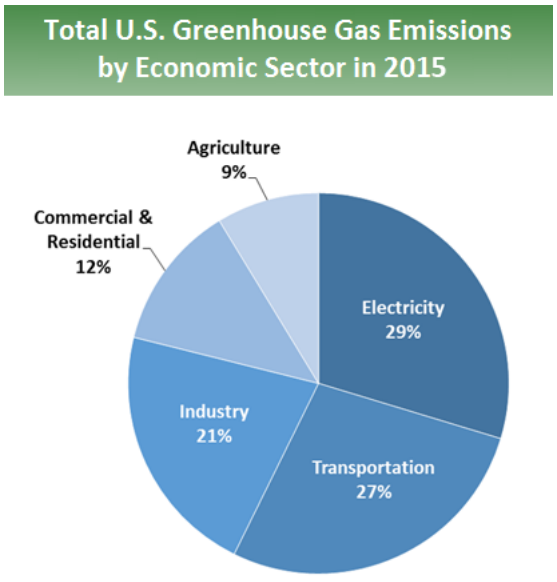

Figure 1.2: Total CO_2 emissions in the US in the year 2015 [5]

Away from the transportation sector, methanol is also one of the most important raw materials for the chemical and pharmaceutical industry where 40 million tonnes of methanol is used each year to produce

chemicals such as formaldehyde, acetic acid and ethers. Although methanol currently is produced mostly from fossil based resources, hydrogenating CO_2 to produce methanol is growing in interest as a more sustainable way. The Olah plant in Iceland produces over 3500 tonnes of methanol from waste CO_2 gases and geothermal energy. Using cheap, geothermal energy to produce hydrogen by electrolysis and using CO_2 captured from neighbouring power plants, methanol is produced in more sustainable fashion.

1.3. THESIS OUTLINE

With the discussed advantages of a bio-based economy and methanol as a move towards sustainability, the study is aimed at investigating methanol production from biomass to further understand the challenges in this process. This study includes chapters organised in a sequential manner

Chapter 2 is a summary of literature studied pertaining this thesis. This chapter reviews in brief different types of gasification technologies currently developed, new trends and technologies in gas cleaning and the downstream applications of methanol synthesis and also about implications of firing syngas in a conventional gas turbine.

Chapter 3 outlines the methodology and steps carried out building a kinetic model in Aspen Plus. The background design of the models as well as the assumptions and laws taken into account in its use are also discussed. This chapter also introduces different case studies done pertaining to different choices of technologies in the process.

The results of the proposed case studies are then discussed in chapter 4 of this thesis. Since the model developed has a number of intricate processing steps to convert biomass to methanol, a number of key parameters that influence the process are identified and are discussed later in this chapter.

Finally, chapter 7 provides a conclusion of the project. Subsequently, few recommendations for further research are given.

2

LITERATURE STUDY

2.1. BIOMASS AS AN ENERGY SOURCE

Biomass can be generalised is all materials of organic origin. To be more specific, biomass can also be defined as a complex mixture of organic materials (carbohydrates,lignin, fats and proteins) with small amounts of minerals (sodium, phosphorus, calcium and iron) ([7]). Currently, biomass is the fourth largest energy resource after coal, oil and natural gas [8]. Lignocellulosic biomass sourced from plants is a renewable and sustainable natural resource that can be engineered into feedstock for producing heat, power and chemicals. Although the potential of biomass derived energy is large due to its abundance, there is a growing criticism of bio-energy competing with food production. However production of bio-energy from non-food lignocellulosic biomass has been extensively studied as more sustainable form of energy in different parts of the world [9].

To realize the full potential of biomass as an alternate energy source, biomass needs to undergo several process routes, shown in Figure 2.1. The process steps involved and the process order is usually determined mainly by the end product required and also by the nature of biomass used. Since biomass is a very broad term by definition, there is a significant variety in the physical and chemical properties between different biomass sources. Biomass usually contain a significant percentage of moisture (from 20% to 60%), organic matter and also some trace elements such as chlorine, alkali and more. The physical and chemical properties of the biomass and its elemental composition can pose a limitation on different downstream processes and hence warrant more attention.

With energy conversion based on biomass as the main theme behind this thesis, this chapter discusses in detail the different processes used to produce power and methanol from biomass. In order to realize the potential of a renewable energy source, biomass has to undergo different process steps. *Each of these process steps have a unique purpose and produces a variety of products which could be useful for different purposes.* This conversion process can be classified in numerous ways. The most apt classification pertaining to this study is with the end product required. Several examples of biomass utilization process routes are shown in Figure 2.1. Hence to completely understand and design a system to produce energy and fuel from biomass, intricacies within these numerous intermediate steps need to be understood.

It can be observed from Figure 2.1, that Thermochemical (Example 3) and Biochemical (Example 1 and 4) conversion are the two main process routes. The main difference between the two routes is the chemical process driver [11]; Micro organisms and enzymes utilization drive the biochemical process route whereas thermal energy drives the chemical process in the thermochemical process route. The main process in the biochemical route is the fermentation of glucose present in the biomass by enzymes secreted by micro-organisms, to produce the required final products (Bio-fuels). Since Biochemical processes depend primarily on the micro-organisms used, the temperature of such processes are usually low and close to ambient. In contrast, the thermochemical process with thermal energy as the key driver, is usually operated at much higher temperatures. For example, Gasification, the process of decomposing biomass into calorific volatile gasses is operated at temperature range between 700°C and 1200°C. Biochemical processes have been deemed eco-

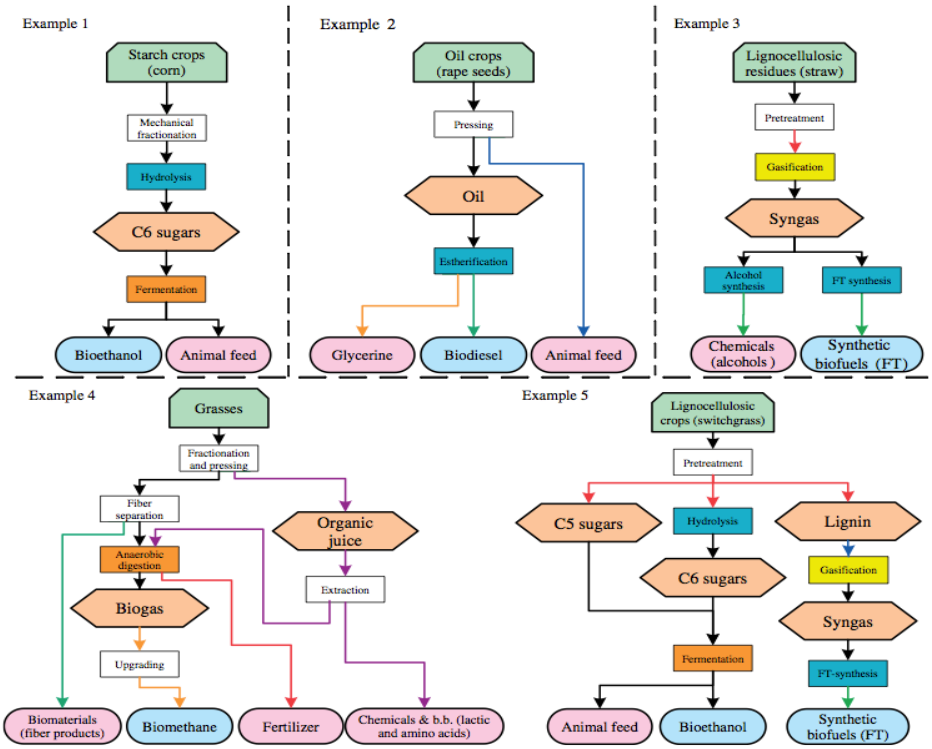

Figure 2.1: Different Process Routes for Biomass Utilization [10]

nomically competitive when first generation biomass such as feedstock used for food production is used as fuel [11]. Despite the relatively noncompetitive economics of thermochemical process, the ability of thermochemical process to produce power or chemicals with biomass that don't compete with food is considered a major advantage [11]. Only Thermochemical conversion is within the scope of this study and this chapter discusses in detail different steps involved in this conversion.

To choose a particular biomass to model this system is a very important task as the composition of the chosen biomass has a significant influence on the composition of the syngas produced. The efficiency of the net system is very much dependent on the biomass chosen to model. Torrefied wood is chosen as the biomass source for this study. Torrefaction of wood is very advantageous as it reduces the moisture content and enriches the carbon composition of the fuel, resulting in a much more concentrated fuel source [12].

2.2. GASIFICATION

Gasification is the thermo-chemical decomposition of a solid or a liquid substance into calorific gasses by under-stoichiometric addition of gasification agents such as oxygen, air, steam or carbon dioxide [13]. Gasification is a thermo-chemical conversion process that involves several steps, each consisting of different complex reaction pathways occurring in parallel since the products and reactants of each of these steps are usually the same. Gasification forms a key part of the process of producing power or fuels from biomass or coals.

The process of gasification can be described to consist of three distinct steps: Drying, Pyrolysis and Gasification. The Figure 2.2 explains graphically the process of gasification. The first step would be the heating of the fuel which causes the moisture in the biomass to evaporate. Biomass usually contains a significant percentage of moisture and for each kilogram of moisture in the biomass, 2.2 MJ (Enthalpy of vaporization of water) of energy needs to be expanded from the gasifier to vaporize this moisture content. This energy demand increases with increasing moisture fraction in the biomass, making a drying step upstream of the Gasifier a very necessary in case of biomass with moisture contents of 20% or more.

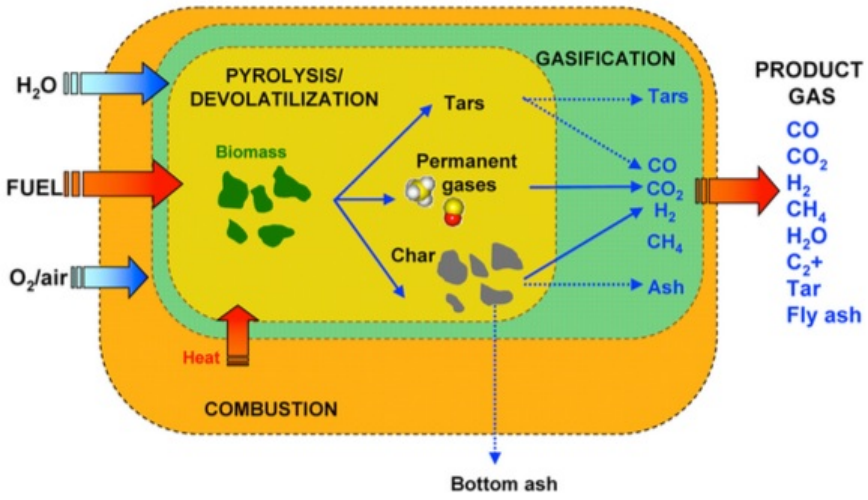

Figure 2.2: Process of Gasification [14]

Table 2.1: List of Gasification Reactions [15] [16]

Reaction Name	Reaction Type	Reaction Expression
Pyrolysis	Devolatilization	$\text{Biomass} \longrightarrow \text{Volatiles(VM)} + \text{Char} + a_1C_6H_6 + a_2C_6H_6O + a_3C_7H_8 + a_4c_{10}H_8 + a_5H_2O$ $\text{VM} \longrightarrow b_1CO + b_2CO_2 + b_3H_2 + b_4CH_4 + b_5N_2 + b_6C_2H_4 + b_7C_2H_6$
Char Gasification	Heterogeneous	$C + 1.2H_2O \longrightarrow 0.8CO + 0.2CO_2 + 1.2H_2$
Boudouard Reaction	Heterogeneous	$C + CO_2 \longrightarrow 2CO$
Water Gas Shift	Homogeneous	$CO + H_2O \longleftrightarrow CO_2 + H_2$
Naphthalene - Tar Reforming	Homogeneous	$C_{10}H_8 \longrightarrow 9C + \frac{1}{6}C_6H_6 + \frac{7}{2}H_2$
Toluene - Tar Reforming	Homogeneous	$C_7H_8 + H_2 \longrightarrow C_6H_6 + CH_4$
Phenol - Tar Reforming	Homogeneous	$C_6H_6O \longrightarrow CO + 0.4C_{10}H_8 + 0.15C_6H_6 + 0.1CH_4 + 0.75H_2$
Benzene - Tar Reforming	Homogeneous	$C_6H_6 + H_2O \longrightarrow 3C + 2CH_4 + CO$
Char Oxidation	Heterogeneous	$\alpha C + O_2 \longrightarrow 2(\alpha-1)CO + (2-\alpha)CO_2$
Hydrogen Combustion	Homogeneous	$H_2 + 0.5O_2 \longrightarrow H_2O$

As the fuel is heated up, the water molecules bound loosely in the fuel evaporates at 100°C (at atmospheric pressure) and when the temperature reaches around 300 – 600 °C during pyrolysis, the organic matter in the fuel is decomposed into gases, char and liquids. Further, during the gasification step, the temperature is raised to between 700°C and 1200°C in the presence a gasification agent. Gasification agent (Steam, Air, Oxygen or Carbon Dioxide) is the reactant added into a gasifier along with the biomass to partially oxidise or convert the biomass into the required product gas. This process of gasification is endothermic and hence heat or energy needs to be supplied to continue this process. The product gas thus produced during gasification consists mainly of combustible gas hydrogen, Methane and Carbon Monoxide and incombustible gas Carbon Dioxide, Water vapor and Nitrogen. The product gas also usually contains traces of different organic volatiles and inorganic compounds which will be discussed later. The composition of this product gas is heavily dependent on the residence time in the reactor and the temperature of gasification and hence the kinetics and the mass transfer properties of the complete process needs to be completely understood to predict the effectiveness of the gasification process.

2.2.1. GASIFICATION TECHNOLOGY

Gasification reactors can be classified in several different ways primarily based on the gasification agent used and on the nature of transport process within the gasifier.

By virtue of the gasification medium used, we can classify gasifiers as the following,

1. Air blown gasifiers
2. Steam blown gasifiers
3. Oxygen blown gasifiers
4. CO_2 blown gasifiers

The gasification medium reacts directly with the biomass and the volatiles emitted by the biomass and hence has a direct impact on the composition, and the properties of the product gas produced during gasification. The simplest medium used for gasification is air, but because of the significant fraction of nitrogen in air, the product gas obtained is much diluted with nitrogen. Hence, by using pure oxygen instead of air, product gas produced have significantly higher heating values when compared to air blown gasifiers [16]. When either oxygen or air is used as the gasification medium, the product gas has a higher volume fraction of carbon-based components (CO and CO_2) than hydrogen. However, in this case, the excess air ratio of the supplied oxygen must be closely monitored; when an excess air ratio of greater than one is maintained, the product gas produced during gasification would be completely oxidised (or combusted) to result in a outlet flue gas (CO_2) stream rather than the desired product gas stream. Alternatively, using steam as the gasification medium results in a product gas that can be relatively richer in hydrogen than CO or CO_2. Hence a mixture of air/steam or oxygen/steam could be used to tailor the CO/H_2 ratio of the product gas.

By virtue of the nature of transport process within the gasifier, the gasification technology can be classified as,

1. Fixed bed gasifiers
2. Fluidized bed gasifiers
3. Entrained flow gasifiers

FIXED BED GASIFIERS

Fixed bed gasifier is a medium temperature gasifier, where the gasification medium (Oxygen, air or steam) flows through a fixed or slowly moving bed of the biomass. Fixed bed gasifiers can be of two types based on the direction of flow of the gasification medium and the fuel(biomass): updraft and downdraft fixed bed gasifiers. The fuel is usually fed from the top in both the cases, but air (gasification medium) is fed from the bottom in case of an updraft gasifier and from the top in the case of downdraft gasifier. This difference in direction of flow of the gasification medium causes significant differences in the nature and the order of zones that are formed within the gasifier. The consequences are that the updraft gasifier is much more efficient than

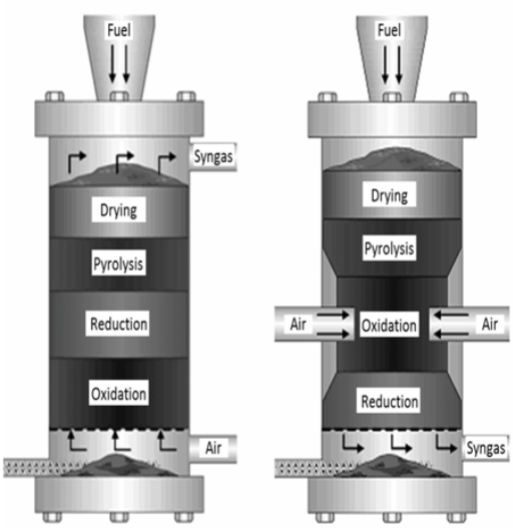

Figure 2.3: Fixed Bed Gasifiers: Updraft (left) and Downdraft (right) configurations [17]

the downdraft gasifier, mainly because, the outlet temperature of fuel gas in the updraft gasifier is much lower than in the downdraft gasifier. This temperature difference in the fuel gas is the amount of energy consumed within the gasifier to dry the top layer of the biomass fuel which leads to higher conversion efficiency in the updraft gasifier. However, this also leads to substantially higher tar and particle concentration in the fuel gas [13].

Generally, the fixed bed reactor is very simple in design and operation. The updraft and downdraft fixed bed gasifiers are usually operated in a 'dry' mode, avoiding the formation of molten ash by maintaining the operation temperatures below the melting temperature of ash. Fixed type of gasifiers usually use air as the gasification medium and this results in a very diluted fuel gas that is produced. Replacing air with oxygen to avoid nitrogen dilution complicates operation by localized increase in temperature causing molten ash formation within the reactors.

FLUIDIZED BED GASIFIERS

In a fluidized bed gasifier, the biomass fuel is added to a bed material and is fluidized by the gasification medium. Fluidized bed gasifiers and combustors are used widely in solid fuel systems such as in coal fired power plants. The fluidization helps achieving better heat and mass transfer coefficients than conventional fixed bed gasifiers. The bed material chosen varies from ordinary sand to a catalytically active material such as dolomite or olivine to reduce tars. The main purpose of this bed material is to distribute heat in the gasifier equally, thereby eliminating any local heat spot formation. When a catalytically active material is used as the bed material, tars can be reduced considerably [18, 19].

Fluidized bed gasifiers can be classified as either Circulating Fluidized Bed or Bubbling Fluidized Bed based on the fluidization velocity. Figure 2.4 below shows different fluidization regimes resulting from increasing the fluidization velocity of the gas blown through the bed. Bubbling Fluidized Beds operate primarily in bubbling regime whereas the Circulating Fluidized bed operates somewhere between the turbulent and fast fluidization regimes shown in Figure 2.4. In a BFB, the gasification medium is fed from the bottom, forming bubbles. These bubbles flow at a gas velocity which is much higher than its minimum fluidization velocity but much lower than its terminal velocity to ensure that the material is not blown out of the gasifier during the process. The fuel distribution within the gasifier tends to deteriorate with increasing diameter of the reactor and limits the scale of a BFB to less than 10 MW_{th} [21].

With increasing velocities, the bed material and the fuel that gets entrained with the flow needs to be recycled. This is done usually in one or more cyclones which separate the produced fuel gas from the entrained

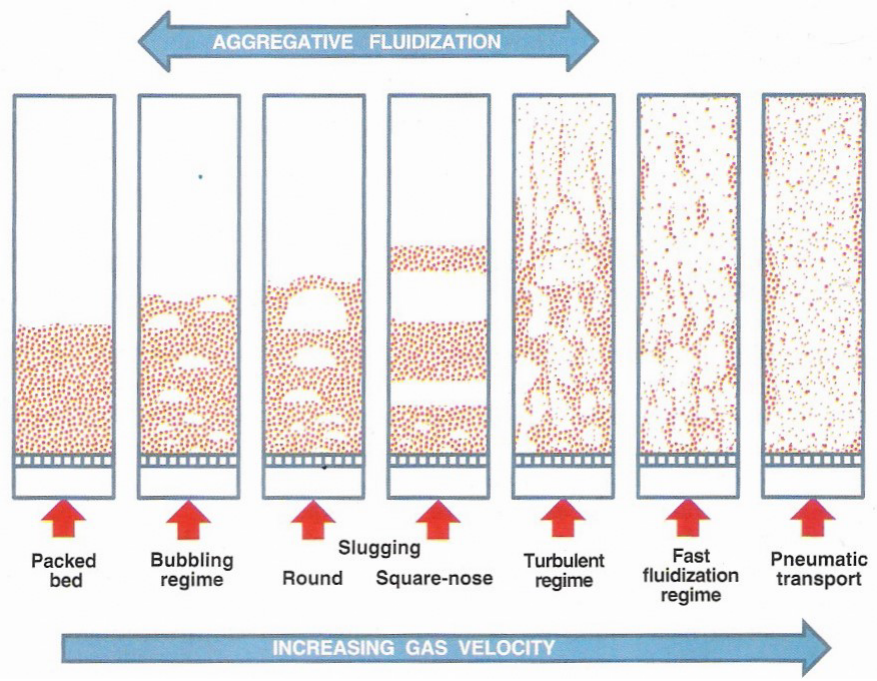

Figure 2.4: Different flow regimes during Fluidization of the bed material [20]

particles, which are then recycled to the reactor. This recycling results in an increased carbon conversion percentage of CFB than the BFB. However, due to the absence of different process zones within the gasifier, the fuel gas produced from the fluidized bed gasifiers usually contain relatively high amounts of tars (1–30 g/Nm^3) and particles (1–100 g/Nm^3). However, higher biomass flow rates required due to rapid conversion results in higher capacities of operation.

Separating the gasification of biomass and the combustion of the produced char in different reactors leads to indirect or an allothermal gasification technology. The process of gasification is very endothermic and hence energy needs to be supplied to sustain gasification. In an indirect or Allothermal gasifier, the biomass fed to the gasifier is gasified to produce syngas and char. A fraction of this char is then combusted in a separate combustion reactor along with the bed material to produce heat. Hot solid particles (bed material) from the combustor is then recycled back to the gasifier to sustain gasification. Hence by separating combustion from gasification, it is then possible to avoid mixing of flue gas from the combustor and product gas stream from the gasifier, yielding in a product gas much less polluted and of higher heating value than conventional gasifiers.

ENTRAINED FLOW GASIFIER

Entrained flow gasifiers are high temperature gasifiers which are used to produce syngas usually from pulverized fuel. The product gas from entrained flow gasifiers are practically free of methane and other heavier hydrocarbons. Entrained flow gasifiers are operated at temperatures close to 1400 °C and at this high temperature tars formed are completely cracked and the produced syngas is usually devoid of any tars. To ensure complete conversion of the input fuel, the fuel is typically subjected to pre-treatment process such as drying and maybe torrefaction. The pre-treated biomass is then pulverized to a very fine grain size. Since the fuel is pulverized to a very fine grain size, the residence time for completely gasification of the fuel is practically instantaneous and hence is why entrained flow gasifiers have been used on much larger scales (100MW ~ 1GW) in co-fired coal power plants. However, since there is a very stringent requirement in the fuel size and type, entrained flow gasifiers are not yet very suitable for biomass gasification. With a syngas practically devoid of tar, this type of gasifiers are the most preferred in methanol production (Fischer Tropsch Synthesis) from coal gasification.

Table 2.2: Typical Syngas Composition from different Gasifiers [22]

		Fixed Bed Concurrent Gasifier	**Fixed Bed Counter-current Gasifier**	**CFB Gasifier**
Fuel moisture	%mf	6 - 25	n.d.	13 - 20
Particles	mg/Nm^3	100 - 8000	100 - 3000	8000 - 100000
Tars	mg/Nm^3	10 - 6000	10000 - 150000	2000 - 30000
LHV	MJ/Nm^3	4.0 - 5.6	3.7 - 5.1	3.6 - 5.9
H_2	vol.%	15 - 21	10 - 14	15 - 22
CO	vol.%	10 - 22	15 - 20	13 - 15
CO_2	vol.%	11 - 13	8 - 10	13 - 25
CH_4	vol.%	1 - 5	2 - 3	2 - 4
C_nH_m	vol.%	0.5 - 2	n.d.	0.1 - 1.2
N_2	vol.%	Rest	Rest	Rest

DIFFERENT IMPURITIES IN BIOMASS GASIFICATION AND REDUCTION TECHNIQUES

With increasing emphasis on utilizing biomass based sources for both power (IGCC) and bio-fuel production, numerous studies on the suitability of different types of biomass for Fuel or power production have been actively conducted. Properties of various biomass streams predominantly determine the quality and quantity of the product gas obtainable from the gasification process. For example, herbaceous and domestic biomass sources are relatively richer in alkali metal, chlorine, sulphur species compared to woody biomass and hence make the study on the composition of various biomass streams very necessary.

Similar to how biomass can be composed of moisture, organic matter and inorganic trace elements, these impurities can also be divided into either organic or inorganic. The impurities of inorganic origin can be classified as three main categories: Alkali, Sulfur and Chlorine based compounds. The organic impurities are primarily the tars and heavier hydrocarbons produced during the gasification process. These impurities are discussed further in this section.

Power generation through IGCCs (Integrated Gasification Combined Cycle) and fuel production via the Fischer Tropsch process impart a considerable constraint on the composition and quality of the product gas produced from the gasifier. A very narrow range of impurity levels, tars and the CO/H_2 fraction desired makes gas cleaning and conditioning a very important step after gasification. Typical syngas quality achieved by different gasification technologies and typical quality requirements for various downstream applications are shown in Table 2.2 and Table 2.4 below.

Currently a separate gas-cleaning unit downstream of the gasifier is used to condition and remove impurities from the product gas produced. Usage of suitable sorbents to reduce the impurities within a gasifier could hold a number of advantages. Bed agglomeration due to alkali species and chlorides, corrosion of gasifier walls and linings due to sour gases (HCl for example) that are produced during gasifier operation can be reduced by adding different sorbents and additives to the bed material. Using partial oxidation or catalytic reforming of tars in the free-board of the gasifier not only reduces the load on the downstream gas cleaning unit but also increases the yield of the complete process. This section summarizes in brief the current research on reducing impurities and tars in the product gas stream.

INORGANIC IMPURITIES

ALKALI SPECIES

With biomass relatively very rich in chlorine and alkali metals such as potassium and sodium, KCl formation during the gasification process is very likely. These alkali species contribute to bed agglomeration and induce corrosion in the inner lining of the gasifier and hence must be reduced. The biomass type used has a very significant effect on the alkali species concentration in the product gas. When elemental concentrations of alkali species was measured for different types of biomass ([23]), the concentration of KCl was usually much higher than NaCl [13]. When KCl concentrations are reduced to values typically as low as ppm (parts per million), the condensing temperature of the alkali species would then mainly depend on the condensation

Table 2.3: Classification of Tars [31]

Class	Type	Examples
1	GC Undetectable tars	Biomass fragments, Heaviest tars (pitch)
2	Heterocyclic compounds. These are components that generally exhibit high water solubility	Phenol, Cresol, Quinoline, Pyridine
3	Aromatic Components. Light Hydrocarbons, which are important from the point of view of tar reaction pathways, but not in particular towards condensation and solubility	Toluene, Xylenes, Ethylbenzene (Excluding Benzene)
4	Light Polyaromatic Hydrocarbons (2-3 ring PAHs). These components condense at relatively high concentrations and intermediate temperatures.	Naphthalene, Indene, Biphenyl, Antracene.
5	Heavy polyaromatic hydrocarbons (≥4-ring PAHs). these components condense at relatively high temperatures at low concentrations.	Fluoranthene, Pyrene, Crysene
6	GC detectable, not identified compounds.	Unknowns

temperature of NaCl, since NaCl concentration dominates in comparison with the remaining KCl concentration. This condensation temperature ranges from 530°C to 630°C [13]. Hence for gasifiers with temperature higher than this, the possibilities of fouling are significantly reduced. Aluminosillicates are also extensively studied for removing alkalis to ppb (parts per billion) scales in gasifiers [24–29]

SULFUR SPECIES

Sulfur species in the biomass is usually released as H_2S or COS. This released H_2S and COS are very poisonous to downstream equipment such as fuel cells and FT reactors and hence have to be reduced to a part per million (ppm) scale (Table 2.4). In addition to its poisoning properties, release of H_2S in gas turbine exhaust streams can also be detrimental to the environment. Usually, both H_2S and COS formed are scrubbed during the gas cleaning phase but can also be reduced in the gasifier by adding suitable sorbents and catalysts. Metals and Metal catalyst can absorb sulfur and deposit as metal sulphides in the bed, thereby reducing its concentration in the syngas produced. Calcium and Barium based oxides have been proved to reduce the sulfur levels very efficiently to ppmv (parts per million by volume) scales when operating the gasifier around 900 ~ 1000 °C[13].

HCL

Simillar to the case of alkali species, HCl are produced during gasification due the Chlorine traces in the biomass used. HCl even in small traces is very corrosive and can cause damage to downstream equipment [13]. Calcium or Sodium base sorbents are verified to be very effective in reducing HCl during Gasification[13].

2.2.2. THE TAR PROBLEM

The overall efficiency of the gasification process is in general higher than that of combustion and this has brought about a significant increase in biomass and gasification research. However, one of the biggest challenges with biomass gasification for fuel production is the tar formed during the gasification process. The definition of tars vary considerably between different research groups but tars are officially defined as all organic contaminants with a molecular weight larger than benzene [30]. Tars can be quite vast, ranging from a single ring to five-ring aromatic compounds along with other oxygen containing hydrocarbons and complex PAH (Polycyclic Aromatic Hydrocarbon) [19]. ECN classifies tars in 6 categories as shown in Table 2.3 based on its behavior [31].

Table 2.4: Typical syngas composition required for different end applications [36, 37]

		IC Engine	Gas Turbine	Methanol Synthesis	SNG Synthesis
Particles	mg/Nm^3	<50	<30	<0.2	0
Particles size	μm	<10	<5		
Tar	mg/Nm^3	<100		<0.1	Below Dew Point
Alkali Metals	mg/Nm^3		0.2		<10 ppbV
NH_3	mg/Nm^3			<0.1	<1 ppmV
S Components	mg/Nm^3			<0.1	<1 ppmV
Cl Components	mg/Nm^3			<0.1	10 ppbV
CO_2	Vol.%	n.l.	n.l.	<12	

Class 2 type tars which are water soluble can cause problems when the syngas temperature drops below the dew point of water as they are water soluble and result in a polluted water stream. Similarly, the dew point of the tar concentration of the syngas is determined by the elemental concentration of the above stated categories of tars.

Tars are undesirable for a number of reasons; tar condensation causes fouling clogging of downstream equipment, tar aerosols and tars polymerize to produce heavier and complex organic compounds which may cause problems in the downstream processing equipment and also in gas engines and gas turbines. However, determining an upper limit on the tar concentration in the produced syngas depends mainly on the downstream equipment that is used. For example, tars and dust in the syngas should be lower than 100 mg/Nm^3 (or even lower than 10 mg/m^3 according to [32]) for gas engines, as shown in Table 2.4. There is significant research available on tabulating the different tar requirements for various downstream applications. Milne et al.[33–35] for example, tabulated the tar concentration requirements for each application. The Table 2.4 below gives an idea on syngas purity requirement for various downstream applications. Though literature on tars and various strategies to reduce tars are well available, there is a challenge in comparing different experimental research data mainly because of the difference in the working conditions cited between these studies.

There are number of technologies that are being developed to mitigate this problem of tars. However, to choose a method that is economically feasible and efficient for removing tars without affecting the composition of the produced product gas is a much harder task. Ideally, the entire tar reduction process would be much preferred to be inside the gasifier to reduce downstream equipment. Currently tar reduction methods are classified in two types, depending on the location where they are used, primary – Inside the gasifier, and secondary – downstream, outside the gasifier.

2.2.3. PRIMARY METHODS

Primary methods are the measures that are employed within the gasifier to reduce tars that are produced during the gasification process. To produce a product gas with the tar concentration required from the gasifier would be ideal and hence is why these primary methods are more attractive and actively studied. An ideal primary method for tar removal would eliminate the need for a downstream secondary tar removal system. However, primary methods are not yet completely understood and hence limited in terms of practical implementation. The bed material used in the gasifier can be made catalytic to enhance tar cracking and reforming reactions to reduce tar that is produced during gasification. The temperature of gasification added to the catalytic activity of the bed material should reduce the concentration of the produced tars. The primary methods for reducing tar include, choosing an ideal operating condition, use of proper bed additives and catalysts during gasification and a proper gasifier design [19].

IDEAL OPERATING CONDITIONS

The gasification conditions have a direct correlation with the syngas composition, carbon conversion, tar composition and also tar reduction[19]. Key operating parameters studied are the temperature of gasification, the reactor pressure, Residence time of the biomass in the gasifier, the equivalence ratio (ER), gasification medium, catalysts and additives.

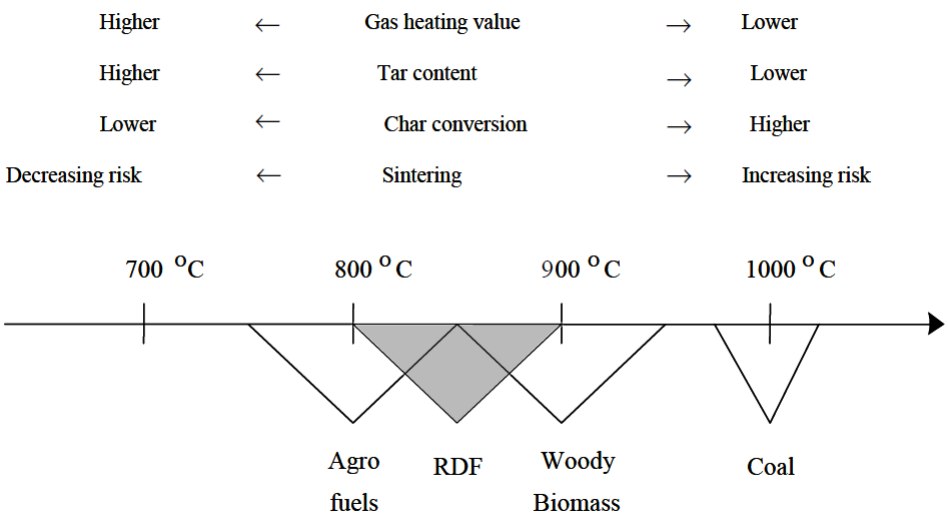

Figure 2.5: Effect of Temperature on the Gasification process [19]

The effect of temperature on the tar concentration is relatively straightforward. Conversion efficiency of tars are strongly related to the gasification temperature and the residence time of the biomass in the gasifier [38]. This process of driving tar cracking reactions by supplying heat is called as Thermal Cracking. There are several studies indicating that higher temperatures are more suitable to reduce the tar concentration of the product gas [39]. Oxygen containing compounds such as phenol, cresol, benzo-furan were found in much lower concentrations at temperatures above 850 °C [19]. An experiment performed on birch wood gasification observing the effect of temperature on tar concentration inferred a 40% reduction in tar concentration when the gasification temperature was raised from 700°C to 900°C [40]. Though the increase in temperature favours the reduction in oxygen containing tar components, it also promotes the formation of 3 and 4 ring aromatic compounds such as naphthalene, phenanthrene etc.[19]. In a similar experiment of birch wood pyrolysis, the concentration of phenol and toluene (50% reduction) reduced but the concentration of benzene and naphthalene showed a considerable increase when gasification temperature was increased from 700°C to 900°C [41]. However, there is a positive increase in H_2 and CO concentration in the product gas when the gasification temperature is increased.

It is also very possible to reduce the tar concentration by increasing the free-board temperature of the gasifier. Free-board is the area in the gasifier above the bed where the product gas rises towards the riser. Increasing the temperature in the free-board reduces the residence time required for the tars to crack and hence has a constructive effect on the tar reduction. Besides reducing tar concentration, increasing temperature can also help reducing ammonia (NH_3) concentration in the product gas[19]. However, there are several other factors that limit the gasification temperature. The catalysts used may lose activity and stability at elevated temperatures and also elevated temperatures lead to a serious risk of bed material sintering which can be detrimental to the gasification process. Figure 2.5 explains the trade-off of increasing the operating temperature. Main reason behind the recent transition towards high temperature gasification can be inferred to be mainly due to the increased char conversion and tar reduction in the produced product gas. However, in the case fluidized bed gasifiers, the bed material used should be able to withstand the high temperatures preferred. The choice in bed material now becomes an interlinked trade-off between its chemical and thermal properties.

Temperature of gasification and residence time have a very interconnected effect on the tar concentration of the final product gas. When thermally cracking tar, the conversion efficiency is increased with an increase in temperature and the residence time of the product gas inside the gasifier. By increasing the temperature of gasification, the residence time required to achieve a set tar concentration can be reduced [38]. Reduced residence time implies more compact vessels but also results in heavier heat demands due to the increased temperature. This can be easily explained by the plot of residence time of naphthalene vs temperature of

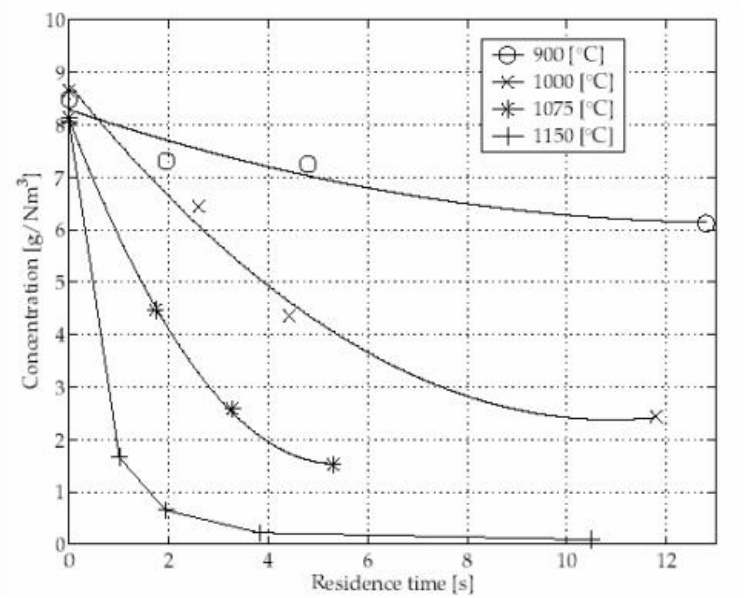

Figure 2.6: Effect of Residence time and Gasification Temperature on Naphthalene Concentration [42]

gasification in an experiment conducted by Søren et al [42] shown in Figure 2.6. As observed, the residence time for naphthalene concentration to reach zero decreases drastically with increase in temperature.

The gasification medium used in the reactor has a direct consequence on the composition and quality of the final product gas obtained from gasification. The gasification medium currently used/studied are air, oxygen, steam and CO_2. With air gasification, tar content decreases with increasing the Equivalence Ratio (ER) since higher ER provides more oxygen to react with the tars in the pyrolysis zones. However, the ER has a strong influence in the type of gasification products that are produced. The higher the ER, lower the concentrations of H_2 and CO and higher the concentration of CO_2 and H_2O. This leads to a product gas much lower in heating value. With increasing ER at a temperature of 700°C, the phenol were completely converted but the fraction of PAH, benzene, naphthalene and other 3-4 ring compounds increased in the total tar composition [19, 43]. Steam gasification promotes hydrogen (50% of product gas) production and the product gas is more or less free of nitrogen [19]. As the steam/biomass ratio is increased, an increase in H_2 and CO_2 was observed with a decrease in CO and CH_4. However, there was a reduction in tar content in the final product gas which can be attributed to be the reaction rate of char with steam causing a reduction of tar through secondary reactions. Steam with oxygen can be used to design an auto-thermal gasifier where the heat required for steam gasification is provided by the oxidation due to oxygen. Similar research on the effect of gasification ratio (GR) (ratio of Steam + oxygen and biomass) concluded that even at low GR, only light tars were produced and these light tars can be easily eliminated by using catalysts during gasification [44]. Further research by Gil et al. [45] recommend an optimal operating conditions of gasifier temperature around 800 ~ 860°C and a GR of 0.8 ~ 1.2 with a residence time of 2s. Steam/air mixture produces measurably lesser tar than air as gasification medium [45].

Gasification with CO_2 is increasing in interest due to its easy availability within the gasification process (By-product). Dry-reforming reactions of CO_2 enhances tar reduction. Minkova et al. studied the effect of CO_2 and CO_2/steam mixtures on gasification effectiveness [46]. The activity of char produced by CO_2-steam gasification is high and in-turn catalyses the secondary reaction and thereby reducing tars. CO_2 gasification increases the H_2 and CO yields and also reduces the CH_4 and the fraction of lower hydrocarbons (Ethane and less) and hence increases the heating value of the product gas. Also the fraction of CO_2 in the output product gas is less than what was supplied, implying that CO_2 can participate in the gasification process and can also disassociate to produce products [19]. The biggest disadvantage of using CO_2 as a gasification medium is the soot formation and carbon deposition on the bed material and catalysts which can be avoided by adding CO_2 in excess [19].

BED ADDITIVES AND CATALYSTS

The main purpose of the bed material in a fluidized bed is to store heat and transfer heat between different endothermic (Gasification, Pyrolysis, Desorption) and exothermic process (oxidation, sorption reactions) and thereby acting as a thermal flywheel by function. In the case of indirect gasifiers where the combustor and gasifier are physically and functionally separated, heat produced by char oxidation in the combustor heats up the bed material and this heat is then transported to the endothermic gasification reactions in the gasifier. By doing so, the bed material in the fluidized bed achieve a uniform temperature profile inside the gasifier or combustor. With combustion temperatures around 950°C, using a sufficiently large bed material recirculation could prevent damage to the inner linings of the combustor due to local temperature surges.

Ideally, the bed material is assumed to be inert during the complete gasification process. Sand (Quartz)-most commonly used bed material, comes the closest to being inert. Even sand, considered relatively inert can combine with alumina or sodium in the gasifier to produce glass like substance at high temperatures. In most bed materials commonly used (apart from sand), the interaction between different fuel constituents (Biomass) and rapidly varying temperature profiles can cause changes in its physical characteristics. This degradation of the bed material is commonly called bed agglomeration and is highly undesirable. A very special advantage of using fluidized bed is the usage of bed material with catalytic properties to enhance certain reactions involved. Using such catalytically active bed materials can improve the output composition of the gasifier by increasing Hydrogen yield and/or by reducing tar and methane amounts in the product gas. The key advantage of using catalytically active bed material is that a very efficient catalytic activity in terms of tar reduction could possible eliminate the need for downstream tar removal equipment. Hence these catalysts can act as in-situ catalysts promoting several tar removal reactions within the gasifier itself [19]. Besides tar reduction, these active bed materials also prevent solid agglomeration and the subsequent choking of the bed[19]. Usage of a catalytically active bed materials during gasification have hence been extensively studied[18, 19]. Criteria for choosing a catalyst would include not only its ability to reform tars but also on various other properties such as its ability to reform methane, its suitability to maintain a required syngas composition and also mainly on its resistance to abrasion and deactivation due to carbon deactivation and sintering.

Naturally occurring metal oxides derived from ores such as dolomites, olivines, calcites and magnesites appear to be more suitable for use as a catalytic bed material when compared to the commercial Ni based catalyts and zeolites [47]. This is mainly because of their non-toxic nature and their increased activity at higher temperatures achieved commonly during gasification. A key disadvantage of these ores is their low attrition resistance compared to sand. Since the costs of these ores are not as high as the commercial Metal-based catalysts, they make an attractive option to be used as bed materials in gasifiers[47]. Though there have been a number of catalysts that have been identified, not all identified catalysts have been actually tested inside a gasifier during active gasification.

One of the first additives to be used in a gasifier as a catalyst was limestone. Steam gasification of manure using 75%wt silica sand and 25% limestone was studied and this experiment confirmed how catalysts enhance the heating value of the final product gas [40]. Also, addition of limestone helped preventing agglomeration of the bed[48]. Among all active materials, the most studied material are the dolomites. Activity of dolomite is found to be the greatest in all of the calcinated rocks, concluded from the experiments done by Delgado et al. [49] This high catalytic activity of dolomite has sparked research on usage of dolomite in both primary and secondary tar reduction measures. In such a study, University of Zaragoza found the in situ use of dolomite within the gasifier less effective than the using dolomite as a downstream tar reduction measure[50]. A key disadvantage with dolomite use as a part catalytic bed material with sand is that dolomite is very soft and can be easily eroded by sand (Silica) in fluidized beds [47]. This usually leads to higher carryover of solids from the gasifier resulting in higher particulates in the product gas. This could partly explain why dolomite performs better as a secondary measure than a primary tar reduction measure. Olivines on the other hand are quite similar in activity as dolomite but much more abrasion resistant and has the same strength and texture as silica sand even at elevated temperatures.

Another type of catalysts that can be used in the gasifier are the Ni based catalysts. Both Ni based and Alkali Carbonate catalysts are very efficient in producing high yields in product gas. The main challenge with Ni based catalysts is its rapid deactivation due to carbon deposition and H_2S poisoning [51, 52]. However as discussed in the previous section, carbon deposition and H_2S poisoning of Ni-Based catalysts can be reduced

by increasing the gasification temperature. There do exist serious questions on the operating lifetime of these Ni-based catalysts. Shorter lifetimes lead to more frequent catalyst replenishment which could cause detrimental effects on the overall economics of the gasification process.

More advanced synthetic catalysts such as FCC (Fluid Catalytic Cracking) and transition metal based catalysts are also being studied. Zeolites are the most commonly studied FCC catalysts and are a class of crystalline aluminosilicate which catalytically crack heavier hydrocarbons to lighter hydrocarbons [19]. The silicon/Aluminium ratio and the nature of preparation of the zeolites have a very strong effect on its catalytic activity [53]. Similar to Ni-based catalysts, coke deposition and loss of active sites due to deactivation by foreign substances causes its catalytic ability to deteriorate fast during gasification. Steam, coke, basic nitrogen compounds and alkaline materials react with the catalyst's active sites to poison the catalyst[53]. The economic advantage of zeolites is easily negated by its rapid deactivation due to coke formation.

Transition metal based catalysts are considered as good catalysts for dry reforming and steam reforming of methane and other hydrocarbons[53]. Transition metal catalysts are very attractive because they can attain complete tar elimination at a temperature around 900 °C[53]. Furthermore, these catalysts can also favour water gas shift reaction, increasing the hydrogen yield in the produced product gas. Ni based catalysts are also around 8-10 times more active than dolomite. However, rapid deactivation due to sulphur and also coke deposition due to high tar contents in the gasifier coupled with them being relatively expensive, makes usage of transition metal based catalysts as a primary tar reduction measure highly uneconomical at this time[44, 54]. However, using transition metal based catalysts for secondary tar reduction downstream of the gasifier is still promising and there are some studies in this direction[53].

Char although not an additive in the gasification process, is continually formed during the pyrolysis and devolatilization of biomass inside the gasifier. Char have been known to catalytically accelerate the reforming reactions of both tars and methane during the gasification process [55]. A study comparing the catalytic activity of different additives for tar conversion showed that char is even more active than dolomite at 900°C[56]. This high activity of char is attributed to the continuous activation of char by steam and CO_2 [47]. However the main challenge in realizing this catalytic ability of char in-situ during gasification is in increasing the interaction times between tars and char within a very rapid and dynamic gasification process. New gasifier concepts such as ECN MILENA and FICFB and other indirect gasifiers employ such char recycling to produce syngas of better quality than that of conventional gasifiers. The following section deals with greater detail on such gasification technologies.

2.2.4. CURRENT GASIFICATION TECHNOLOGIES

ECN MILENA

The Energy research Centre of Netherlands (ECN) is currently working on a gasifier technology to produce bio-SNG (Synthetic Natural Gas) from biomass called MILENA gasifier technology. MILENA is an indirect gasifier with both the gasifier and the combustion reactors are constructed within the same shell. The schematic of the MILENA gasifier is shown in the figure below.

WORKING

The MILENA gasifier is an indirectly heated gasifier in which the gasification of fuel is carried out in two reactors. Both the reactors are within a common shell as shown in Figure 2.7. The Gasifier is in the middle (riser) and is a circulating fluidized bed type whereas the combustor surrounds the gasifier and it is operated in a bubbling fluidized bed mode with pre-heated air to burn the char to produce heat required to sustain gasification.

Biomass is fed into the gasifier from the bottom and steam is injected into the biomass. Hence the bottom of the gasifier forms the dense zone where most of the gasification takes place. Hot bed material and combusted char (around 925°C) are recycled from the combustion reactor through small ports opposite to the biomass feeding port. This hot char and bed material provide the necessary heat for gasification. The steam injected from the bottom creates the linear upward velocity for fluidization [21]. Steam is used as a gasification medium to mitigate nitrogen dilution of the produced fuel gas. The biomass undergoes devolatilization and this released gas moves upward with a vertical velocity of about 6 ms^{-1}. This upward velocity creates a turbulence within the material in the vertical riser. The density of the material in the riser reduces along the

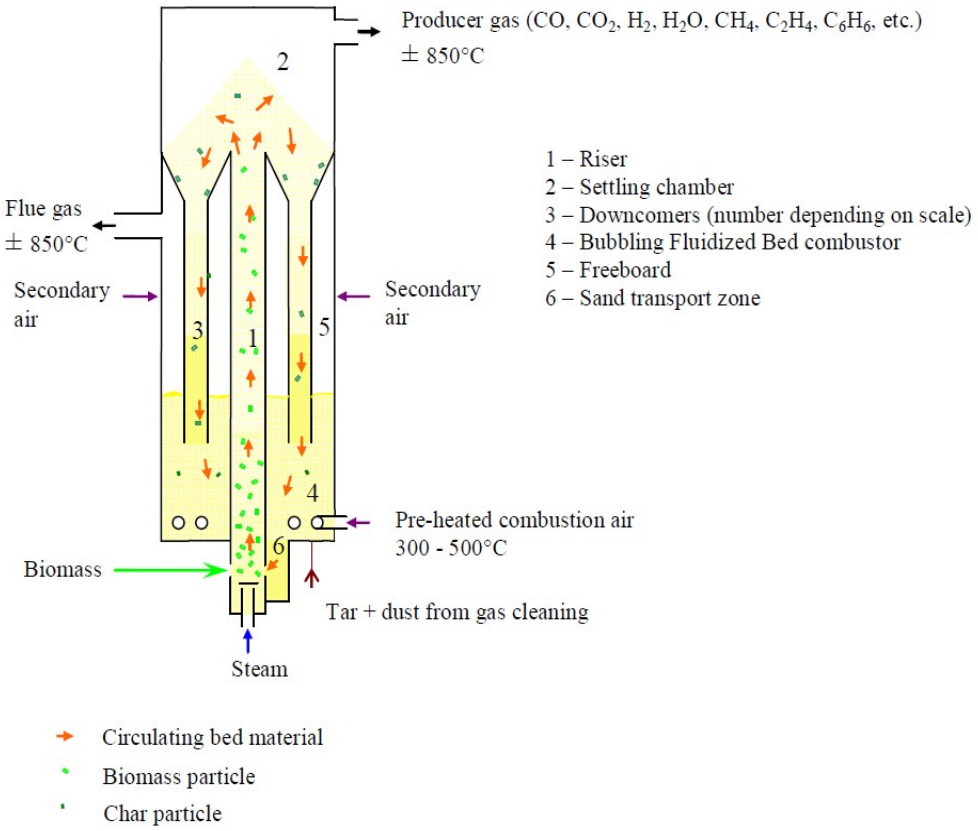

Figure 2.7: ECN MILENA Gasifier [21]

Table 2.5: Reported Composition of Syngas from Pilot Plant of FICFB [57]

Hydrogen	30 - 40%
Carbon Monoxide	20 - 30%
Carbon Dioxide	15 - 25%
Methane	8 - 12%
Nitrogen	1 - 5 %

	Raw gas	**Clean gas**
Tar	0.5 - 1.5 g/Nm^3	<20 mg/Nm^3
particles	10 - 20 g/Nm^3	<10 mg/Nm^3
Ammonia	500 - 1000 ppm	<200 ppm
Hydrogen Sulfide	20 - 50 ppm	

height of the riser and this less dense region is where most of the tar cracking reactions happens. The turbulent nature of the gas flow entrains some solid particles (bed material and char, ash) with it and these solid particles are removed partially at the settling chamber. From the vertical riser into the settling chamber, the flow area (Volume) increases sharply causing the flow velocity to decrease. This decrease in velocity helps not only with removing the entrained particles but also increasing the residence time of the fuel gas within the reactor. With gas flow speeds of 6 ms^{-1} within the riser, the residence time of the gas in the riser in of a few seconds and this is not enough for complete gasification of the biomass and to crack the produced tars. The increased residence time due to the settling chamber helps increase the carbon conversion and to reduce the tar concentration in the product gas.

The solids that separate from the product gas fall down into the downcomer and into the combustor. The product gas coming out from the settling tank can be filtered later for tar and dust and the tars can also be recycled to the combustor. The char and tars along with bed material in the combustor are burned at a temperature of around 925 °C with air as the oxidizing medium. An air stream (primary) is injected from the bottom of the bubbling fluidized bed combustor and a secondary stream of air is added in the free-board of the combustor to reduce the CO and hydrocarbon emissions from the combustor. This flue gas from the combustor is extracted separately and mixing of the flue gas from the combustor preventing mixing of flue gas and the product gas from the gasifier. Hence the fuel gas produced is much richer and with a higher heating value. The flow rate of the char and bed material from the combustor and the new biomass is monitored to maintain a gasification temperature of around 850 °C.

FICFB GASIFIER, GUSSING

The FICFB (Fast Internally Circulating Fluidized Bed) gasifier concept at Gussing was developed first by the University of Vienna and is one of the first two dual fluidized bed concepts to be proven in an industrial scale. By operation, it is quite similar to the ECN MILENA gasification technology of a physically separate combustor to supply the heat required for gasification. The gasification reactor in the FICFB gasifier is a bubbling fluidized bed reactor (opposite to that of ECN MILENA) working with steam as the gasification medium. Figure 2.8 shows the schematic of the FICFB concept. Gasification temperature is maintained between 850°C and 900°C[13]. Bed material along with the produced char is continuously recirculated through a chute and a loop seal to the combustion reactor functioning as a circulating fluidized bed reactor. The char is then completely combusted in the combustor with air and with additional fuel if required to produce heat and increase the temperature of the bed. The combustor is maintained at temperatures between 950°C and 1000°C and the hot bed material is then recirculated to the gasifier by means of a second loop seal . The loop seals are placed to avoid mixing of the flue gas and the product gas stream. The produced syngas entrains a considerable amount of solids (because of the bubbling fluidized bed gasifier) and that is separated from the produced syngas in the cyclone. Since steam is used as the gasification medium, nitrogen dilution is avoided and the nitrogen found in the product gas composition is primarily from the biomass. The heating value of the product gas obtained from such is typically of the range of 12 – 14 MJ/Nm^3[57].

The bed material initially used was quartz sand which is catalytically inert and the tar concentration in the final product gas measured was less than 1 g/Nm^3[57]. Composition of the raw and cleaned product gas produced from the pilot plant with wood chips as the biomass fuel is shown in the Table 2.5[57].

Experimental results of the pilot plant of FICFB are available from literature and these results help us understand the effect of various operating parameters such as the Steam to Biomass ratio and gasification temperature on the final product gas composition and quality[57–59]. Moreover, there have also been tests conducted in this pilot plant on the effect of Ni based catalysts on tar reduction and Tar content was shown to reduce with increase in catalyst percentages and at 43% Ni, the tar concentration drops to levels less than

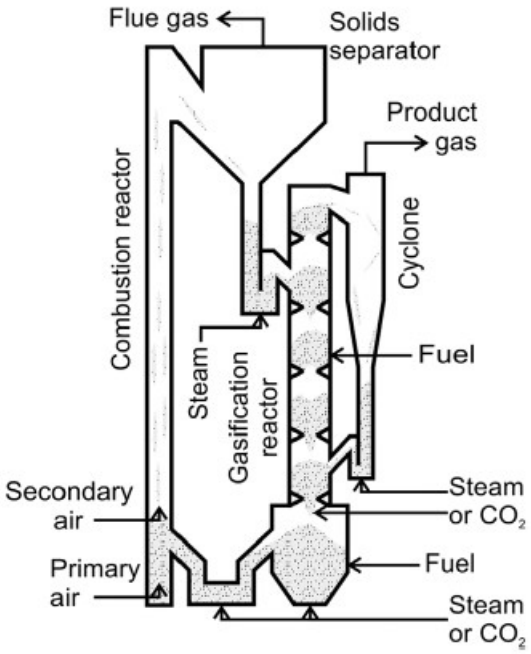

Figure 2.8: Schematic of the FICFB Gasifier, Gussing[35]

0.5 g/Nm^3[57]. As expected from theory, the hydrogen yield of the product gas increases with an increase in catalyst percentage in the bed material[57]. This hydrogen yield is attributed to the decrease in methane concentration in the product gas composition. The measured tar levels are low enough for direct use of the product gas in an SOFC (Solid Oxide Fuel Cell) [57]. The final gasifier efficiency was measured to be around 70 - 85% and was strongly influenced by the steam/biomass ratio.

2.2.5. ABSORPTION ENHANCED REFORMING (AER)

Hydrogen fraction of the syngas produced from an allothermal gasifier can be enhanced by using a CO_2 absorbing sorbent inside the gasifier. In other words, the CO_2 produced during gasification can be reduced to promote the Water Gas Shift and Char Gasification reactions mentioned in Table 2.1 to increase the hydrogen fraction of the produced syngas[60]. This process of enhancing the reforming process by removal of CO_2 is called Absorption Based Reforming (AER). CaO (Calcium Oxide) rich materials such as Dolomite and other ores are studied actively for their CO_2 absorbing property. CaO reacts with CO_2 at gasification temperatures to produce $CaCO_3$ which is shown in the Equation 2.1. The CO_2 absorbed to produce $CaCO_3$(Calcium Carbonate) can be released by the calcination (reverse) reaction (Equation 2.2) which happens at temperatures close to the combustor temperatures in an allothermal gasifier.

$$CaO + CO_2 \longrightarrow CaCO_3 \qquad \Delta H^{\circ}_{298} = -178\ \text{kJ mol}^{-1} \tag{2.1}$$

$$CaCO_3 \longrightarrow CaO + CO_2 \qquad \Delta H^{\circ}_{298} = +178\ \text{kJ mol}^{-1} \tag{2.2}$$

AER is a very attractive concept for an allothermal gasification process because, dolomites and other CaO rich sorbents can be used as bed material. Apart from just transferring heat from from the combustor to the gasifier, they can also help increase hydrogen yield by removing CO_2. The forward reaction, $CaCO_3$ formation is an exothermic reaction, which increases the gasification temperature increasing both the hydrogen yield and promoting tar cracking to an extent [60, 61]. Although the reverse reaction, calcination is an endothermic reaction, it is thermally compensated by the exothermic forward reaction. A simple functional schematic of such an AER concept is shown in Figure 2.9.

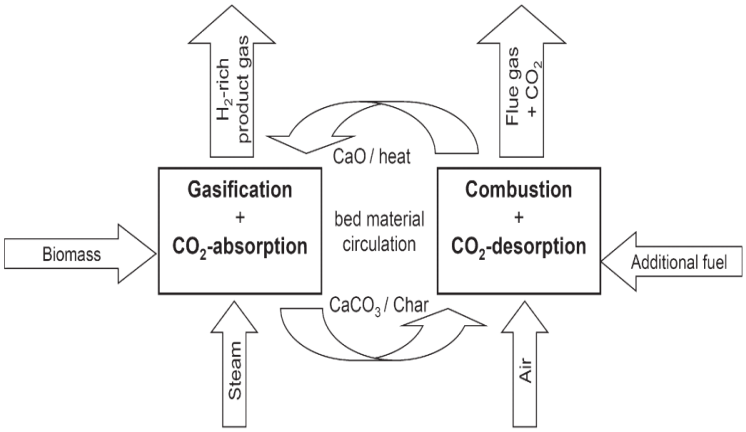

Figure 2.9: Absorption Enhanced Reforming (AER) - Use of Dolomite for In-situ CO2 capture during Gasification [60]

The CO_2/CaO equilibrium shown in Equation 2.1 mainly depends on the process temperature and the partial pressure of CO_2 in the reactor[60]. Florin and Harris [62] state that the this CO_2 capture process is favored between the temperatures 450°C and 750°C. It has to be noted that this temperature range is quite low when compared to the gasification temperatures of most allothermal gasifiers found in literature [21, 57, 63]. However, at temperatures higher than 850°C. the formed $CaCO_3$ calcinates to produce back CaO.

2.3. GAS CLEANING

The next step after gasification is the processing of the produced syngas. Even with the most novel gasification technology, the produced syngas more often than not needs to be cleaned for downstream needs. Gas Cleaning process often involves removal of particulates that entrains with the syngas and removal/breaking down tars and other impurities. Gas Cleaning technologies can be divided into two, dry gas cleaning and wet gas cleaning. Currently, majority of industry-wide gas cleaning performed by low temperature gas scrubbers (Wet Gas cleaning) such as the RECTISOL process, which is a cryogenic scrubbing process with methanol at very low temperatures [64]. The major drawback of such low temperature wet scrubbers are that the syngas has to be cooled down before gas cleaning and then subsequently reheated to downstream synthesis temperatures. This significantly reduces the exergy efficiency of the whole process while also increasing its complexity. This section provides a short introduction to both dry and wet gas cleaning methods.

2.3.1. DRY GAS CLEANING

To increase the exergy efficiency of the overall gasification and gas cleaning process and to circumvent the added complexity of incorporating a complicated energy recovery network, there have been a number of studies on High Temperature Gas Cleaning. Most effective heat recovery practice would be to perform gas cleaning at the gasification temperature and then subsequently cooling the clean syngas to synthesis temperature. Moreover, performing gas cleaning very close to the synthesis temperature would require designing heat transfer equipment to work with a very crude impure syngas which would require a higher dust loading.

Two cases of Dry Gas Cleaning are actively studied: one, a high temperature gas cleaning system operating at around 800°C, corresponding to the gasification temperature and second, a Moderate temperature gas cleaning line operating at a temperature around 450°C - 500°C. Karlsruhe Institute of Technology (KIT) proposed a High Temperature High Pressure (HTHP) gas cleaning process line for a biomass based syngas with high ash content based on a High –Efficiency particle filter combined with sorption units for sulphur and chlorine removal [64]. Tars and other contaminants such as ammonia are treated in a catalytic bed subsequently. This gas cleaning concept was designed to be operated downstream of an entrained flow gasifier

for coke oil slurry gasification and upstream of an FT reactor to produce bio-fuels[64], with the key objective of producing a clean syngas stream with the required purity as shown in the Table 2.4 using sorbents that are currently available. Added constraint in such a high temperature system is the softening of ash in the syngas stream at this temperature.

Although very promising in design, high temperature filters are still not a mature technology. Key challenges including, resistance to abrasion, operational time and clogging remain a major setback to its development.

2.3.2. WET GAS CLEANING

Cold or wet gas cleaning methods tend to remove or reduce tar and other contaminants by mainly using scrubbers and various absorbing liquids. Wet gas cleaning at low temperatures is a fairly mature technology, very effective and hence shifting the focus of majority of the recent research towards the Hot Gas cleaning methods. A key advantage of using a wet gas cleaning method is that wet gas cleaning methods offer a complete and comprehensive solution to remove various contaminants with just a single technology. However, there are a few disadvantages with wet gas cleaning such as, the syngas when cooled to lower temperatures from high gasification temperatures has a detrimental impact on the overall efficiency of the system. Additionally, the cooled syngas after the Gas Cleaning unit has to be reheated to the required downstream temperatures. The scrubbers usually employed for wet gas cleaning generate waste streams which cannot be directly disposed without prior treatment [65].

In wet gas cleaning, the tar molecules are first physically removed by cooling the syngas to a temperature below the dew point temperature of the tars. This cooling process is usually done with an absorbing agent to avoid fouling due to liquid tars. Obviously, the tar dew point temperature and solubility of tars in the absorbing liquid medium play a significant role in the effectiveness of the system. Furthermore, there is no risk of catalyst deactivation and no heat requirement for this type of gas cleaning. The main concern of wet gas cleaning is in the waste streams that are produced during operation, which do limit its scale in modern applications.

ABSORPTION BASED GAS CLEANING - AN INTRODUCTION

In absorption systems, a gas mixture is contacted with a liquid absorbent or solvent to selectively dissolve a particular set of components by mass transfer from the gas stream to the solvent stream. The components absorbed or removed are called solutes or absorbate.The opposite of this absorption process is a process called stripping where, a single or set of components are selectively removed from a liquid stream by mass transfer between the liquid and a gas stream [66]. Liquid-gas scrubbers are commercially used to remove tars and particulates from syngas.

Absorption and stripping are technically mature separation operations; water based scrubbing systems have been used for gas cleaning. The process of absorption based scrubbing can be of two types; Physical and chemical absorption. When water and other hydrocarbon oils are used as absorbants, there are no significant chemical reactions occurring between the solutes and the solvents. This kind of absorption is called physical absorption. On the other hand, when Monoethanolamine is used to absorb CO_2 from the flue gas stream, a reversible reaction takes place. This kind of absorption is called chemical Absorption. This research focuses on developing a liquid gas absorption system for syngas cleaning because of its relative technical maturity in industrial availability. The following section discusses in brief a novel Gas Cleaning unit developed by ECN for tar removal.

OLGA GAS CLEANING

OLGA (Dutch Acronym for Oil-based Gas washer) is part of the integrated gasification system developed by ECN. The main objective of such a gas cleaning system is not to completely remove tar in a product gas stream but to remove all tar related problems in a product stream. A pilot plant of this gas cleaning unit has been realized in early 2003 and the experimental verification of its feasibility has been carried out from then [65].

The primary objective of the OLGA was set for selective tar removal (No removal of water or other product gas such as H2, CO and CO_2) and to completely remove water soluble heterocyclic tar components which

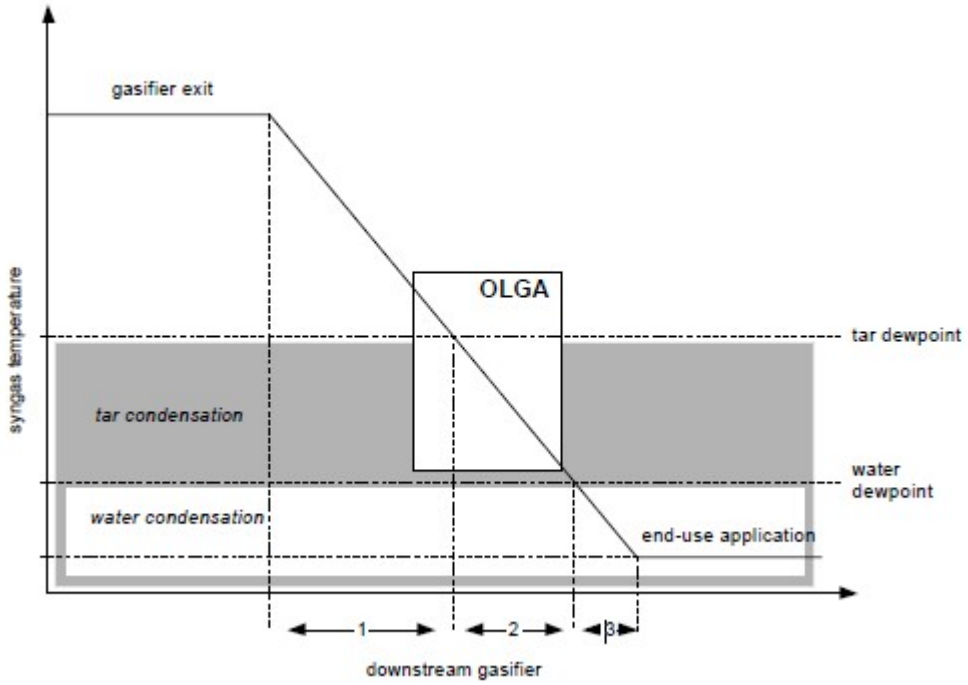

Figure 2.10: OLGA - Working conditions [65]

could cause process water contamination problems downstream. Scrubbing liquid consumption was designed to be a minimum, mainly on account of process economics and also high consumption would taint the sustainability of biomass gasification [65]. A Common problem with tars downstream is its condensation. Deep removal of tars from class 1 to 5 is required to reduce the tar dew point to be lower than the downstream operational temperatures. The actual collection efficiency of the system depends on the volume and composition of tars in the process stream. Since the type 2 tars are water soluble, collection efficiency of tars of class 2 (Heterocyclic tars) is very essential to prevent pollution of process water.

The inlet gas temperature of OLGA is kept above the tar dew point temperature to avoid any condensation related problems upstream of the OLGA system. The outlet temperature is however kept above the dew point temperature of so that water is not absorbed in the scrubbing liquid. The Figure 2.10 illustrates the working limits of the OLGA [65].

The secondary objective of OLGA was to operate as an integrated system to remove tars, particulates and inorganic impurities as a system. The produced product gas is first de-dusted and cooled upstream of the OLGA. Downstream of the OLGA, water in the cleaned gas is condensed by water quench and major inorganic impurities such as ammonia and HCl are removed by scrubbing. The product gas produced is now available for most downstream applications. Additionally, the scrubbing liquids can be cleaned and the produced tar and the unrecovered scrubbing liquid as well as the ammonia from the wet scrubber can be recycled to the combustor, preventing any additional waste streams. The scrubbing liquid consumption is designed to be a maximum of 0.5% by weight of the biomass feed. Experiments at ECN show that tars are completely destroyed in the Combustor of the gasifier (when the tars are recycled back to the MILENA) and most of the ammonia removed from the product gas are converted into elemental nitrogen.

DESIGN

The schematic of the OLGA system is shown in the Figure 2.11. The product gas flowing through the OLGA is cooled to a temperature slightly higher than the dew point of water. As the gas is cooled, the liquid and and gaseous tars are collected by the scrubbing liquid. This absorption process is carried out in two separate scrubbing columns, the Collector and the Absorber. Liquid tars are then separated from the scrubbing liquid and sent back to the gasifier (Combustor part of MILENA when air is used as stripping agent) where the tars

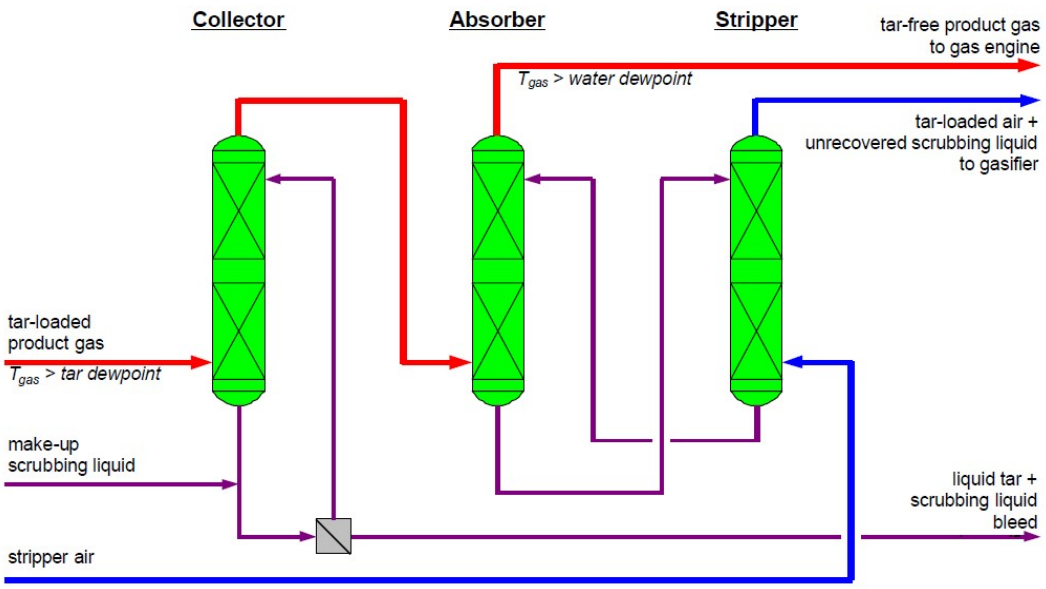

Figure 2.11: Functional Schematic of the OLGA Gas Cleaning Unit [65]

were broken down during gasification. The scrubbing liquid with tars dissolved then flows into the stripper, the third column. The whole process of tar absorption and stripping is same as in a classical absorption - regeneration process. The gasification medium (or air, even when air is not used as the gasification agent) used in the gasifier is used as the striping agent and blown through the stripper. The gasification medium with the stripped tars are then sent to the gasifier. The scrubbing liquid entrained with the gasification medium is monitored to be minimal. The design criteria used when designing OLGA is that 95% of phenols and 100% of poly-aromatic compounds are removed so that no condensation occurs downstream[65].

EXPERIMENTAL RESULTS OF PILOT OLGA

The test setup at ECN for testing OLGA consists of a bubbling fluidized bed gasifier connected to a pilot sized OLGA through a ceramic high temperature filter [65]. Temperature of the product gas drops from 330 - 350°C to 60 ~ 100°C. Key operational parameters for tar collection within the system are the scrubbing liquid to gas flow ratio and the Temperature [65]. The product gas from the outlet of the gas cleaning unit were then measured for elemental composition. A 75 hour operational test was conducted to demonstrate the tar reduction capability of the system and the results are shown in Figure 2.12. A 98% removal of tars within the OLGA was observed. None of the main product gas elements such as CH_4, H_2, CO , CO_2, H_2O were removed and the dew point was reduced to around 20°C [65].

2.4. METHANOL SYNTHESIS

Systematic synthesis of methanol has a history of over 100 years, when it was first produced by destructive distillation of wood [67]. Methanol has since been used as a 'building-block' chemical, solvent and more recently, as combustion fuels and more. Interest in methanol has increased recently because of its potential use as an alternate fuel or as its precursor (Bio-Diesel production). The first commercial synthesis of methanol was done as a high pressure-synthesis process and since then the the process of producing methanol has moved to a low-temperature synthesis. The most common practice of methanol synthesis is typically from syngas produced from steam reforming of natural gas but there are a variety of process that produce methanol from different sources.

2.4.1. CONVERSION OF SYNGAS TO METHANOL

Synthesis of methanol from syngas is commercially carried out over a heterogeneous catalyst system, usually a $Cu/ZnO/Al_2O_3$ catalyst[67]. Methanol synthesis is in itself reasonably complicated with a number of chemical reactions proceeding simultaneously inside the reactor. The principal three stoichiometric reac-

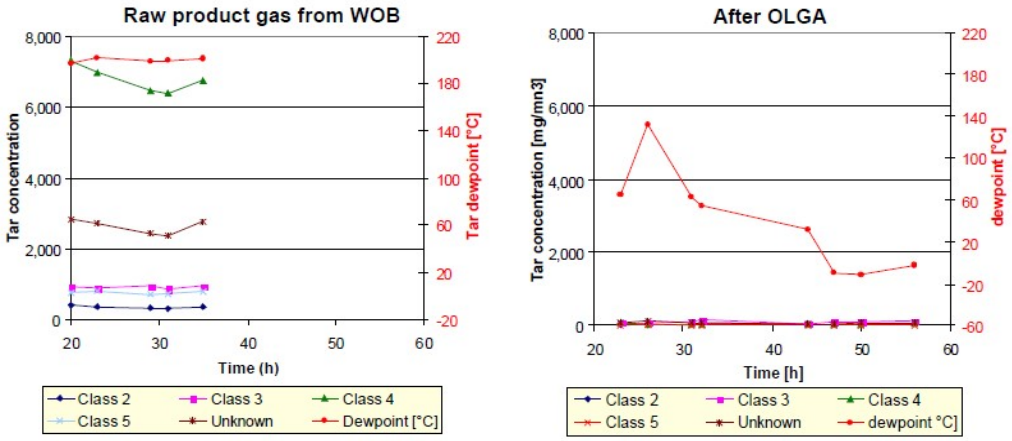

Figure 2.12: OLGA Gas Cleaning Unit Results [65]: 75 Hour test demonstrates the removal efficiency of different classes of tars in the product gas.

tions considered in this chemical conversion are,

$$CO_2 + 3H_2 \longrightarrow CH_3OH + H_2O \qquad \Delta H^\circ_{298} = -54\,931\ \text{kJ mol}^{-1}\ [68] \tag{2.3}$$

$$CO + 2H_2 \longrightarrow CH_3OH \qquad \Delta H^\circ_{298} = -98\,438\ \text{kJ mol}^{-1}\ [68] \tag{2.4}$$

$$CO + H_2O \longrightarrow CO_2 + H_2 \qquad \Delta H^\circ_{298} = +43\,466\ \text{kJ mol}^{-1}\ [68] \tag{2.5}$$

Among these three chemical reactions, only two equations are stoichiometrically independent; a linear combination of any of the two equations would yield the third equation. The choice of selecting either CO or CO_2 hydrogenation along with the water gas shift reaction as the key chemical reactions for methanol production is very controversial in most literature [67, 69, 70].

The effect of temperature and pressure of the methanol, synthesis on the equilibrium and the kinetics of the methanol reaction are to be studied closely to choose an optimum working condition for the methanol synthesis process. Both the methanol synthesis reactions, CO and CO_2 hydrogenation reactions are kinetically not favored at low pressures and high temperatures. This is shown in the Figure 2.13, a plot of equilibrium constants of the three reactions versus Temperature [67, 69]. Kinetically, reducing the temperature would decrease the reaction rate and thereby reducing the methanol yield following an Arrhenius type of dependency on temperature whereas the equilibrium conversion is thermodynamically unfavored with an increase in the reaction temperature. Hence, the synthesis process is primarily performed at relatively higher temperatures, pushing the pressure requirements even further. However, elevated temperatures do make the process more complicated, increasing the likelihood of potential thermal deactivation of the catalysts. The exothermic nature of the synthesis reaction would also add to this thermal stability problem within the reactor. Increasing the reaction pressure on the other hand would increase the complexity of the process with higher energy demands and capital investments supporting the process.

Optimizing these constraints would mean that the process is usually operated in an unfavorable equilibrium nature, leading to a typically low single pass conversion. All commercial methanol production processes employ a recycle to increase overall conversion. Typical operating conditions for methanol synthesis is around 220°C to 270°C and 50 to 100 bars [67].

Determining the optimal conditions for methanol production is much complicated by the interlinked nature of the reactants and also by standard operating parameters such as temperature and pressure. Increasing the temperature would increase the rate of methanol synthesis reaction following an Arrhenius type of temperature dependency. However equilibrium conversion of this synthesis reaction reduces with increasing temperature. the operating temperature of the catalyst and the process impart an additional constraint

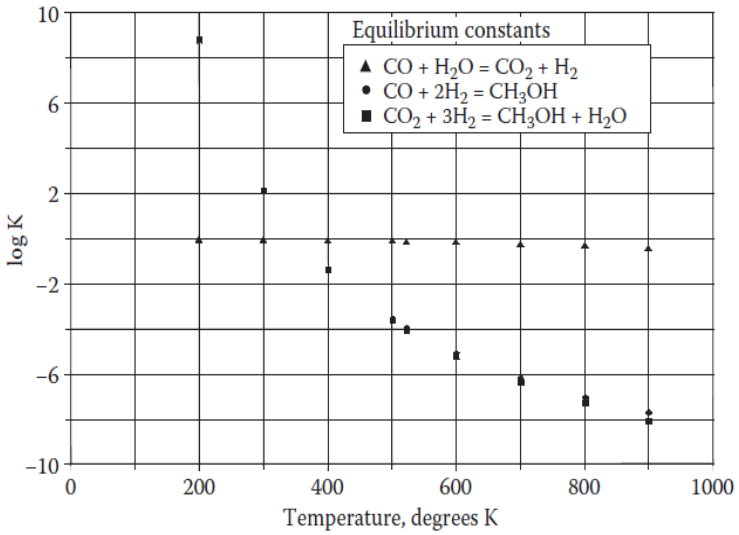

Figure 2.13: Temperature dependence of Equilibrium constants of different methanol synthesis reactions [67]

on this maximum synthesis temperature. Temperatures of 280°C - 300°C are considered as maximum and beyond this temperature, the catalyst used would be subjected to sintering and essentially lose its catalytic ability. Since the methanol synthesis is quite exothermic, the reactor along with the process needs to be designed carefully to avoid good dispersion of this exothermic heat produced during the synthesis to avoid any local hot spots to enhance conversion efficiency.

In literature pertaining to methanol synthesis, the term *'Balanced Gas'* is very commonly used. This Balanced Gas refers to 2:1 mixture of H_2 and CO in the syngas supplied for methanol synthesis [67]. Irrespective of the main methanol synthesis pathway (CO or CO_2 hydrogenation), this 2:1 mixture is a stoichiometric assessment of methanol production as a direct combination of 1 molecule of CO and 2 molecules of H_2 [67]. Different methanol synthesis technologies use different H_2/CO fractions, primarily depending on the nature of the process and the nature of the biomass/fuel source used. However, the theoretically optimal stoichiometric ratio of the the syngas used is given by the formula shown in Equation 2.6. This stoichiometric ratio, a function of the molar flows of Hydrogen, Carbon Monoxide and Carbon Dioxide has to be tailored to be around 2.05 to have optimal methanol Yield [67, 71] (2.1 when a recycle within the methanol synthesis process is considered).

$$\text{Stoichiometric Ratio} = \frac{H_2 - CO_2}{CO_2 + CO} \tag{2.6}$$

2.4.2. LURGI PROCESS FOR METHANOL PRODUCTION

Lurgi Process for methanol, production is designed to be operated as a single-train process to produce methanol from natural gas or other oil-based gasses. A schematic of this Lurgi process for methanol synthesis is shown in Figure 2.14. Natural gas is reformed with steam to produce a synthesis gas consisting only of H_2, CO, CO_2 and a small fraction of unconverted CH_4. Schematic of the Lurgi process is shown in Figure 2.14. Heat required for this reforming process can also provided by partial oxidation with a small fraction of O_2 supplied.

Stoichiometric feed for methanol synthesis is achieved by supplying pure hydrogen, produced by pressure swing adsorption (PSA) to required the H_2 - CO ratio. A water cooled reactor is used for the methanol synthesis process, where a part of the product gas is recycled to increase methanol yield. Exothermic heat produced from the synthesis reaction is used to boil the cooling water and thereby maintaining near-isothermal conditions during the synthesis process. The reactor effluent gas is then cooled to 40°C and flashed at a lower pressure to separate methanol and water from the unreacted gases. the released gases are partly recycled into the methanol reactor as mentioned before. the methanol and water mixture is then sent to a distillation column where methanol is separated from water. Process enhancements have been made to improve the overall

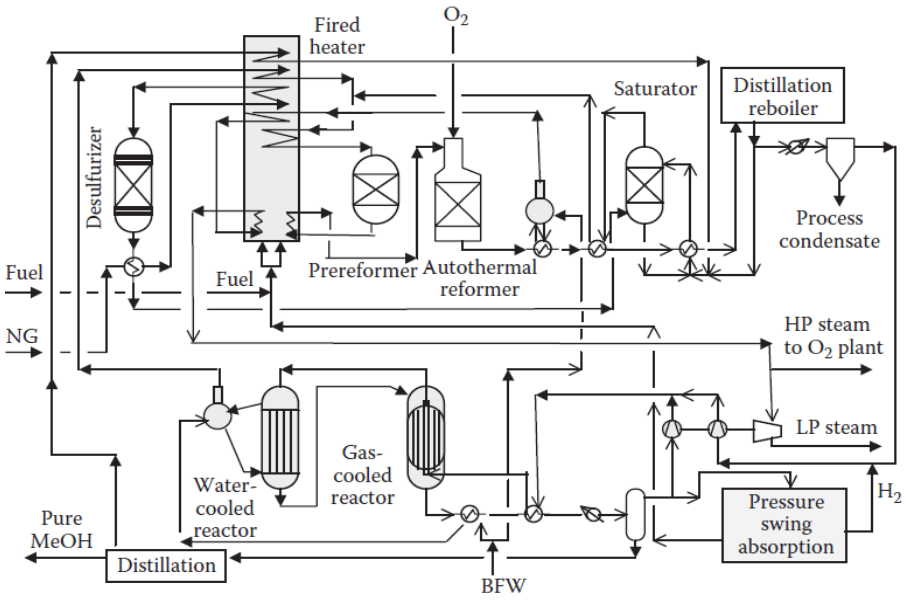

Figure 2.14: Lurgi Process for Methanol Synthesis - Schematic [67]

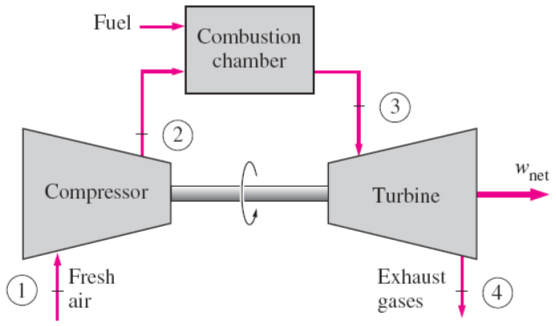

Figure 2.15: Schematic of a Gas Turbine system

yield of the process and to achieve a recycle ratio as low as 2 [67].

2.5. GAS TURBINES

The Gas Turbine engine is a prime mover used to produce mechanical work from a gaseous working fluid. Similar to an internal combustion Engine, such as an Diesel engine but with a significant difference that the Gas turbine system produces mechanical power from a gaseous fuel source continuously and not intermittently. A Gas Turbine system consists of a compressor, a combustion chamber and a turbine but usually integrated into a single unit. Air is initially compressed to a higher working pressure inside the compressor and then this compressed air is used to oxidize the gaseous fuel inside the combustion chamber. The hot, high pressure flue gas is then expanded in the turbine, back to atmospheric pressure producing mechanical work. The compressor, turbine and the generator are usually coupled with a common shaft; The turbine work produced is partially used to run the compressor. Schematic of a Gas Turbine system is shown in Figure 2.15. Gas Turbine cycles are usually coupled with a suitable bottoming cycle to improve the overall energy efficiency.

2.5.1. GAS TURBINE SUITABILITY FOR DIRECT SYNGAS COMBUSTION

Major efforts were devoted in the 1990's to improve the prospect of Gas Turbines as high efficiency means to produce electricity from Natural gas [72]. However, the recent diminishing economic advantage of using natural gas for power production coupled with the increasing drive towards zero emission power production has resulted in an increase in research towards integrating a gas turbine system for power production from

synthesis gases produced from coal/biomass gasification. Co-firing syngas in gas turbines has however been studied and realized industrially since 1960 [73]. There are numerous research on incorporating a GT system with a gasifier network. Tijmensen et al. [74] proposed a system where a Gas Turbine is used to fire the off-gas from a Fischer-Tropsch (FT) reactor, producing energy and biofuels. Li et al. [75] discuss the possibility of utilizing a GT for firing unreacted syngas from methanol synthesis to produce power. Either way, various models are being developed using a GT either as a standalone power production unit firing syngas directly from the gasifier or also using GT essentially as a power producing alternative to flaring off-gas (waste gas or flash gas) from various process. Cleaning requirements for GT/CC installations are relatively less stringent than for FT/Methanol synthesis, making integration more attractive [74]. This is also illustrated in Table 2.4. This lesser syngas (or fuel) purity requirement could attract the potential use of gas turbines for producing power from different calorific waste gases produced during different synthesis processes such as methanol synthesis process.

This transition from using natural gas to syngas as the gaseous fuel is complicated by the diversity in composition of syngas produced from different gasification technologies. Since syngas contain a significant fraction of hydrogen, steam formed upon combustion results in a firing temperature around 110 - 180°C lower than that of the natural gas equivalent [76].

Major Gas Turbine producers such as GE and Siemens both have gas turbines which are capable of firing syngas in an industry-scale. Siemens for example, have projects on designing Gas turbines for syngas dating back to the 1960s [77]. The main concerns for firing syngas directly in Gas turbines is the lower heating value of syngas when compared with conventional natural gas or methane and also, the purity of the syngas fired. Reduced heating value of syngas would imply a higher a mass flow into the turbine, increasing the power produced. However, with significant fraction of steam in the flue gas (due to combustion of hydrogen), questions on blade lifetime and operations have been widely raised [77] However Research on improving syngas combustion and power production have been very active and promising in the last decade, making the use of Gas Turbines for power production from biomass derived syngas a very close reality [78].

2.5.2. IMPACT OF FIRING SYNGAS IN A GAS TURBINE

The technical impact of firing a non-conventional fuel such as syngas in a Gas Turbine can be analyzed by studying the change in behaviour between a Gas Turbine system firing a conventional natural gas a fuel and the same gas turbine system firing syngas as fuel. Since IGCC's have been very well studied for clean energy production, research of this kind can be found in literature [77, 79, 80]. Although the detailed design of a gas turbine system capable of firing syngas is beyond the scope of this research, it is necessary to understand the practical challenges involved in the operation of such a system. The impact of firing syngas in a GT system can be split into two parts, between the combustor and the moving parts such as the turbine and the compressor.

COMBUSTION OF SYNGAS

Despite the aged interest and promise of the IGCC technology, numerous failures have been reported from the previous IGCC plants, particularly with regard to the synthetic gas turbine combustor[79]. Lee et al. studied the combustion of a wide array of CO: H_2 mixture as fuel and the results of this study can help understand the Gas Turbine combustion characteristics of syngas[79]. Since syngas is predominantly a mixture of CO and H_2, the combustion properties such as the flame temperature, flame speed etc. vary significantly from that of methane (natural gas). The flame temperature of syngas was found to be approximately 100°C higher than that of natural gas and this difference increased with increase in hydrogen fraction of the syngas used[79]. There was also a notable difference in nozzle temperature, which was attributed to the increased flame speed of syngas (primarily due to the hydrogen fraction)[79]. Burning velocity of syngas is affected more by the burning speed than the convective speed, which could imply that an increased fraction of H_2 or CO in the syngas could cause severe nozzle damage due to flashback[79].

Oluyede et al. analyzed the impact of firing syngas in a GT by comparing the theoretical creep life of the turbine blades between the cases of natural gas and syngas as fuel[80]. Since Hydrogen constitutes to a significant portion of the syngas fuel, the fraction of H_2O in the flue gas stream is significantly larger than when natural gas is used as fuel. This increased fraction of water vapor increases the specific heat of the flue gas stream. This increased heat capacity of the flue gas would result in higher heat transfer from the flue gas to the turbine blades and vanes in the turbine during expansion. This additional heat input causes the hot metal

temperature of the blades and vanes to increase. Hence with increasing fraction of water vapor in the flue gas, the hot material temperature was shown to increase[80]. As a result, the theoretical creep life of the turbine blades dropped by 20% when syngas with 12.1% Hydrogen fraction was fired in a gas turbine[80], compared to the natural gas case. In order to maintain the durability of the hot sections, GE hence recommends the firing temperature to be lowered as hydrogen fraction in the syngas increases[80]. This is one of the key reasons why the turbine Inlet temperature (TIT) of hydrogen rich syngas fired gas turbines are limited to 1000°C.

IMPACT ON THE TURBINE AND COMPRESSOR

A significant effect of using syngas as a fuel in a Gas Turbine system would be the increased mass flow in the compressor and turbine when compared to a natural gas fired gas turbine. This increase in mass flow is due to the reduced heating value of syngas, which would require an increased syngas flow to achieve the same firing temperature. Johnson et al. predicted the off-design performance when firing coal derived syngas in a natural gas based gas turbine and the results of this study can be used to understand the key impact of this fuel change. For a choked turbine inlet condition, the mass flow of an ideal gas can be shown as,

$$\dot{m} = P_i * A^* \sqrt{\frac{MW}{T_i}} \sqrt{\frac{\gamma}{R_u} * (\frac{2}{\gamma+1})^{\frac{\gamma+1}{\gamma-1}}} \tag{2.7}$$

The equation shown in Equation 2.7 is a rearranged form of the traditional equation and was obtained from [81].

When syngas is fired in a gas turbine, the mass flow ($\dot{m}$) shown in Equation 2.7 increases (due to lower heating value) to maintain the same firing temperature T_i. Now, when γ (ratio of specific heats) and the molecular weight (MW) are approximated to be constant, the increase in mass flow into the turbine could be accommodated by increasing either the total pressure (P_i) or the critical area (A^*). If increasing the critical area of the turbine can be safely ruled out as realistically impractical for a GT system frequently switching between two different fuels, the compressor pressure ratio must be increased or compressor mass flow must be reduced. Operating at an increased pressure ratio presents several challenges on the turbine and the compressor. Apart from the increased thermal loads on the turbine blades, the increased pressure can push the compressor operating point towards surge. Surge is a complicated, transient flow reversal that can cause severe damage to the compressor. Hence, to achieve the theoretical advantage of producing relatively more power when firing syngas, the compressor must have a sufficient surge margin to sustain the effects of this increased pressure ratio[81].

2.5.3. INVERTED BRAYTON CYCLE

The thermodynamic cycle explaining power production in a Gas Turbine is the Brayton Cycle. The working gas (air) is compressed in the compressor and then combusted along with a gaseous fuel in the combustion chamber. This high pressure hot flue gas from the combustion chamber is then expanded in a turbine resulting in a net mechanical work produced. However, the efficiency of such a Brayton cycle is maximised by decreasing the temperature of air and fuel before compression and in theory, maximising the temperature before expansion. Hence for a case where a hot gaseous fuel (or flue gas) at atmospheric pressure is to be combusted in a Gas Turbine, the gas has to be cooled to near atmospheric temperatures to reduce the compressor power consumption. This would require an additional Heat Exchanger to cool the fuel stream, reducing the compactness of the complete system.

However, Net specific work can be extracted from a hot gas at atmospheric pressure by expanding the gas below atmospheric pressure,cooling and then finally re-compressing it back to ambient pressure. These tasks can be performed with a turbine, recuperator and a compressor, respectively, which are the same components of a conventional Brayton Cycle (GT). This cycle is similar to a Brayton cycle but "reversed' in flow and hence commonly called as the Inverted Brayton Cycle (IBC). A simple schematic of this inverted Brayton cycle with Exhaust gas recirculation is shown in the figure 2.16. The reversed nature of flow can be observed by comparing the schematics of the conventional Gas Turbine system (Figure 2.15) and the Inverted Brayton Cycle system (Figure 2.16).

In a recuperated IBC, inlet air is heated by the exhaust flue gas and combusted with fuel at atmospheric pressure, eliminating the need for a separate fuel gas compressor. Since the combusted flue gas is expanded

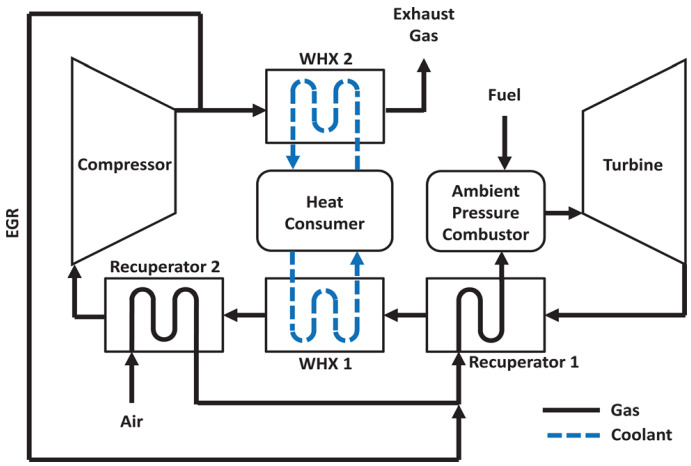

Figure 2.16: Schematic of a Inverted Brayton Cycle with Exhaust Gas Recirculation [82]

to very low sub-atmospheric pressures, increased volumetric flow rates would enable the use of bigger turbines and recuperators. Increased size of the compressor and turbine would reduce the heat losses and thereby increasing the isentropic efficiency compared to smaller compressors and turbines. Studies of IBC such as [82] and [83] show that recuperated IBC cycles can be much more efficient that conventional Gas Turbine systems in the micro-GT range.

2.6. RESEARCH OBJECTIVE

This report introduced the key aim of this study as to investigate Biomass gasification and its practical importance. To elaborate a bit more on what exactly follows within the gasification process and its subsequent steps, chapter 2 (background) discussed in better detail on different technologies of gasification, Gas Cleaning and certain downstream applications such as Methanol Synthesis, Gas Turbine systems and their respective challenges. Upon understanding the theory behind each of these processes, we now define the main objective of this master thesis. The key aim of this study is develop a model of a system which would be capable of producing both Methanol and power from Biomass. Having defined this objective, the research can be divided into different focuses based on chronology.

Since the process of converting biomass to fuel (Methanol) or power involves a number of steps (such as Gasification, Gas cleaning etc.). These identified steps of processing to convert biomass to methanol can be considered as individual functional blocks. The first focus would be to identify and examine different technologies for each of these *blocks*. To be more precise, this part would involve splitting the model into different functional sub-models such as Gasifier, Gas Cleaning Unit, Methanol synthesis and the Gas Turbine part. The Second Focus would be in optimizing each of these sub-units upon modeling each unit separately. The next step would be integrating each of these sub-units into a single generic model.

previously in this chapter, various technologies for each of these functional blocks were discussed in brief. As the first step, the bounds of this study are fixed in terms of the inputs and technologies considered. This research would focus on a kinetic based modeling study of Indirect (Allothermal) Gasification of Torrified wood for Methanol and power production.

The above mentioned research focuses can be consolidated into the following research questions which this master thesis aims to answer.

1. Taking into consideration different experimental results of Gasification studies, how accurately can this model predict the composition of the major product gas and operational conditions?

2. With the discussed advantages of Absorption Enhanced Reforming (AER) on the gasification process, What are its effects on the overall process, producing methanol and power from biomass gasification?

3. Could this model be used as a generic tool to compare the effect different choices in technology of these

identified blocks on the performance of the overall process? For example, comparing the choices of gasification parameters such as the choice of bed material, and the Gas Turbine system (Conventional GT vs IBC) on the overall process efficiency.

3

MODEL DEVELOPMENT AND VALIDATION

The main objective of this research is to create a model on Power and Methanol production from biomass gasification and then subsequently validating the developed model with data from literature. After the validation step, this research then focuses on optimising the model not just economically but in terms of energy consumed and wasted. chapter 2 provided a detailed background study for the different blocks of the model being developed. Aspen (Advanced System for Process ENgineering) Plus was used to develop this model and the simulation results were compared with literature to validate the model. Aspen Plus® is a very favourable simulation tool to develop a model comprising of different processes such as reactors, gas cleaning systems etc.. Its integration with FORTRAN also helps in implement different customised bounds which could make the model much more sturdy and compact. By incorporating calculation Methods for Vapour-Liquid Equilibrium such as NRTL, UNIFAC or many more, Aspen Plus® is quite accurate in predicting results. The model developed in this research also uses Cycle-Tempo to simulate the energy (steam) network and the Gas Turbine part of the model.

The model is split into different blocks, as shown in the schematic. A model for each of these blocks was first developed and the simulation results were validated with data from literature. This chapter discusses in detail on how these blocks were modeled and also on how a final model was developed by linking all these blocks. Some base assumptions were considered to simplify and develop this model, these are discussed in the next section. Following which, model development and validation are discussed.

3.0.1. TARGETS AND ASSUMPTIONS

In the first part of this thesis, some of the newer technologies of different blocks such as the Gasifier, Gas Cleaning Unit (GCU), Methanol Synthesis and Gas Turbine were discussed. Amongst the different options considered, the best, practically available options were chosen. The model developed was aimed at maximising the methanol yield and overall energy efficiency of the process. As an added motive, even though the economics of the overall process is not within the scope of this study, equipment size and wastage of streams such as the scrubbing liquid were aimed to be minimal.

Peng-Robinson Equation of state was used as the primary property methods throughout the model with a few exceptions. The reason behind the choice of Peng-Robinson equation of state (EOS) is its popularity in literature on gasifier modeling [84, 85]. Blocks such as the Gas Cleaning Unit where accuracy in VLE data are required, the activity Coefficient model, UNIQUAC was used. the property method used in each of these blocks are discussed later in this section. Unless explicitly specified, the property method used is Peng-Robinson.

- The process is assumed to have reached Steady-State of operation.
- Pressure drops in components are assumed to be zero unless mentioned upon.
- The rate expression, reaction order and kinetic expressions for different reactions were taken from literature. The experimental conditions of these kinetics and expressions are assumed to be compatible with the conditions modeled in this research.

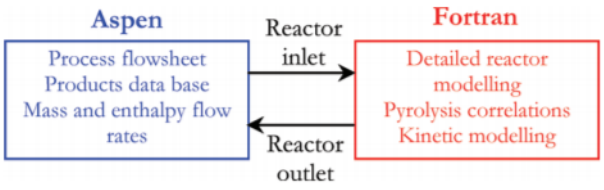

Figure 3.1: Principle of coupling Fortan calculator to the developed Aspen Plus® model

- Biomass is modeled in Aspen Plus® as a Non-Conventional solid and the enthalpy and specific heat calculated by Aspen Plus® are used for calculations.
- The biomass is assumed to be ash free. Similarly, the biomass is assumed to be free of Nitrogen, Sulfur and Chlorine.
- Tars are represented by 4 species, Benzene, Toluene, Phenol and Naphthalene.
- Char resulting from pyrolysis is simulated as pure Carbon (Graphite). Char was initially simulated as a non-conventional solid with varying composition depending upon the process conditions. However, since kinetic data on such an approach were scarce in literature, the accuracy produced by using char as a non conventional solid was very low. Simulation results of using char as a non conventional solid is shown in Appendix D

IMPORTANCE OF FORTRAN IN THE MODEL

None of the commercial and open source process simulation software such as Aspen Plus®, Hysys, ProII etc. have predefined models to simulate biomass gasification. Since gasification is a process that can be understood better as a group of functional sub-processes, gasification is usually not modelled as one block to reflect the functional differences between the different sub-processes. Although Aspen Plus® is capable of calculating energy and mass balances, specific customized balances and inputs can not be directly simulated easily. Aspen Plus® however has the flexibility to allow the incorporation of Fortran blocks which could be a better method to achieve these user defined balances.

There are two ways to insert a fortran subroutine in Aspen Plus®: to include an external fortran code by means of a dll file or to use inbuilt Fortran calculators within Aspen Plus®. For simpler applications, the calculator blocks within Aspen Plus® are much easier to use but these calculator blocks soon lose both stability and accuracy upon increasing complexity [84]. Therefore, for complex and highly re-iterative fortran computations (especially for convergence related Enthalpy balances), using an separate external fortran file is recommended. For the model developed in this study, a number of Fortran sub-routines have been used as calculator blocks which are discussed more in the following sections in this chapter. A simple schematic to understand how an Aspen Plus® Flow sheet works in tandem with a fortran calculator is shown in Figure 3.1.

3.1. MODEL DEVELOPMENT - CREATING THE FUNCTIONAL BLOCKS

3.1.1. BIOMASS GASIFICATION

BIOMASS FEEDSTOCK

A very wide variety of biomass resources can be used as feedstock for gasification. Conventional sources such as wood and unconventional sources such as agricultural and municipal wastes, organic sludge etc. are also considered as potential fuels. The significant difference in physical and chemical properties of biomass between different sources were also discussed briefly in Section 2.1 For this research, clean torrefied wood has been used as the biomass feedstock. Clean wood is shown to produce relatively clean syngas with a lower concentration of impurities, making the gasification process relatively simple [74]. However, it is highly expected that dedicated plantations and unconventional sources such as sludge and wastes would replace wood as primary sources of renewable biomass in the future [12].

Torrefied wood is a clean, renewable energy source which is more energy dense than wood and almost as dense as coal. Torrefied wood is produced by subjecting clean wood to a process called torrefaction. Torrefaction is a process of roasting wood or any biomass at high temperature to remove moisture and other

Table 3.1: Physical Properties of the Biomass used - Ultimate and Proximity Analysis

Ultimate Analysis	
Element	**Mass %**
Carbon (C)	48.08
Hydrogen (H)	6.22
Oxygen (O)	45.70

Proximate Analysis	
Constituent	**Mass %**
Fixed Carbon	16.2
Volatiles	83.8
Moisture Content	20%
Computed LHV	15.20 MJ/kg

low energy volatiles to produce a product which is energy dense and easier to transport. Torrefaction is usually done at a temperature between 230°C and 300°C in a oxygen low environment to prevent oxidation of fuel. The low volatiles produced during torrefaction are usually oxidized in the process to produce the energy required for torrefaction. The elemental composition of the torrefied wood used is shown in Table 3.1.

3.1.2. GASIFIER

The first and the most significant part of the model is the gasifier. In the previous chapter, section 2.2 discussed in detail different gasification technologies currently used and their corresponding strengths and challenges. Upon comparing literature on different gasification technologies currently available, this study focuses on designing a allothermal gasifier, similar in functionality to the ECN Milena and the gasifier at FICFB, Gussing mainly because of its reported higher hydrogen fraction in the final product gas. A brief literature study was then performed to better comprehend the practical performance of these two gasifiers (ECN Milena and the FICFB gasifier). Both ECN Milena and FICFB Gussing had operational pilot plants which recorded significantly increased Hydrogen yields compared to conventional autothermal gasifiers. However, experimental data from FICFB Gussing was more comprehensively available in literature than from ECN Milena's, and hence the gasifier was modeled to the comparable to the pilot plant of FICFB Gasifer at Gussing.

The gasifier block was modeled in Aspen Plus® with Peng-Robinson as the base property method. Although the gasifier in reality is just one reactor, it can be functionally decoupled into three functional parts: The pyrolysis zone, the heterogeneous reaction zone and the Free-board. Biomass and Hot bed material flow (in this case, inert quartz Sand) in near opposite directions, causing a distribution of temperature within the gasifier. The three zones and their corresponding temperatures are shown in Figure 3.2. The Aspen Plus® model developed for the gasifier is also decoupled corresponding to functionality to three different reactors, one fore each function. A Flowsheet of the developed Aspen Plus® model is shown in Figure 3.3.

This model was developed and simulated to understand the effect of using a catalytic bed material (discussed in section 2.2.3) on the total gasifier performance. Dolomite was chosen as the catalytic alternative to an inert quartz (silica) sand. A unique advantage of using using Dolomite instead of sand is that the Calcium Oxide (CaO) and Magnesium Oxide (MgO) in dolomite has an ability to chemically absorb Carbon Dioxide (CO_2) by sorption to produce their respective carbonates. The CO_2 can be recovered by heating the carbonates at high temperatures in the combustor. The application of dolomite as a catalytically active bed material is shown in Figure 2.9. This sorption property of dolomite and other ores were discussed in brief in Section 2.2.3. The composition of dolomite used in this study is given from the CaO to MgO molar ratio of **1.17**, obtained from Mostafavi et al. (2012) [86].

SCHEMATIC

Schematic of the Aspen Plus® model developed is shown in Figure 3.3. The stream Biomass is the fuel input to the gasifier and its composition is mentioned in Table 3.1. The stream Biomass is declared as *Non-Conventional solid* stream with proximate and ultimate analysis data entered as input into the Aspen Plus® model. However, the enthalpy and specific heat and the density are calculated by the ***HCOALGEN*** and ***DCOALIGT*** property methods of Aspen Plus®. The other inputs to the model are the air for the combustor and steam input for the gasifier. Input parameters of all the three input streams are shown in Table 3.2. Each reactor in the schematic has a particular function and they are discussed in better detail in the following sections.

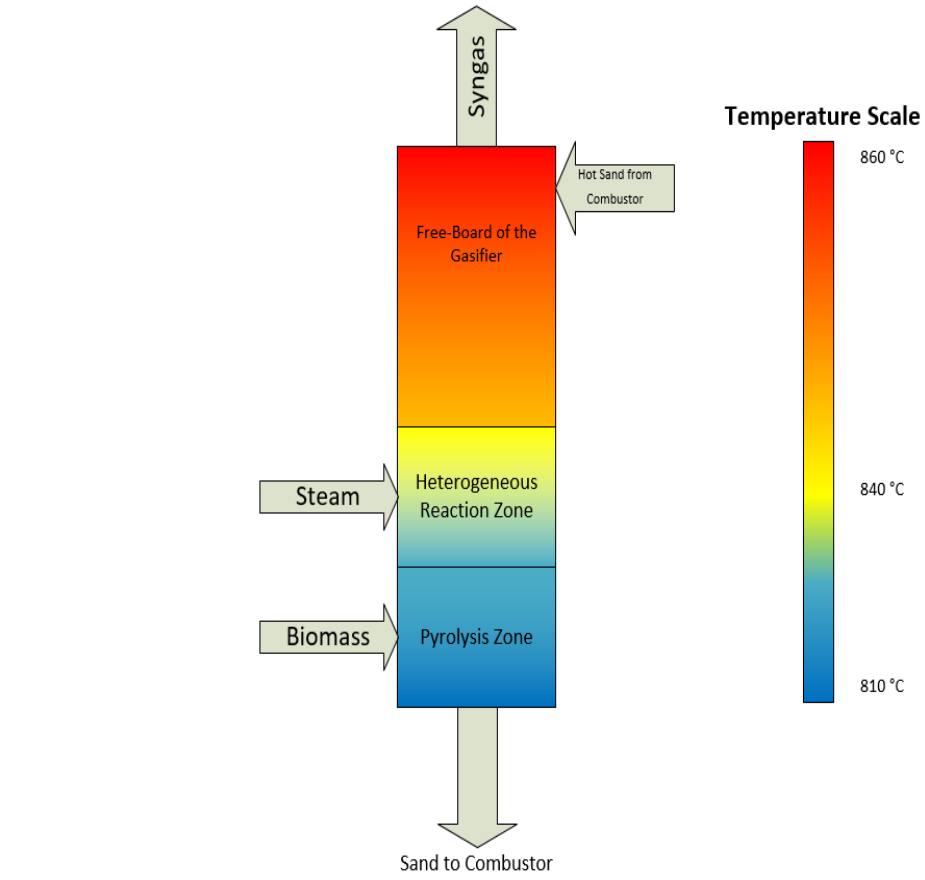

Figure 3.2: Temperature Profile and Different Zones formed within the Gasifier

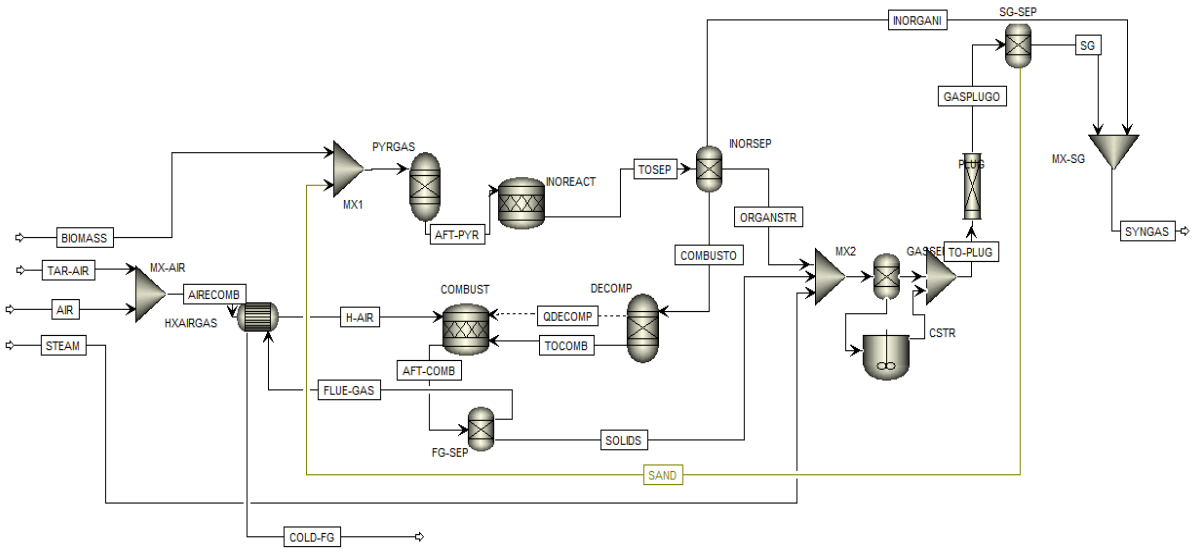

Figure 3.3: Schematic of the developed Aspen Plus® model of the Gasifier Block

Table 3.2: Main Input Parameters for the Gasifier block of the Aspen Plus® Model

Input Parameter	Input	Ref.
Inlet Temperature, Pressure of Biomass	25°C and 1 atm	
Composition of Biomass used	Table 3.1	[84]
Moisture Content of Biomass used	20%	[84]
Bed Material Flow Rate (kg/s)	37	[58]
Steam To Biomass Ratio (mass basis)	0.5	
Steam Pressure inlet	1.5 Bar	
Gasification Pressure	1 atm	
Gasification Temperature	860°C	

PYROLYSIS

Biomass is fed into the gasifier from the bottom, and forms a zone of pyrolysis at the bottom of the Gasifier. This pyrolysis zone is simulated by using an RYield reactor block in the Aspen Plus® model. An Ryield block is used when the the mass yield or molar yield of the products of the reactants are exactly known. The model uses empirical correlations for mass yields as a function of the gasifier temperature, based on results found in literature. Dufour et al performed experiments to determine the mass yield resulting from wood pyrolysis in a tubular reactor at temperatures in the range of 700°C - 1000°C [87]. Although the gasifier considered in this study is not tubular, assuming a uniform temperature of the bed material within the gasifier is a reasonable assumption, especially when considering the significantly large mass flow of bed material when compared to the biomass flow rate (Table 3.2). L. Abdelouahed et al quantified the results of Dufour et al into an empirical correlation with the bed material temperature as the only variable [84, 87]. Mass yields used in this study based on the empirical correlations developed by L. Abdelouahed et al. are shown in Table 3.3.

Char mass yield was then calculated to achieve mass and mole balance based on the mass yields of the other pyrolysis products. However, the first step simplifying the gasifier part was to assume the char produced is pure carbon (Graphite). Hence the mole balance was closed by releasing the calculated hydrogen and oxygen fraction of char. Calculated mass flows of different pyrolysis products are shown in Appendix C. These mass yields are calculated in a FORTRAN calculator block within Aspen Plus®. This FORTRAN code uses the temperature of bed material from Aspen Plus® and calculates the mass yield which is then returned to the Aspen Plus® model. Since the empirical data is based on experiments performed in the temperature range of 700°C and 1000°C, this pyrolysis block is modeled to operate only within this range.

The pyrolysis products, syngas and char, then enter a stoichiometric Reactor (RSTOIC reactor in Aspen Plus®) INOREACT where all the fuel bound nitrogen (N_2), sulfur (S) and chlorine (Cl_2) are converted into NH_3, H_2S and HCl respectively. The produced NH_3, H_2S and HCl are then separated from the main stream in the Separator block (SEP Block in Aspen Plus®) INORSEP, and then later added back to the gasifier outlet stream. This separation is based on the assumption that the produced NH_3,H_2S and HCl are inert and do not contribute to any of the other gasification reactions. The reactor INOREACT is adiabatic, the heat of the reactions discussed above is absorbed by the stream, which relates to an actual gasifier operation.

HETEROGENEOUS REACTION ZONE

The Aspen Plus® CSTR reactor, RCSTR (in Figure 3.3) with no heat loss is used to simulate the the heterogeneous reactions of gasification such as, the char gasification and the Boudouard Reaction. A Continuously stirred tank reactor (CSTR) is used to model this heterogenous phase reactions because this study assumes that the solids, char and bed material are uniformly mixed and this is practically achieved in a CSTR. All the gasification reactions shown in section section 2.2 are modeled kinetically in the the two gasification reactors, the RCSTR block (CSTR in Figure 3.3) and the RPLUG (PLUG in Figure 3.3) reactors. The CSTR reactor performs the char gasification and the other solid-vapor reactions (heterogenous phase reactions). Kinetics of the reactions used are shown in Section B.1 of Appendix B. Aspen Plus® requires either the reactor volume or the residence time within the reactor to be specified. Reactor dimensions of the pilot FICFB Gasifier at Gussing could be found from literature and this data is shown in Table 3.4 [59]. Heterogeneous reaction zone

Table 3.3: Pyrolysis correlations used in the Gasifier model. Empirical correlations for mass yield as a function of bed material temperature were developed by [84]. Mass Yields are in the format $Y_i = aT^2 + bT + c$ with T (temperature of bed material) in Kelvin.

Product	**a**	**b**	**c**
CH_4	-4.341×10^{-5}	10.12×10^{-2}	-51.08
H_2	1.362×10^{-5}	-2.517×10^{-2}	12.19
CO	-3.524×10^{-5}	9.770×10^{-2}	-24.93
CO_2	3.958×10^{-5}	-9.126×10^{-2}	64.02
C_2H_4	-6.873×10^{-5}	14.94×10^{-2}	-76.89
C_2H_6	8.265×10^{-6}	-2.105×10^{-2}	13.38
C_6H_6	-3.134×10^{-5}	7.544×10^{-2}	-42.72
C_7H_8	-4.539×10^{-6}	0.687×10^{-2}	1.462
C_6H_6O	1.508×10^{-5}	-3.662×10^{-2}	22.19
$C_{10}H_8$	-8.548×10^{-6}	1.882×10^{-2}	-9.851
H_2O	5.157×10^{-5}	-11.86×10^{-2}	84.91

Table 3.4: FICFB Pilot Gasifier physical data [59]

Thermal Output	100 kW
Fuel Used	Wood Pellets and Wood Chips
Reactor Diameter	300mm
Riser Diameter	100mm
Riser Height	4250mm

is assumed to be one third of the total volume and this is used as the CSTR Reactor Volume. This assumption is based on the observed volumetric flow rate of the solids (char and bed material) from the Pyrolysis reactor in the Aspen Plus® model, which is roughly one third of the pilot plant reactor volume. Since the RCSTR module of Aspen plus® requires either the reactor volume or the residence time within the reactor to compute and also since this heterogeneous reactor represents the dense part of the gasifier above the pyrolysis part of the gasifier, the reactor volume corresponding to the mass flow of rate of the solids from the pyrolysis was chosen (Approximately one third of the reactor volume).

FREE-BOARD OF THE GASIFIER

The free-board of the gasifier as shown in the Figure 3.2 has the highest temperature within the gasifier. In reality, hot bed material from the combustor falls into the gasifier from the top while gases and entrained char move upwards from the bottom. However, the heat consumed within the gasifier is much less when compared with the other two parts of the gasifier primarily because of relatively higher volumetric flow than the other parts of the gasifier. For this reason, it is assumed in the developed Aspen Plus® model that the inlet temperature of the CSTR and the free-board (PLUG) are nearly the same. The Free-board is modeled in the model with an adiabatic RPLUG reactor with no heat loss named PLUG. A plug flow reactor would imply a uniform radial temperature profile within the plug which is practically relatable for high bed material flow rates.

Gas Phase reactions mentioned in Table 2.1 are modeled in this reactor. Kinetics provided as input for this reactor is shown in section B.1 of Appendix B. Both the PLUG and the CSTR are modeled to be adiabatic; in other words, the energy required for the gasification reactions is provided by the hot bed material flowing from the combustor. The output of the free-board (PLUG) is a product gas-bed material mixture which the separator block SG-SEP splits into gas and solid bed material streams.

COMBUSTOR

In an allothermal reactor, the combustion and gasification processes are separated physically and the heat required for gasification is usually provided by the bed material moving between the combustor and the gasifier. In the considered case of FICFB, char and some recycled tars from a downstream gas cleaning unit are combusted in a separate combustor along with a chemically inert bed material, increasing the temperature of the bed material leaving the combustor.

In the Aspen Plus® model, the combustor is simulated by a stoichiometric Reactor (RSTOIC reactor in Aspen Plus®) named COMBUST, which is an adiabatic reactor. When char is declared as an Non-Conventional stream rather than a pure carbon stream (as discussed in the pyrolysis part of Section 3.1.2), the RYIELD reactor DECOMP decomposes the produced char into elemental C, H and O. This decomposition simplifies the combustion simulation, enabling Aspen Plus® to use its inbuilt combustion reactions. The heat of this decomposition process is given as input to the combustor, hence this combination of decomposition and combustion would reflect a practical combustor operation. The RSTOIC reactor module in Aspen Plus® is capable of using an array of auto-generated combustion reactions for different input reactants. The heat of reaction and stoichiometry is calculated by the program and the temperature of this combustor unit is maintained such that the gasifier achieves a temperature of 860°C. A recuperator HXAIRGAS is used to preheat the combustion air to the combustor by recovering heat from the flue gas of the combustor. A typical Shell and Tube heat exchanger was used to simulate this recuperator. Bed material and flue gas are then separated in the separator block FG-SEP. The hot bed material is then sent to the gasifier and the flue gas to the recuperator.

3.1.3. POST-PROCESSING OF SYNGAS

Syngas produced from a allothermal gasifier such as the ECN Milena or the FICFB Gasifier at Gussing has a higher hydrogen fraction than most other gasifier technologies. However, post processing of this produced syngas is often governed by the downstream application for which this syngas is produced. Since methanol production is one of the key objectives of this model, the syngas composition and quality needs to be primarily tailored for the requirements of methanol synthesis. In section 2.4.1, and Table 2.4, the stoichiometric feed ratio and the minimum quality of syngas in terms of tars and other contaminants were discussed. Two key post processing steps modeled in this study are the Water Gas Shift reactor and the Gas Cleaning Unit. This study focuses on using a oil absorption system for gas cleaning, similar to the OLGA gas cleaning concept,

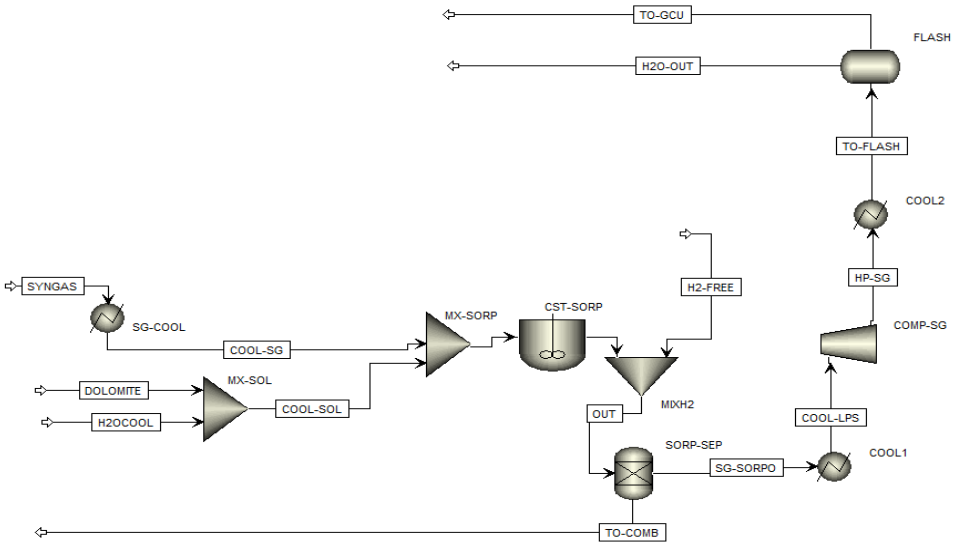

Figure 3.4: Schematic of the developed Aspen Plus® model of the Water Gas Shift Block

discussed in section 2.3.2. Water gas shift reactor is modeled to work at a maximum temperature of 450°C with dolomite as the catalyst. The 450°C temperature limit is from the use of commercial water gas shift catalysts. Although dolomite promotes the water gas shift in a different mechanism (by removing CO_2) than these commercial catalysts, the inlet temperature of this reactor is fixed at 450°C to promote easy comparison between the two practices.

WATER GAS SHIFT REACTOR

The main objective of this water gas shift reactor is to increase the hydrogen fraction in the syngas to achieve a stoichiometric ratio, mentioned in Equation 2.6, close to 2.05. The water gas shift reaction mentioned in Equation B.2 is the primary equation to achieve higher hydrogen mole flow in the product gas. Typical inlet temperatures for commercially used water gas shift reactors are between 450°C - 500°C to limit catalyst sintering and deactivation. Hence in the developed Aspen Plus® Model, a Heat Exchanger HXAIR is used to reduce the temperature of the syngas to the required water gas shift temperature.

Water Gas Shift reactor in reality is catalysed by commercial metallic oxide catalysts. However, in this study, dolomite is used to promote the water gas shift reaction by removing CO_2 in-situ to promote hydrogen production. Although slightly different from Absorption Enhanced Reforming (AER) in terms of purpose, the logic and working remain the same. In Equation B.2, the production of hydrogen can be increased by adding more H_2O or/and removing CO_2 from the syngas mixture in accordance with Le Chatelier's principle. With the CO_2 sorption ability of Dolomite, Dolomite can in theory be capable of promoting Water Gas Shift to produce more H_2 [88]. As an added advantage, since dolomite can be used as bed materials in the gasifier, using dolomite for the Water Gas Shift eliminates the need for an added inventory of catalysts. Hence for the developed Aspen Plus® model, dolomite is used as the bed material for both the gasifier and the water gas shift reactor. Simulations were performed to validate the sorption capability of dolomite with experimental results and its effect on gasification with results obtained from literature. This comparison is discussed later in Section 3.2.1

The Water Gas Shift reactor used in the Aspen Plus® model is an adiabatic RCSTR reactor named CST-SORP. A CSTR reactor was used reflecting the assumption of a well mixed bed within the reactor. This reactor is also modeled kinetically with the reactions and their corresponding kinetics mentioned in Section B.1 of Appendix B. The residence time of the reactor is varied to achieve the stoichiometric ratio mentioned in Equation 2.6. The outlet syngas is then cooled to the required temperature for the Gas Cleaning unit. The bed material from the Water Gas Shift reactor is recycled back to the combustor.

GAS CLEANING UNIT

An Oil Scrubbing system is used for Gas Cleaning, similar to the OLGA concept of ECN (Section 2.3.2) in the developed Aspen Plus® model. The simplest scrubbing liquid that can be used is water, which simultaneously cools and removes the tar species from the produced syngas. However, water scrubbing systems produce a significant quantity of waster water streams which require downstream treatment, thereby shifting complexity from tar removal to waste-water treatment [85]. Also, since most of the tar species are hydrophobic, absorption rates are quite low, requiring larger equipment. Hence a better alternative is to use Bio-diesel based solvents as scrubbing liquids. Nicolaou [22] had simulated Oil scrubbing different scrubbing liquids such as diesel, vegetable oil and Bio-Diesel and had concluded Bio-Diesel and vegetable oil to be a very attractive and efficient scrubbing liquid for Gas Cleaning.

The Gas Cleaning unit modeled in this study is very similar to the OLGA concept with the only difference being pressurized operation. The OLGA Gas cleaning unit is designed to be operated at ambient atmospheric pressures. The advantages of using a pressurized column for absorption was already discussed in section 2.3.2. The syngas from the gasifier is cooled to a temperature just above its tar dew-point. The tar dew-point is the temperature at which the tars in the syngas condense. Condensing tars can create significant problems by corroding and depositing on the walls of downstream equipment and hence have to be avoided. The cooled syngas is then compressed to the Gas Cleaning pressure. Temperature increase due to this compression is then removed by another Heat Exchanger such that none of the tars condense. Due to the significant fraction of water in the syngas, compressing the syngas would cause a stream of free-water. This condensed water has a fraction of tars dissolved (Mainly Naphthalene and Phenol, while Toluene and Benzene remain). This condensed water fraction is then removed in a flash separator before entering the Gas Cleaning Unit.

The Gas Cleaning Unit is an oil scrubbing unit with Bio-Diesel as the scrubbing liquid. The composition of Bio-diesel used is followed from the work of [85]; Biodiesel is considered to be a methyl ester of Vegetable oil and is represented in [85] as a mixture of Methyl Oleate, Methyl Palmitate and Methyl Stearate with a mass fraction of 74, 14 and 12, respectively. The Liquid-Liquid Equilibrium data is another key input required for the GCU simulation. Major consensus in the studied literature recommend the use of Non-Random Two-Liquid (NRTL) model regressed with experimental results for a particular syngas and scrubbing liquid composition [85, 89]. They also conclude that both NRTL and Universal QuasiChemical (UNIQUAC) model work reasonably well. For the purpose of this study, UNIQUAC is chosen as the property method for the gas Cleaning unit and the missing binary interaction parameters were estimated using the UNIFAC method.

SCHEMATIC

The absorption and stripping column of the Gas Cleaning Unit are simulated as two adiabatic RADFRAC columns in the Aspen Plus® model. RADFRAC is a rigorous mixing and distillation module of Aspen Plus® commonly used to simulate separation columns. The Columns COLLECTO and STRIPPER represent the Absorber and Stripper columns in the Gas Cleaning Unit, as shown in Figure 3.5. Bio-diesel is recycled between the two columns and a separate Bio-diesel input stream named OIL-MAKE is added to the recycle stream to compensate the oil loss. The Absorber is operated at 80°C and 20 bar pressure while the stripper is operated at 200°C and atmospheric Pressure. Cooled pressurized syngas is supplied at the bottom stage of the Absorber and Bio-Diesel is supplied at the top. The Number of stages of the Absorber are varied to achieve a tar concentration of less than 0.1 mg/Nm^3. The Stripper works with air as the stripping agent. Air has to be heated to stripper temperature and this is done in a Heat Exchanger extracting heat from the product gas stream from the gasifier outlet. Stripper Temperature chosen has to be lower than the boiling temperature of the scrubbing oil used, to avoid significant oil losses.

Heat Exchanger HX-GC is used to integrate the heating and cooling of the bio-diesel stream from the Absorber and Stripper, respectively. A heater and Cooler OIL-HEAT and OIL-COOL are used to heat the scrubbing liquid to the required Absorber and Stripper temperatures. Using such a interconnected Heat Exchanger between the two streams aids in reducing the net energy demand for gas cleaning. The cleaned syngas stream GAS-C-OU is then directed to the required downstream process. Hot air from the stripper on the other hand has a significant fraction of tars which makes the stream calorifically attractive. This chemical energy in the tar - air stream can be recovered in the gas turbine or in the combustor of the gasifier to reduce the amount of char combusted. This stream is hence partly recycled back to the combustor of the Gasifier. The rest of this

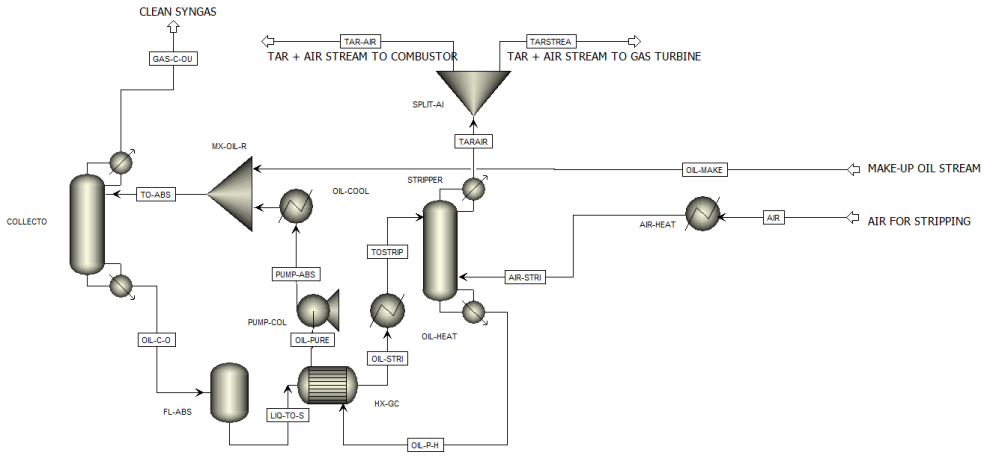

Figure 3.5: Schematic of the developed Aspen Plus® model of the Gas Cleaning Unit Block

stream is combusted in the Gas Turbine to produce mechanical work. The recycled nature of the Gas Cleaning Unit makes convergence slightly complicated and increases the significance of proper input specification.

Sensitivity tests were performed to understand the influence of different operational parameters on the gas cleaning process. By varying the Bio-Diesel flow rate, Absorber pressure, and other operating parameters, several sensitivity tests were performed and the results of these tests can be found in the Section 3.2.2.

3.1.4. METHANOL SYNTHESIS

A brief background on the methanol synthesis process was discussed in section 2.4.1. The Lurgi process model developed by Lei Chen et. al is used for developing this methanol synthesis part of this thesis. The process developed by Lei Chen is a standard Lurgi process for methanol synthesis based on a commercial methanol production facility [71].

In the developed Aspen Plus® model, the core of the methanol synthesis is the RPLUG reactor 'METHANOL' which is kinetically modeled. Considering Carbon Dioxide (CO_2) as the main methanol producing species, the two reactions used are Equation B.1 and Equation B.2 as discussed in Section 2.4.1. The Kinetics used in this reactor were developed by K. M. V. Bussche, G. F. Froment and are shown in Section B.3 of Appendix B [90]. The reactor temperature within METHANOL is adjusted by a counter-current flow of boiling water from a high pressure drum. This high pressure drum is modeled as a flash separator named H2O-FLAS in the Aspen Plus® Model. The main thinking behind using a water cooled reactor is that by supplying hot boiling water and using the heat of synthesis to completely boil the supplied water, the reactor can be made nearly isothermal. The temperature of the Methanol Reactor and thereby the synthesis temperature is therefore fixed by choosing a suitable steam pressure which inturn fixes the saturation temperature of water.

Since the single pass efficiency of methanol synthesis is proven to be quite low (Section 2.4.1), a fraction of the outlet vapor stream is recycled back to the methanol reactor. Since the scale of operation considered by Lei Chen was much higher than the syngas flow modeled in this study, the kinetics were first validated for the similar reported conditions [71]. The reactor dimensions used by Lei Chen also reflect the industrial reactor dimensions. However, the catalyst details are taken to be the same as from Lei Chen [71]. Upon validation of the kinetics, the dimensions of the methanol reactor were scaled down to match the syngas flow from the GCU of the developed Aspen Plus® Model.

SCHEMATIC

The schematic of the Methanol synthesis block developed is shown in Figure 3.6. Cleaned syngas from the Gas Cleaning unit is cooled down to near ambient temperature and then compressed to the required synthesis pressure. The syngas inlet conditions for the methanol synthesis process is fixed as 234°C and 60 Bar [71]. The compressed syngas is then cooled to the required synthesis temperature in the Heat Exchanger COOLMET and then sent to the reactor METHANOL. As explained before, the Flash Drum H2O-FLAS supplies hot

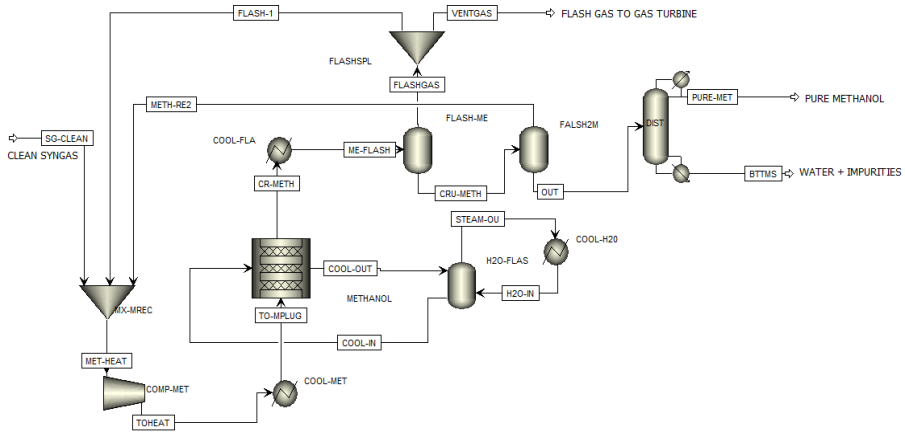

Figure 3.6: Schematic of the developed Aspen Plus® model of the Methanol Synthesis Block

boiling water for the METHANOL reactor. The Flash drum pressure is chosen as 29 bar to achieve a saturation temperature of 232°C. The heat of methanol synthesis is then used to boil the water supplied and the produced steam is then cooled to boiling water through the heat exchanger COOL-H2O. Outlet process gas from the Methanol reactor now consists of a small fraction of methanol and a major fraction of unconverted syngas. This outlet process stream is then cooled to 40°C in the heat exchanger COOL-FLA. Methanol and a fraction of water condense from this stream and are extracted from two flash drums, one at 60 Bar and the other at atmospheric pressure. The Flash gas produced from this expansion process is then partly recycled via the stream FLASH-1 back into the reactor.

Although the Lurgi process is a very conventional process for methanol synthesis, its operational parameters depend significantly on the syngas properties supplied. To choose the ideal operating conditions for synthesis, the effect of these parameters has to be studied more. Different sensitivity analysis were performed to optimize this block and will be discussed later in the subsection 3.2.3. Some of the parameters studied were the inlet temperature and pressure of the syngas, steam drum pressure, reactor dimensions and the recycle ratio.

3.1.5. GAS TURBINE

Both biomass gasification and Methanol Synthesis produce a number of streams which contain significant chemical energy which can be very attractive to produce power though a Gas Turbine System. One of the key objectives of this study is to investigate the integration of a Gas Turbine system into a methanol synthesis process. To achieve this objective, numerous systems were designed by varying the position of the Gas Turbine system and these cases were simulated to evaluate the most optimum case for this integration.The first step done in this direction was to model a Gas Turbine system. A typical Gas Turbine system consists of a Compressor (fuel and Air), Turbine, a Combustion Chamber and if required, a recuperator. Both Aspen Plus® and Cycle-Tempo were used to model this Gas Turbine block.

As discussed previously in Section 2.5, two different arrangements can be used to extract power, A conventional gas Turbine system and an Inverted Gas Turbine system (IGT) (Section 2.5.3). Although physically very different in operation, the IGT is just a 're-arranged' GT system. A schematic of both a conventional and Inverted Gas Turbine system developed is shown in Figure 3.7. Compressors, COMP-AIR and COMP-GT are used to compress air and fuel respectively to the required pressure. A stoichiometric reactor RSTOIC module named GT-COMB is used as the combustion chamber. This GT-COMB is an adiabatic reactor which generates its own combustion reactions. Air mass flow in stream AIR-GT is altered to achieve a turbine Inlet (Exit from the combustion chamber) Temperature of 1000°C. The high temperature flue gas produced from GT-COMB is then expanded in a turbine (TURBINE in the schematic) back to atmospheric pressure. The turbine exit flue gas is still at a considerably high temperature and hence can be used to pre-heat compressed air through a recuperator HX-RECUP. Isentropic efficiency of the turbine and compressor are mainly determined by the size of the Gas turbine and hence are assumed to vary between different cases developed.

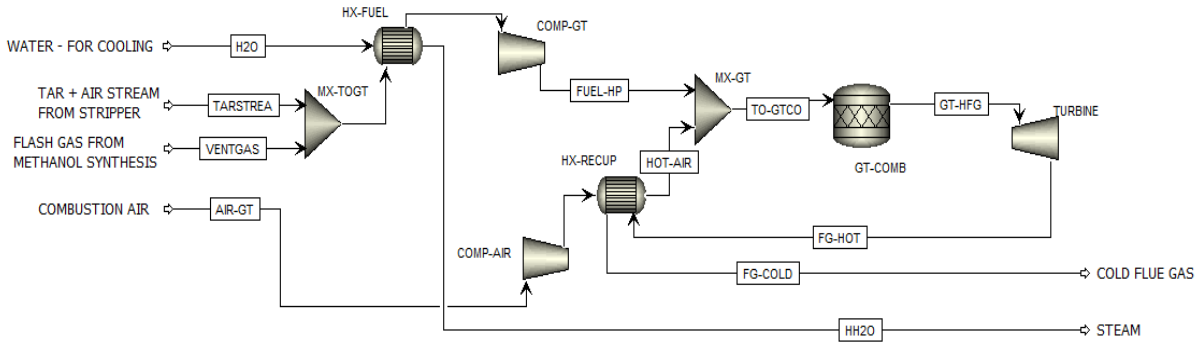

Figure 3.7: Schematic of the developed Aspen Plus® model of the Gas Turbine Block

3.2. UNDERSTANDING AND VALIDATING THE MODEL

Section 3.1 discussed on decoupling the complete model into a number of functional sub-blocks and how these blocks were modeled in Aspen Plus®. The next subsequent step is to validate these blocks by comparing the simulation results with experimental data found in literature. This validation step is discussed in this section.

3.2.1. GASIFIER

The key functional block identified during the course of this study is the Gasifier, mainly because the choice of parameters used in the gasifier defines the quality and composition of the syngas used for both methanol and power production. In the section 3.1.2, the development of the gasifier model was discussed to be based on data from the FICFB gasification process at Gussing. With physical reactor dimensions obtained from the FICFB pilot plant [57–59], the results from the simulated Aspen Plus® model were compared with the actual experimental data from the same pilot plant.

To better understand the results obtained from literature, the variables compared are first identified. The most obvious comparison is the composition of the syngas predicted by the model and the results from the pilot plant. This is obtained by fixing a Gasification temperature (at 860°C) and plotting the syngas composition as a function of the Steam To Biomass Ratio (STBR). The term STBR is defined as shown in Equation 3.1. Increasing the STBR within the Gasifier has a positive effect on hydrogen flow in the syngas at the expense of reduced CO composition. In the developed Aspen Plus® model, this gasification temperature is fixed at 860°C by varying the recycle fraction of the tar stream from the GCU and the heat of gasification is supplied by combustion of a part of char produced from pyrolysis and a part of the tar recycle stream obtained from the Gas Cleaning Unit. Since there are a number of recycle loops spanning between different blocks, convergence of such a model is quite tedious and hence the gasification temperature was maintained between 855°C and 870°C.

$$Steam\ to\ Biomass\ Ratio = \frac{Steam\ Mass\ flow + Fuel\ Moisture\ Mass\ Flow}{Dry,\ Ash\ free\ Fuel\ Feed\ Flow} \tag{3.1}$$

$$Water\ Conversion\ (\%) = \frac{Sum\ Water\ Input\ [kg/hr] - Sum\ Water\ Output\ [kg/hr]}{Sum\ Water\ Input\ [kg/hr]} \tag{3.2}$$

Since the complete gasification process was modeled kinetically, the choice of gasification reactions and their corresponding kinetics have a very definitive impact on the product gas composition obtained. Two sets of kinetics were studied and simulated in the Aspen Plus® model. The two sets of kinetics can be found

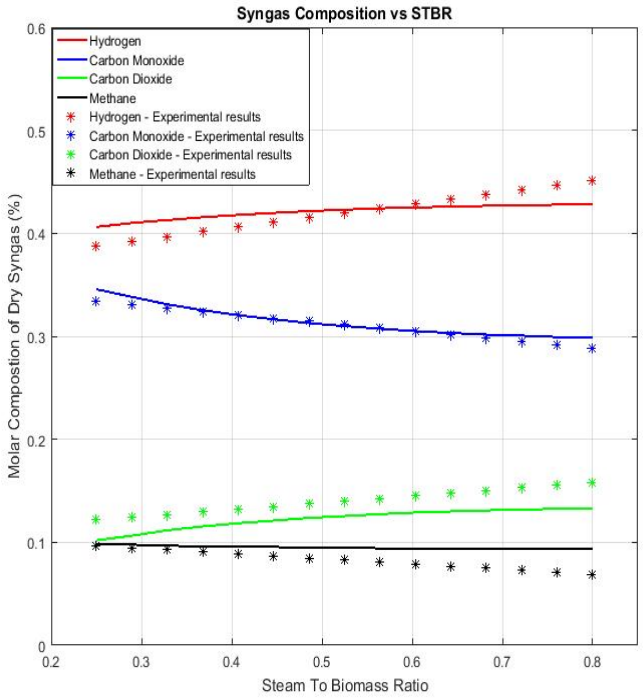

Figure 3.8: Comparison between developed Aspen Plus® Model results and Pilot plant experimental results: Syngas composition vs STBR for Kinetics **set 1** at a gasification temperature of 860°C[59]

in Section B.1 in Appendix B. The results of both the simulations can in Figure 3.8 and Figure 3.9. By varying the STBR from 0.25 to 0.8, Kinetics set 2 can be observed to over predict Methane steam reforming and thereby resulting to a increased hydrogen and Carbon-Monoxide fraction in the final product gas. Kinetics set 1, however predicts the composition of the final product gas very close to experimental data reported in [58, 59]. Although both the sets of kinetics predict the trend between the product gas composition and STBR, kinetics mentioned in tables B.2 and B.3 in Appendix B is chosen to model the gasifier.

The next sampled variable is water conversion. Water conversion is simply put, a measure of steam content used within the gasifier by the gasification reactions. To be more precise, water conversion is calculated as shown in Equation 3.2. Two plots shown in Figure 3.10a and Figure 3.10b compare the predicted amount of water consumed within the gasifier and the actual consumption found in literature [59].

The Concentration of tars in the product gas is a key factor in choosing and designing downstream processes. One of the main advantages of the FICFB gasifier is reduced tars due to the relatively higher gasification temperatures used (Table 2.2). Another minimal factor leading to reduced tar concentration is that by avoiding a significant Nitrogen dilution, the steam concentration inside the gasifier is more than conventional gasifiers and thereby driving the steam reforming reactions. The pilot plant of FICFB was tested to determine the effect of the STBR on tar concentration of the final product gas produced at a particular gasification temperature [59]. Results of this test are shown in Figure 3.11. The developed Aspen Plus® model was simulated in similar fashion, at a fixed gasification temperature of 860°C. The results obtained from both the Aspen Plus® model and literature from FICFB gasifer are plotted in Figure 3.12. Since the experimental data available from [59] is available only until a STBR of 0.5, the trendline shown in Figure 3.11 was extrapolated to a simulated STBR of 0.8.

The kinetics of set 1 although quite accurate in predicting the composition of the four major product gas constituents - H_2, CO , CO_2 and CH_4, is observed to be less accurate in predicting the tar concentration in the product gas at lower values of STBR. However, above a STBR of 0.5, the results from the Aspen Plus® Model

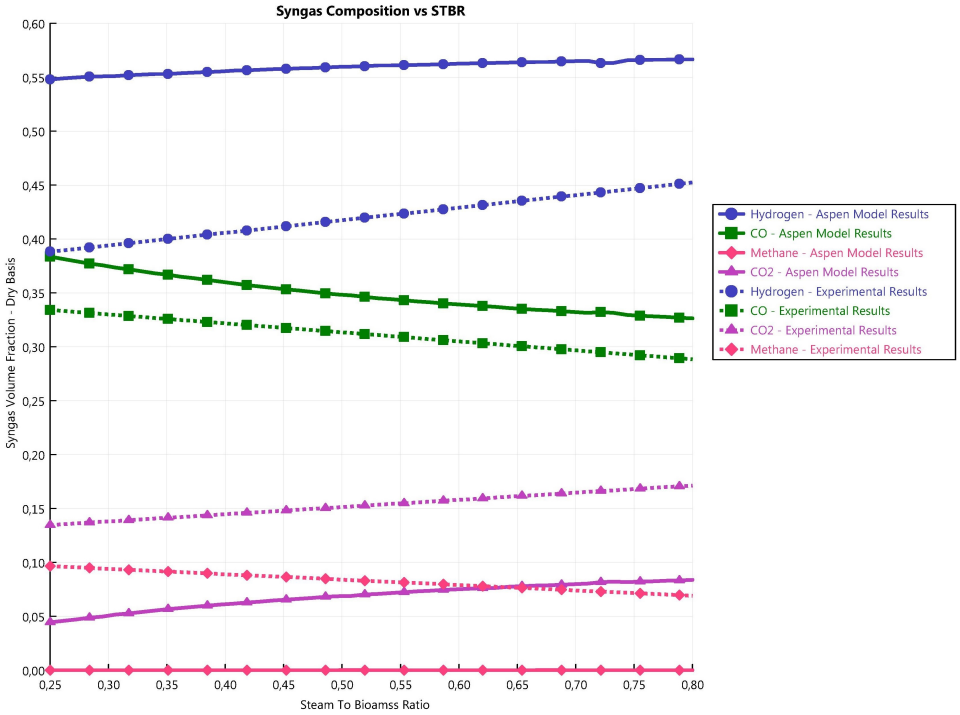

Figure 3.9: Comparison between developed Aspen Plus® Model results and Pilot plant experimental results: Syngas composition vs STBR for Kinetics **set 2** at a gasification temperature of 860°C [59]

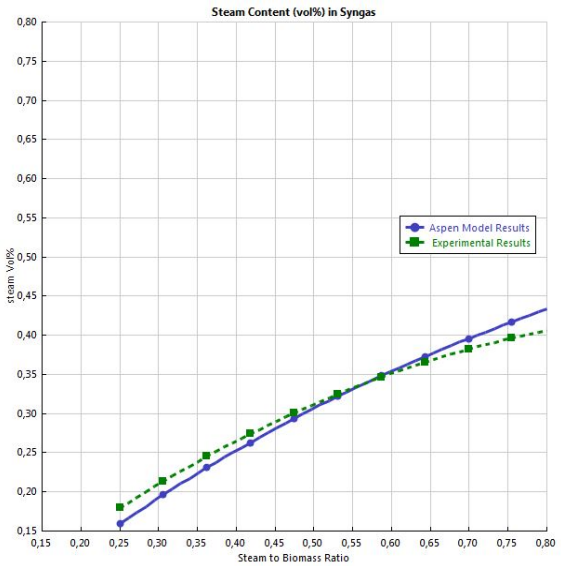

(a) Comparison between developed Aspen Plus® Model results and Pilot plant experimental results: Steam Content in the produced Syngas vs STBR at a gasification temperature of 860°C [59]

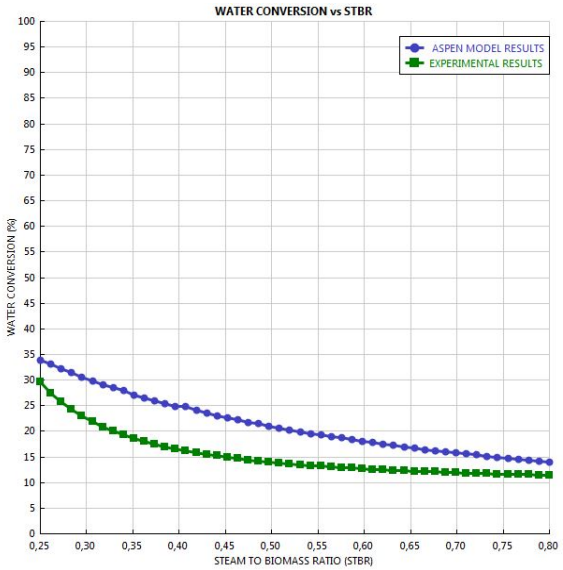

(b) Comparison between developed Aspen Plus® Model results and Pilot plant experimental results: Water Conversion (%) vs STBR at a gasification temperature of 860°C [59]

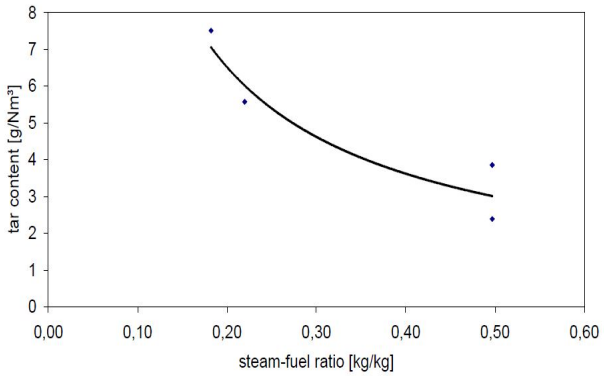

Figure 3.11: Tar Concentration vs STBR at a gasification temperature of 860°C - Experimental Results from FICFB [59]

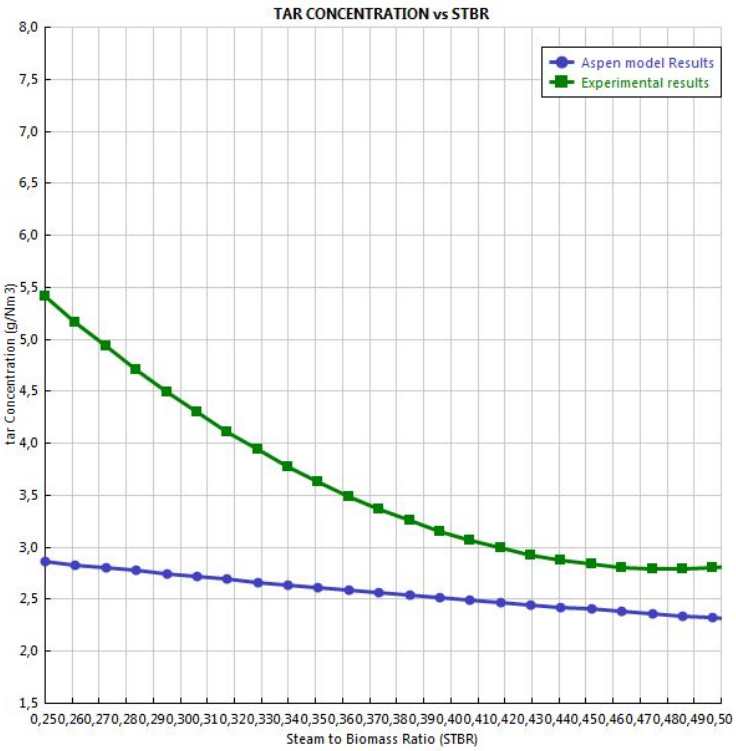

Figure 3.12: Comparison between developed Aspen Plus® Model results and Pilot plant experimental results: Tar Concentration (%) vs STBR at a gasification temperature of 860°C [59]

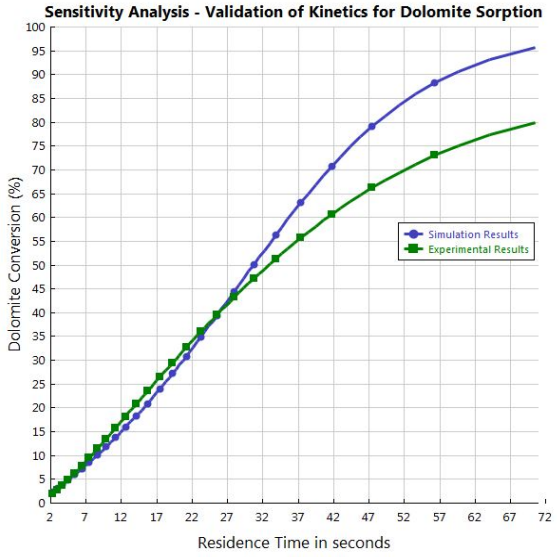

(a) Comparison between developed Aspen Plus® Model results with Kinetics from sun et al. [91] and experimental data from literature [86]

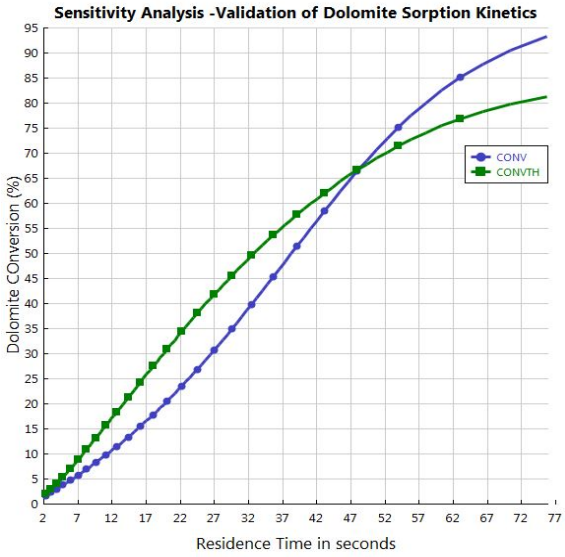

(b) Comparison between developed Aspen Plus® Model results with Kinetics from Mostafavi et al. [86] and experimental data from literature

Figure 3.13: Validation of Dolomite Sorption Kinetics: Sensitivity Analysis Results

appear to be converging with experimental results (Figure 3.12). Since this study considers a STBR of close to 0.5 and that tars are removed in a downstream gas cleaning unit, kinetics set 1 showed in Section B.1 in Appendix B is chosen to be satisfactory.

DOLOMITE

The Gasifier modeled and simulated in the previous section was with silica sand (quartz sand) as the bed material. Silica sand had only one function of distributing and transporting heat from the combustor to the gasifier uniformly. However, the advantages of using a catalytic bed material was discussed in the previous chapter (Section 2.2.3). In this step, Dolomite was used as a catalytic bed material in the place of sand to simulate an Absorption Enhanced Reforming (AER) concept, previously discussed in Section 2.2.5. To simplify this simulation, this study assumes that the sorption reaction of CO_2 is the only chemical reaction in which the dolomite takes part in. As discussed in Section 3.1.2, the composition of dolomite used in this study is given from the CaO to MgO molar ratio of **1.17**. Kinetics from Ehsan Mostafavi et al were used to simulate this sorption reaction within the gasifer [86]. The kinetics used is shown in Table B.7 in Appendix B. The kinetics were first validated by comparing the simulated results with experiments found in literature. Since Dolomite is a naturally occurring ore, its physical and chemical properties vary significantly with location and other related factors. Since experiments on in-situ CO_2 removal within a gasifier is very scarce, the kinetics used were first validated with a different experimental setup. A stoichiometric mixture of CO_2 and Dolomite were introduced into a RPLUG reactor and the sorption results of the model and the experiments were compared.

$$CaO\ \ Conversion = \frac{Moles\ of\ CaO\ reacted}{Total\ Moles\ of\ CaO\ in\ the\ inlet\ stream} \tag{3.3}$$

By fixing the temperature of the PLUG reactor at 675°C, the sorption efficiency was plotted against the residence time of the reactor. Both the kinetics (specified in Table B.7 in Appendix B) were plotted against the experimental results, as shown in figures Figure 3.13a and Figure 3.13b.It can be observed that kinetics by sun et al. [91] has a better agreement with experimental results for shorter residence times. Since the water gas shift reactor and the gasifier operate at very short residence times (less than 15 seconds), the kinetics proposed by sun et al. show more accuracy for this model. The next step would be to simulate this sorption capability of dolomite in the gasifier model developed. It was already discussed in Section 2.2.5 that the gasification temperature must be maintained below 750°C. Hence a second simulation was performed with

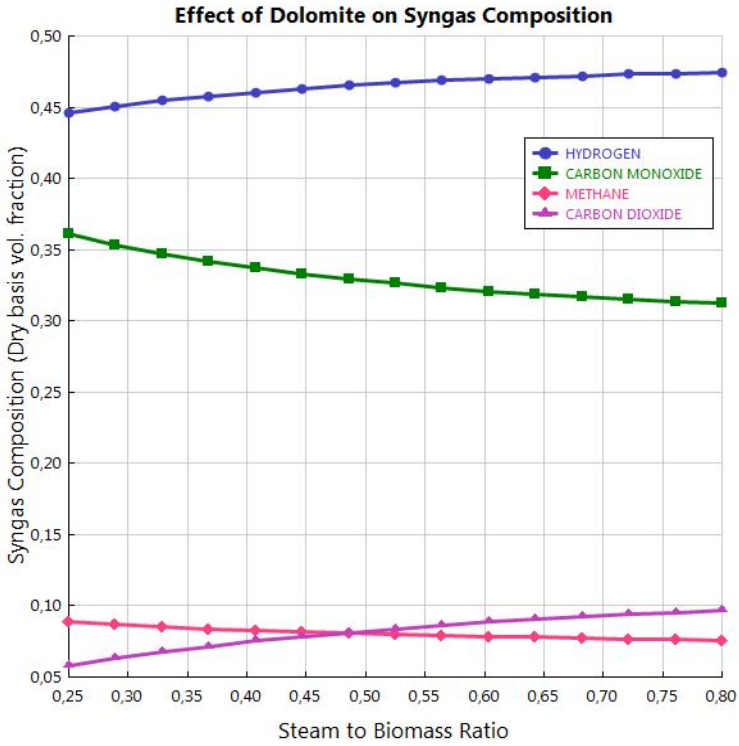

Figure 3.14: Aspen Plus® Simulation results: Syngas Composition (%) vs STBR at a gasification temperature of 750°C with **dolomite** as bed material

a gasification temperature of 750°C and with dolomite as the bed material. To emphasise more on the effect of removing CO_2 in-situ within the gasifer, the simulated results were compared with simulated results with silica sand as the bed material, as shown in Figure 3.14.

It can be observed that the hydrogen fraction in the product gas has increased considerably by using dolomite as the bed material. This increase in hydrogen composition can be explained to be due to two main factors:

1. The gasification temperature now is reduced to 750°C from 860°C. Decreasing the gasification temperature leads to less char combusted and this increased mass of char gasified results in a increased fraction of CO and CO_2 produced within the gasifer.

2. However, since CO_2 is removed from the gasifier by the dolomite, increased *CO* fraction and reducing CO_2 fraction drives the Water Gas Shift reaction (Equation B.2) towards hydrogen production, thereby resulting in a higher hydrogen fraction in the final product gas from the Gasifier.

3.2.2. GAS CLEANING UNIT

The schematic of the Gas Cleaning Unit developed was discussed previously in Section 3.1.3. The model developed is very similar to that of OLGA but with one significant difference of being pressurised in operation. Tar removal techniques widely reported in literature are usually at near atmospheric pressures and the study by Srinivas et. al [85] is the only high pressure tar removal research that is referred in this study. The Gas Cleaning Unit was modelled with input from the gasifier and the output purity fixed by the methanol synthesis requirements. Since Bio-diesel is used as the scrubbing liquid, several sensitivity tests on the operating parameters of the GCU were performed to ensure proper selection of these parameters.

Five key parameters of the GCU were studied by analyzing the results of their variation on the syngas tar concentration achieved. The five parameters varied were, the absorber pressure, number of stages of the absorber, Scrubbing flow rate, stripping medium (air) flow rate and the fraction of scrubbing liquid recycled back from condensing the tar stream from the stripper. The end objective of this study was to mainly en-

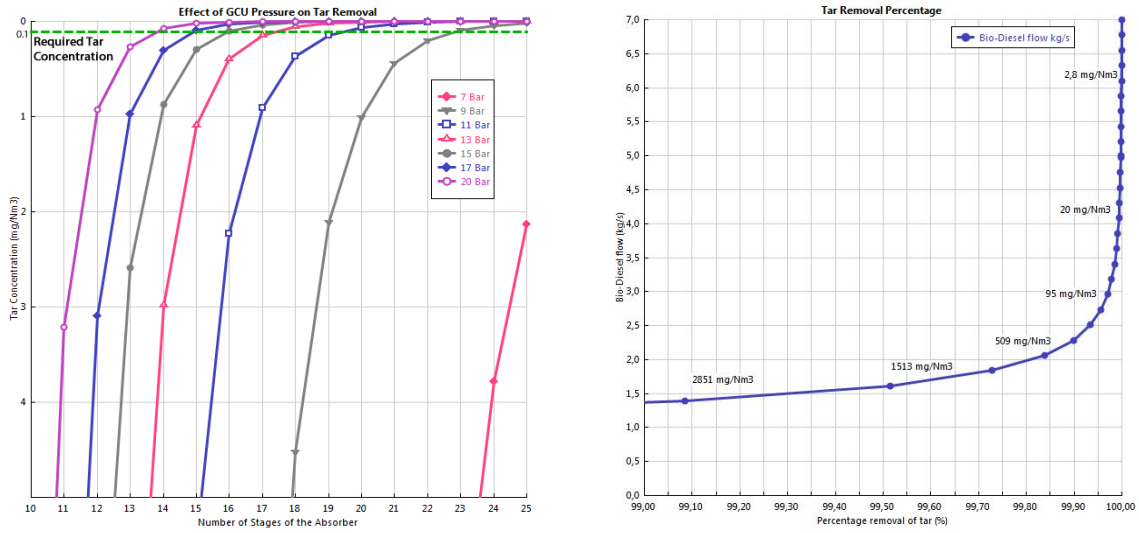

(a) Effect of Absorber pressure and number of stages on Absorber operation

(b) Effect of Bio-Diesel flow on Tar removal Percentage of an 8-stage Absorber at 20 Bar pressure

Figure 3.15: Sensitivity Analysis results on different operating parameters of the Gas Cleaning Unit

sure that the GCU designed is well capable of achieving a tar concentration of lower than 0.1 mg/Nm^3 in the clean syngas stream with minimized power and resource consumption such as equipment compactness and scrubbing liquid consumption.

Results of the first two sensitivity analysis done are shown in Figure 3.15. The first plot is to understand how for a fixed volume flow of Bio-diesel, different physical parameters of the absorber determine the tar concentration of the outlet pure syngas. As a boundary, the maximum number of stages was fixed at 25 and the tar concentration required (<0.1 mg/Nm^3) is from Table 2.4. The number of stages in an absorber can be compared as a direct measure of the absorber size and it can be observed that increasing the pressure of absorber makes the absorber more compact in size. For Absorber pressures of less than 9 Bar, the required syngas purity can not be achieved within 25 stages of operation. Also as the absorber pressure increases, the lines in the plot can be observed to move closer to each other. For example, the minimum number of stages required to achieve the target syngas purity is 16 and 14 for absorber pressures of 15 bar and 20 bar respectively. Increasing the absorber pressure leads to increased energy demands as both the syngas and the scrubbing liquid have to be compressed to the required absorber pressure.

The second plot (Figure 3.15b) shows graphically the effect of scrubbing liquid volume on the tar removal capacity of the Absorber. The absorber pressure and number of stages are fixed at 20 bar and 25 stages respectively. There is an exponential increase in the volume of scrubbing liquid (Bio-diesel) required to achieve the syngas purity required. These two sensitivity tests provide a primitive understanding on how different physical parameters of the absorber determine the Tar removal ability of the Gas Cleaning Unit. Although not within the scope of this research, understanding the practical and economical implications of this sensitivity tests could provide better insight into the optimum parameter selection for the gas cleaning unit.

The last sensitivity analysis done was to analyze the effect of the stripper column on the outlet tar concentration of the syngas. The stripper is responsible for removing the tars absorbed by the scrubbing liquid in the absorber by transferring them onto the inlet hot air. An inefficient stripping column can cause the tar concentration in the scrubbing liquid to increase, thereby impeding its ability to absorb tars in the absorber. Another key variable to be optimized in the GCU is the scrubbing oil lost during operation. Since Bio-Diesel is a very calorific liquid, loss of scrubbing liquid can have significant detrimental impact on the overall efficiency of the GCU and the process. One easy way to reduce the Bio-Diesel loss is by condensing the Bio-Diesel in stripped away in the hot air stream from the stripper and recycling a part of the recovered Bio-Diesel back into the stripper. This sensitivity analysis focuses on investigating the effect of hot air flow into the stripper and the recycle fraction of scrubbing liquid recovered. The results are shown in the Figure 3.16. The most

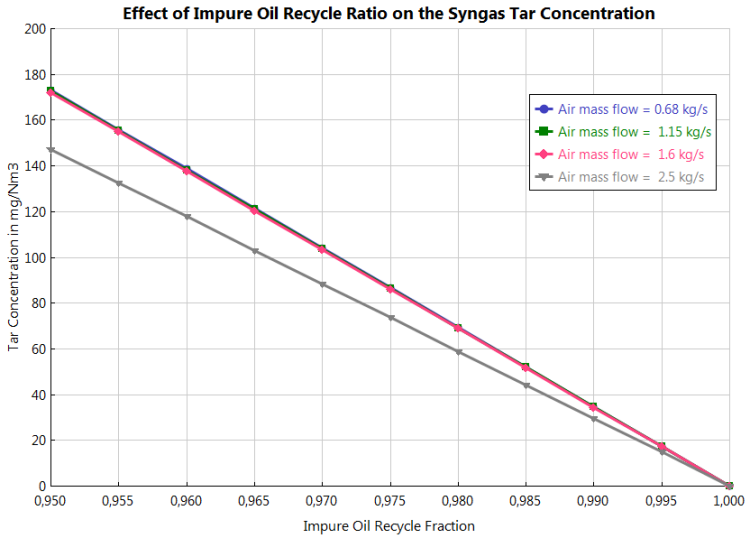

Figure 3.16: Aspen Plus® Simulation results: Effect of Scrubbing oil recycle percentage on Tar Concentration

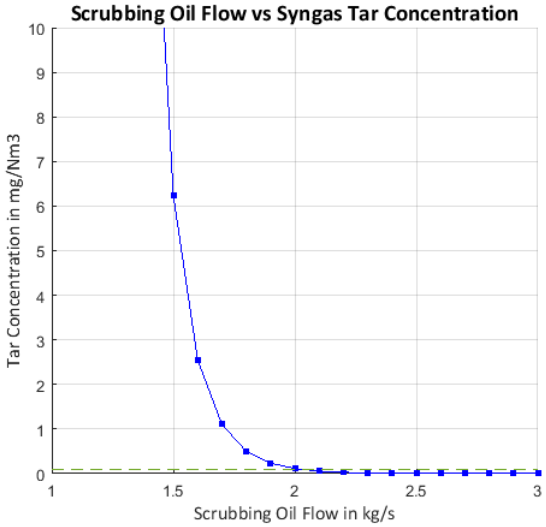

Figure 3.17: Aspen Plus® optimization results: scrubbing oil flow vs outlet syngas tar concentration

straightforward observation is that even a small fraction of the recovered Bio-diesel can compromise the gas Cleaning ability of the GCU, causing the tar concentration to be much higher than the requirement. Also, increasing the hot air flow rate has no effect of tar concentration at no or very less recycles but, increasing the hot air flow rate increases the amount of Bio-Diesel entrained causing increased Scrubbing oil loss. The scrubbing liquid loss was reduced from **9%** to around **4.4%** for the GCU model developed. Nicolaou developed an optimized model for an atmospheric wet gas cleaning system with Bio-Diesel as the scrubbing liquid and reported a scrubbing liquid loss of **9%** [22]. However, in the case of pressurized gasification, the mass flow of stripper and the scrubbing fluid are much higher than the values modeled by Nicolaou. Since the Gas Cleaning Unit (GCU) developed in this study is pressurized in operation compared to an atmospheric GCU simulated by Nicolaou, comparing directly both the results is not wise, but it can be inferred that the loss of such a fraction scrubbing is an unavoidable loss for a wet scrubbing system such as this. Considering these sensitivity tests, the Absorber pressure, number of stages of the absorber and the mass flow of Bio diesel were fixed.

With the results of the sensitivity tests shown earlier, the GCU inputs were optimized for the five key parameters discussed. The Figure 3.17 show the results of the optimised gas cleaning unit operation. The number of stages in the absorber and stripper along with scrubbing oil flow rate and gas cleaning unit pres-

Table 3.5: Input Specifications for Methanol validation : Reactor and Catalyst Specifications on the left, Feed and Coolant Specifications on the right [71]

Reactor Tube Diameter (m)	0.04
Reactor Length (m)	7
Number of Tubes	1620
Catalyst Particle Density (kgm^{-3})	1190
Bed Void Fraction (m^3m^{-3})	0.285
Heat Transfer Coefficient ($Js^{-1}K^{-1}m^{-2}$)	118.44

	Feed	**Cooling Water**
Temperature (°C)	225	220
Pressure (Bar)	69.7	29
Mole Flow ($kmol.hr^{-1}$)	6264.8	766
Vapor Fraction	1	0
Component Flow Rates ($kg.hr^{-1}$)		
CO	10727.9	
CO_2	23684.2	
H_2	9586.5	
H_2O	108.8	13800
Methanol	756.7	
CH_4	4333.1	
N_2	8072	

Table 3.6: Comparison of results of Simulation and Literature [71].

	Mass Flow in $kg.hr^{-1}$		
	Literature Results	**Simulation Results**	**Deviation**
CO	4921	4898	-0.48%
CO_2	18316	18316	0%
H_2	8014	8010	-0.05%
CH_4	4333	4333	0%
H_2O	2309	2306	-0.13%
Methanol	11283	11335	0.46%

sure were optimised to arrive at these results. The scrubbing liquid flow rate in the shown figure, was varied to achieve the required purity in the final syngas. The plot shown is similar to the previous sensitivity test shown in Figure 3.15b but after optimization. The drop in scrubbing oil flow rate is very significant and it can be seen from the Figure 3.17 that a minimum scrubbing oil flow rate of more than 2.1 kg/s is required for achieving the required tar concentration of 0.1 mg/Nm^3 in the cleaned syngas. Hence the scrubbing oil flow rate was fixed at 2.2 kg/s for the gas cleaning unit model.

3.2.3. METHANOL SYNTHESIS

Similar to the case of pressurized Gas Cleaning, literature on kinetic modelling of the Lurgi process is relatively scarce. Kinetic studies by Bussche et al. [90],Graaf et al. [92], Luyben et al.[93] and Lei Chen et al. [71] were studied to develop the methanol synthesis block of the model. Kinetics of Bussche et al. was used along with some equilibrium constants taken from Graaf et al. The kinetics used are shown and explained in better detail in Appendix B.

Lei Chen et al. used the same set of kinetics to validate the Lurgi process used in a commercial methanol production plant [71]. Although the Lurgi process is a much matured technology for methanol synthesis, experimental data on this Lurgi process is very scarce to find in literature. With the kinetics shown in Table B.8 of Appendix B, the first step was to compare the results of predicted methanol yield with results published by Lei Chen et al. [71]. The scales of these methanol synthesis plants is significantly higher than that of the model being developed in this research. To avoid ambiguity in scaling, a separate simulation was performed with the inputs corresponding to the plant.

The schematic used in for validation of this methanol synthesis block is very close to the schematic shown in Figure 3.6 but without a cooling water recycle stream and a product recycle. The main reason behind changing the model schematic is that the validation found in literature was for a single-pass conversion of methanol which was simulated and compared to validate the kinetics used in this model [71]. Inputs used

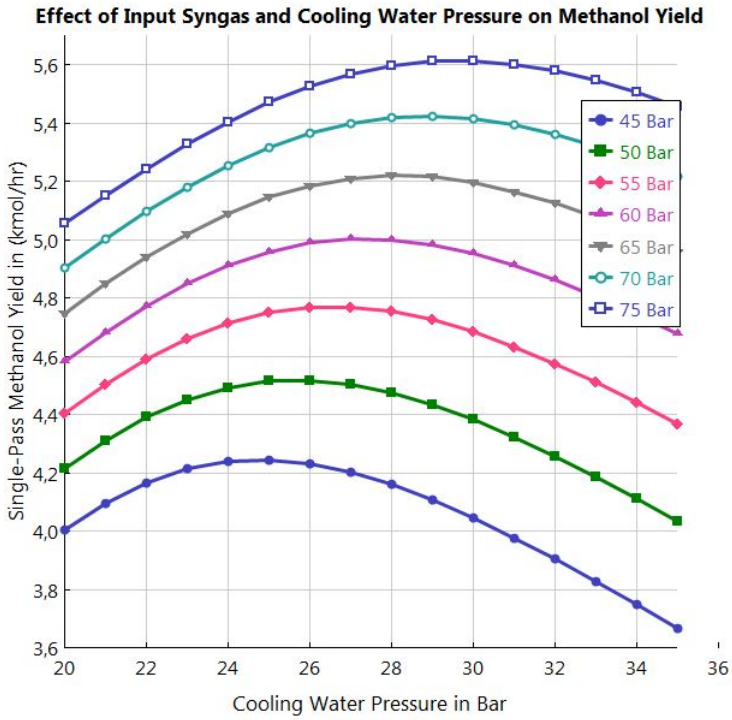

Figure 3.18: Sensitivity Analysis: Effect of Inlet pressure on Single-Pass Methanol Yield. Inlet Syngas pressure is plotted as the parametric Variable

and results of this simulation are shown in Table 3.5. The kinetics used were validated by comparing the results of the simulated model with the actual data from the Methanol synthesis Plant. A comparison of the results is shown in Table 3.6. It can be observed from the results that the kinetics are very accurate to obtain a end methanol yield which is in very close agreement with the results documented from a commercial methanol plant. The study by Lei Chan ventures further to optimize various input parameters such as the inlet pressure and temperature of both the syngas and the coolant water stream, physical parameters such as the length of the reactor and more.

The reactor dimensions used were scaled down for the syngas mass flow rates used in this study. With the current scales, several sensitivity tests were performed to understand the behaviour of this block and thereby selecting appropriate input conditions. The input pressures, pressure of the syngas stream and the cooling water stream were varied and the corresponding single-stage (No recycle) methanol yield was obtained and plotted in Figure 3.18. Although increasing the input syngas gas pressure has a positive effect on the methanol yield, it also increases the energy demand of the whole process as compression work increases. A more important observation is that there exists a inlet Cooling water pressure for which methanol yield peaks and this corresponding cooling water pressure depends largely on the syngas inlet pressure. To be more precise, the inlet cooling water pressure corresponding to the local maximum of methanol yield increases with increasing syngas inlet pressure.

Similar sensitivity tests were done on the reactor physical dimensions such as the number of tubes within the reactor and the length of the reactor. The results of these analysis are shown in Figure 3.19. In the Figure 3.19a, It can be easily observed that the methanol composition in the gas stream reaches a 'equilibrium' after a length of around 7 meters. Increasing the reactor any more would only increase the equipment cost of the reactor without an appreciable increase in methanol yield. On the other hand, increasing the number of tubes (Figure 3.19b) leads to an almost linear increase in methanol yield. Choosing an optimum number of tubes would require further investigation into the construction and economics of the reactor which would fall outside the scope of this thesis. The objective of such a sensitivity analysis is to understand the interplay between different parameters in maximising methanol yield and a more detailed economic analysis would help better in choosing the optimum operating conditions for such a process.

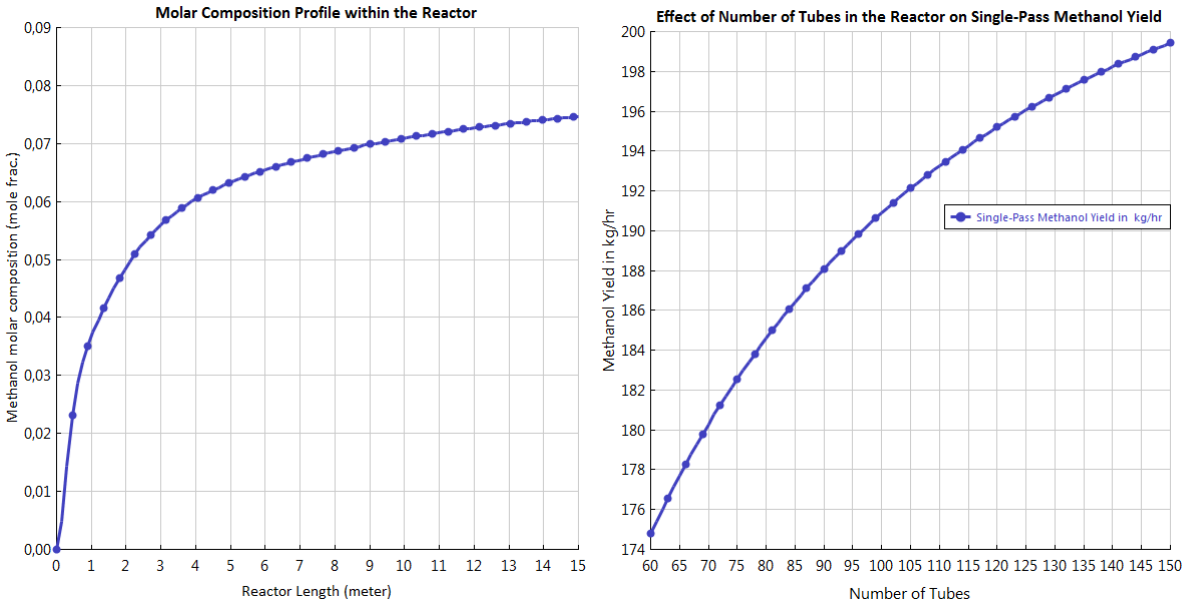

(a) Effect of Reactor Length on Single-Pass Methanol Yield (b) Effect of Number of tubes on Single-Pass Methanol Yield.

Figure 3.19: Sensitivity Analysis: Effect of Reactor Dimensions on Methanol Yield

One of the key parameters in this methanol synthesis block is the composition of syngas used. The stoichiometric ratio of close to 2, given by the Equation 2.6, provides a theoretical optimum for the syngas composition. Since tailoring the composition of the syngas for the methanol synthesis block is carried out in the shift reactor, this dependence of methanol yield on syngas composition needs to be understood better. A sensitivity analysis was performed by varying the Hydrogen flow rate in the supplied syngas and the corresponding methanol yield was simulated. In the previous tests, a water cooled reactor was used to simulate the methanol synthesis reactor but as a simplification to understand the effect of the stoichiometry, a isothermal reactor was used in this test. The simulation results are shown in Figure 3.20a. It can be observed that the methanol yield reaches a maximum earliest at a Stoichiometric ratio of close to 2.1 for a simulation with no recycle. This implies that adding more hydrogen to increase the stoichiometric ratio will have no constructive effect on the methanol yield past a stoichiometric ratio of 2.1. However, a methanol, synthesis process without recycle is highly inefficient and the result of recycling lowers the stoichiometric ratio of the inlet feed to the reactor. This is the main reason why the stoichiometric ratio of the product gas from the shift reactor is tailored to be marginally above 2.1 so that the inlet feed for the methanol reactor would be at a stoichiometry of 2.

The last sensitivity test done was on the recycle fraction in the methanol synthesis process. Since the single pass efficiency of the methanol synthesis process is very low, there is a need to recycle some of the unconverted gas back into the reactor to increase the end methanol yield. Figure 3.20b shows the results of this sensitivity analysis. Two output parameters were sampled with varying recycle fraction. It can be seen from the plot that both end methanol yield and the net throughput through the methanol reactor increase with increasing recycle fraction. Although, an increase in end methanol yield is an encouraging result, the sharp increase in throughput signifies an increase in reactor size. Moreover, since the recycle gas is at a lower pressure (Due to the flash to separate converted methanol), it has to be compressed back to synthesis pressure. Hence increasing the recycle fraction would cause an increase in both investments as well as operational costs at the expense of increased methanol yield. Since this recycle is unavoidable, a recycle fraction of 0.9 is chosen, since beyond 0.9, the throughput increases much faster.

3.3. COMPLETE MODEL

By combining different blocks developed and validated in the previous sections, different schematics were developed to better understand the integration process of these blocks. The end objective however remains unchanged from methanol and power production. Four main cases or scenarios were developed, each vary-

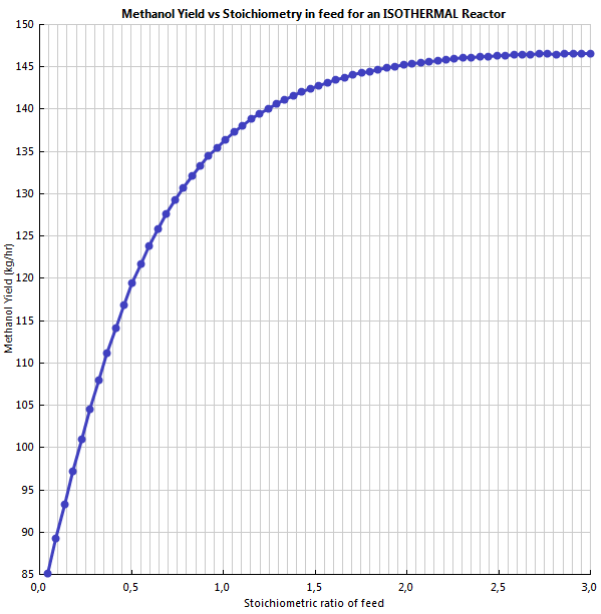

(a) Sensitivity Analysis: Effect of Inlet Syngas Composition on Single-Pass Methanol Yield

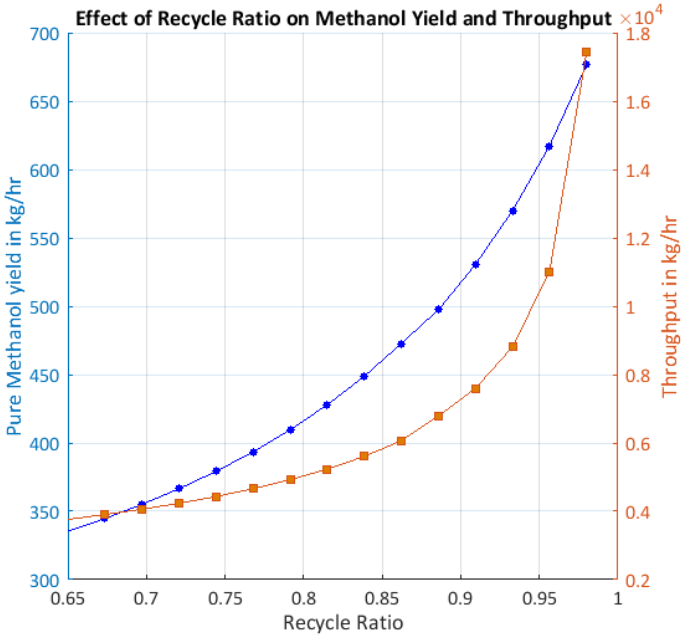

(b) Sensitivity Analysis: Effect of recycle ratio on the methanol yield and the throughput within the reactor

ing only in terms of positioning of different blocks. Net productivity and Energy efficiency of each of these blocks were computed and compared.

3.3.1. CASE A: CONVENTIONAL METHANOL PRODUCTION PROCESS

The conventional Methanol synthesis process combines all the five functional blocks as shown in schematic A of Figure 3.21. Case A represents the conventional methanol synthesis route from biomass gasification. A gas turbine is used to flare the vent-gas or the off-gas arising from the methanol synthesis reactor. A key upgrade of this conventional route in the developed model is the use of the tar loaded stream from the Gas Cleaning Unit as a part fuel in the gas turbine unit. The Gas Turbine combustion temperature should be sufficiently high enough to completely combust the tar species produced during gasification. A steam network is also added to utilize the waste heat produced during the course of this process. The model proposed in developed completely in Aspen Plus®. Since its a combination of all the blocks discussed in the previous section, the model looks very complex and hence a simple block schematic is shown in Figure 3.21. The actual schematic can be found in the Appendix C.

3.3.2. CASE B: THE FREE ELECTRICITY CASE

The second case considered is a very practical application of the Case A (conventional methanol synthesis route). A key energy and economic demand during the conventional methanol synthesis process is the shift reactor unit which operates at a temperature of 450°C. Dolomite, the bed material used, needs to be cooled down to the shift reaction temperature and then has to be re-heated back to gasification temperature. This cooling down and subsequent heating of dolomite can cause a energy demand, increasing the amount of Char that is combusted, leading to reduced efficiency of the gasifer. Although not ideal, this shift reactor is an absolute necessity in attaining stoichiometry in the feed for methanol synthesis.

Recently, integrating electricity produced from different non-renewable sources such as solar power and wind energy are growing in interest. A main challenge with these renewable sources is their intermittent availability which could cause a surge in surplus electricity produced as Germany experienced recently[94]. On the other hand, hydrogen is also produced as a by-product in numerous chemical plants. Hence to utilize these free sources of hydrogen and electricity, a second model was proposed. This model uses the free-electricity to produce H_2 and O_2 by electrolysis. The H_2 produced is added directly to the syngas stream and the O_2 produced from the electrolysis is then used to combust the char in the combustor. By doing so, the

function of the shift reactor is then eliminated, leading to a lesser heat demand and an increased fraction of char gasified. This would as a net result increase the overall system efficiency of the process. This model was intended to be a practical integration of this process and hence as a simplification, the electrolysis part is not modeled in detail but simply as a RYIELD reactor in Aspen Plus®. A functional block Schematic of this case is shown in Figure 3.21.

3.3.3. CASE C: POWER PRODUCTION FROM BIOMASS GASIFICATION - INTEGRATED GASIFICATION COMBINED CYCLE (IGCC)

The third case modeled is similar to that of an Integrated Gasification Combine Cycle system. Syngas produced from the gasifier is directly fired in a gas turbine to produce power. A steam cycle is modeled as a bottoming cycle to extract heat from the flue gas stream from the gas turbine. A functional block Schematic of this case is shown in Figure 3.22.

The dual gasifier concept modeled is advantageous for its relatively low tar concentration in the produced product gas. The tar concentration is at a level which can be fired directly in a Gas Turbine. The particulate matter entrained with the product gas however needs to be removed. A separate model is also modeled without the Gas Cleaning Unit but with a High Temperature particulate filter to remove the entrained particulate matter.

3.3.4. CASE D: POWER PRODUCTION FROM BIOMASS GASIFICATION VIA AN INVERTED BRAYTON CYCLE(IBC)

Case D is very similar to the IGCC case (Case C) but differs only in the gas turbine technology used. Since the product gas obtained from the gasifier is at a considerably high temperature (800°C), the stream has to be cooled down before compression to minimise compression work. This cooling down process would require a separate heat exchanger and hence would decrease the net energy efficiency of the process and also increase the costs of the overall system. The Inverted Brayton Cycle, discussed in subsection 2.5.3, is a novel idea to utilize the energy from high temperature fuels. By combusting at atmospheric pressure, the need for compression is eliminated. However, the constraints on particulate matter concentration in the syngas stream would warrant a high temperature filter unit, causing the syngas stream to be at 450°C. The Inverted Gas Turbine is coupled with a steam network to extract waste heat and to increase the energy efficiency of the overall process. A functional block Schematic of this case is shown in Figure 3.22. The results of the cases C and D are compared for energy efficiency in the next chapter.

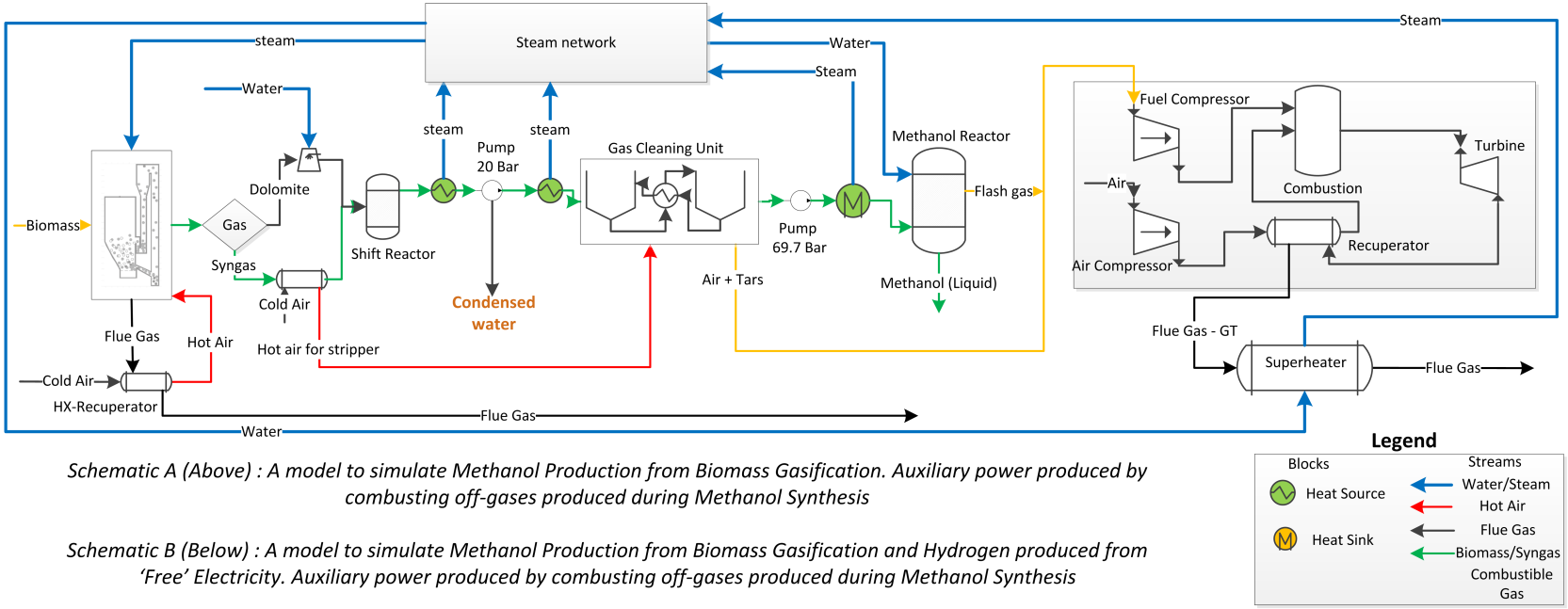

Schematic A (Above) : A model to simulate Methanol Production from Biomass Gasification. Auxiliary power produced by combusting off-gases produced during Methanol Synthesis

Schematic B (Below) : A model to simulate Methanol Production from Biomass Gasification and Hydrogen produced from 'Free' Electricity. Auxiliary power produced by combusting off-gases produced during Methanol Synthesis

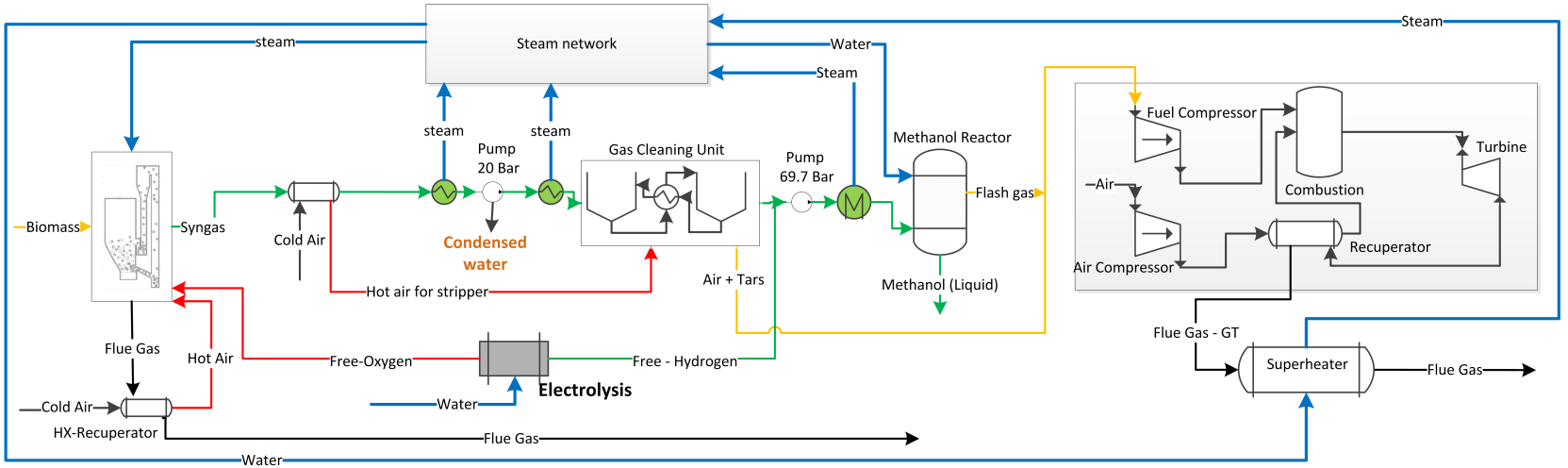

Figure 3.21: Functional Schematics of the cases A and B.

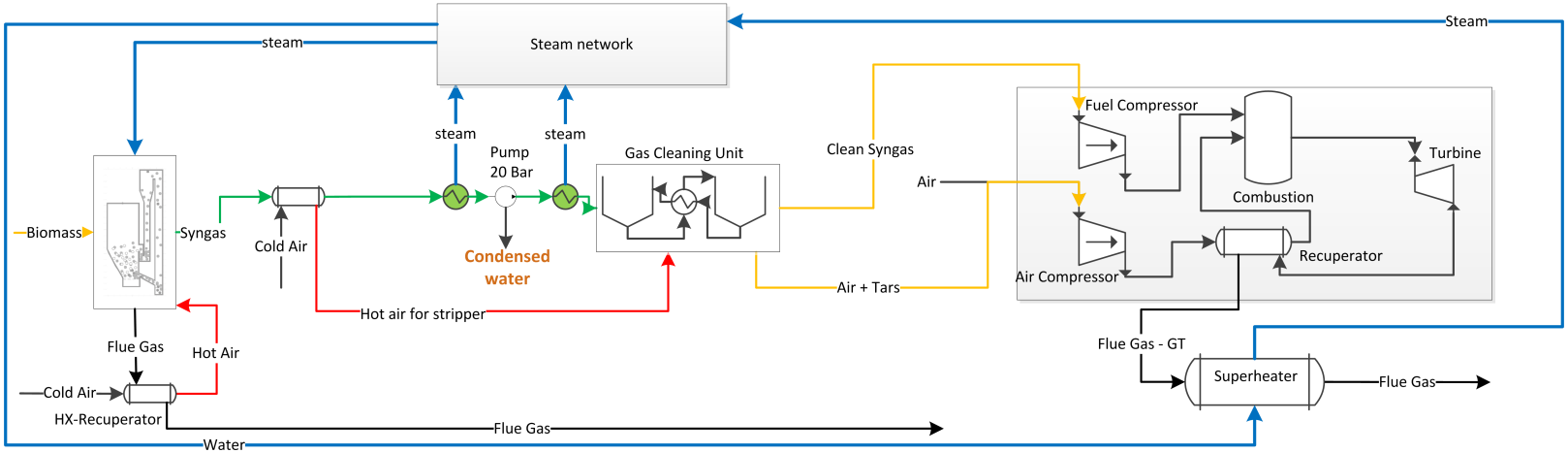

Schematic C (Above) : A model to simulate only Power production from gases arising from Biomass Gasification. Cleaned Syngas is combusted in a gas turbine to produce power.

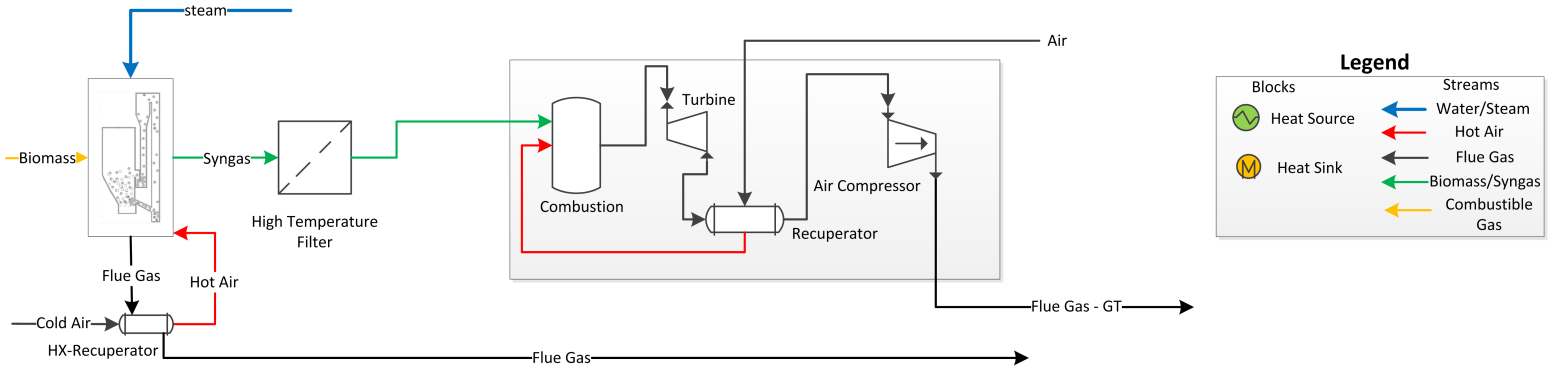

Schematic D (Above): A model to Simulate Power production from gases arising from Biomass Gasification. A Inverted Brayton Cycle is used to produce power directly from the high temperature Syngas produced.

Figure 3.22: Functional Schematics of cases C and D

4

Results and Discussion

Section 3.3 in the previous chapter discussed briefly about the different cases that were modeled. The four cases discussed form the key objectives of this study. In all the four cases modeled, two choices in the bed material used can be made; either the catalytic dolomite or the inert silica sand. The difference apart from the CO_2 removal by dolomite sorption is that the gasification temperature is limited by this choice. In section 2.2.5, the sorption capability of dolomite was discussed and this limits the gasification temperature to a maximum at 750°C. Removal of CO_2 has shown to promote other gasification reactions increasing the hydrogen yield comparable to a higher temperature gasification process. On the other hand, increasing the gasification temperature has a positive effect on the hydrogen fraction in the produced product gas, thereby increasing its heating value. But the use of silica sand would require a dedicated catalyst for the water gas shift reactor. Two sub-cases have been studied within the scope of this project, one with dolomite as bed material at a gasification temperature of 750°C (Corresponding to AER) and the other is with dolomite but with a gasification temperature of 860°C (No CO_2 removal considered).

Hence, the four cases are modeled for both dolomite and silica sand to make this comparison more prominent. For the case of silica sand, a gasification temperature of 860°C was fixed, which corresponds to the data from the FICFB. Since, the model is assumed and modeled for steady state operation, silica sand is simulated by dolomite but by excluding the CO_2 reaction from the list of reactions used. List of reactions used are shown in Appendix B. A Sankey Diagram and list of efficiencies for each of these cases were also computed from the simulation results. The results of the simulations are discussed in the following sections.

4.1. Case A: Conventional methanol production process

This case of a conventional methanol synthesis process was previously discussed in the previous chapter. The functional schematic followed to build the Aspen Plus® model for this case was also shown in the previous chapter (Figure 3.21). The product gas produced from the gasifier was cleaned process and the cleaned syngas was used to produce methanol. The developed model can be found in the Appendix C. The results of this case can be discussed in two parts: first, by calculating the Cold Gas Efficiency and the net efficiency of the process. Second, by drawing a Sankey diagram for visualising the conversion of biomass into the products desired. The model can be divided into four blocks, the syngas production and processing step, the Gas Cleaning process, the Gas Turbine system and the Steam Network. Since dolomite is used in both the gasifier and the water gas shift reactor, they both are coupled into the same step.

Syngas Production and Processing

Biomass with composition shown in Table 3.1 was used as input fuel for the gasifier model. The gasification temperature required was obtained by recycling a fraction of char (Carbon) and a fraction of the tar stream from the Gas Cleaning unit (Appendix C). Input air for gasification is heated up in a recuperator by cooling down the flue gas stream from the combustor. The produced product gas and a fraction of the dolomite stream is then cooled to the water gas shift temperature and then fed into the water gas shift reactor. The residence time of the water gas shift reactor was varied to attain stoichiometric ratio (Equation 2.6) of around 2.1. Key inputs for this block for both the sub-cases are shown in Table 4.1.

Table 4.1: Inputs for the Gasifer and the Shift Reactor for the Case A

	sub-case A	**sub-case B**
Gasification Temperature	**860°C**	**750°C**
Gasifier:		
Biomass Flow rate (kg/s)	0.65	0.65
Bed Material Flow Rate (kg/s)	37	37
Steam to Biomass Ratio	0.48	0.48
Water Gas Shift reactor:		
Residence time within the reactor	14s	5s
Inlet Temperature of product gas	450°C	450°C

Table 4.2: Inputs for the Gas Cleaning Unit

GCU operation pressure	15 Bar
Mass flow rate of Bio-Diesel in the GCU	2.20 kg/s
Absorber	
Number of Stages considered	14
Absorber Pressure	15 Bar
Syngas Inlet temperature	110°C
Bio-Diesel inlet temperature	80°C
Stripper	
Number of Stages considered	25
Stripper Pressure	1.013 Bar
Air Inlet temperature	200°C
Bio-Diesel inlet temperature	200°C

GAS CLEANING UNIT

The tailored product gas obtained from the water gas shift reactor is then cleaned in the Gas Cleaning unit. The product gas is first pressurized to the absorber pressure and then the water content in the stream is removed. A fraction of tars is absorbed by the condensed water but the authors of [85] believe the impurity concentration in such a stream would not pose a threat to necessitate a downstream waste water cleaning unit. The pressurized gas is then fed to the absorber where a Bio-diesel stream removes the tars. The tars in the oil are then stripped in the stripper column by a hot air stream. Input to this unit is shown in the Table 4.2. Since the bed material has no effect outside the gasifier, inputs shown are the same for both the sub-cases.

METHANOL SYNTHESIS

Cleaned syngas from the Gas Cleaning Unit is then compressed to the required synthesis pressure and then cooled down to the required temperature in the subsequent heat exchanger. The synthesis reactions are simulated in the plug flow reactor METHANOL. The products of the reactor are then flashed in two flash separators, separating the gaseous stream from the liquid stream. The gaseous stream does contain some methanol absorbed and similarly, the liquid stream of water and methanol do contain some gases absorbed. A fraction of the flash gas is recycled back into the methanol reactor and the rest sent to the Gas Turbine unit. The liquid stream is then distilled in a distillation column to produce pure methanol. Inputs to this block are shown in Table 4.3.

GAS TURBINE UNIT

The Gas Turbine Unit is designed to utilize any waste calorific streams that may result as a byproduct of any of the other functional blocks. The three main calorific streams combusted in the gas turbine are the Flash gas from the methanol synthesis block, the Tar stream from the Gas Cleaning Unit and the flash gas produced during gases escaping the scrubbing liquid in the gas cleaning unit. Since the fuel stream (mixture

Table 4.3: Inputs to the Methanol Synthesis block

Methanol Synthesis Pressure	69.7 bar
Methanol Synthesis Temperature	236°C
Plug Flow reactor inputs	
Length of the reactor	7 m
Number of tubes	85
Diameter of a single tube	0.04m
Cooling water pressure	29 Bar
Flash temperature	40°C
Flash Separator 1 pressure	40 Bar
Flash Separator 2 pressure	1.013 Bar
Recycled fraction	0.90
Distillation Column Inputs	
Methanol purity required	0.99
Number of Stages	15

Table 4.4: Inputs to the Gas Turbine block

Turbine Inlet Temperature	1000°C
Isentropic Efficiency	
Compressor - Fuel	0.7
Compressor - Air	0.8
Turbine	0.8
Pressure Ratio	20
Air Inlet temperature	25°C

Table 4.5: Inputs to the Steam Network block

Steam network pressure	25 Bar
Turbine Inlet temperature	400°C
Turbine outlet Pressure	0.04 Bar
Flue Gas exit temperature	100°C
Minimum Pinch temperature	10°C

of the three streams) is a mixture of different species, the combustion process within the gas turbine can be relatively more complicated than a conventional natural gas fired gas turbine. With tars and hydrogen as reacting species in the fuel, the turbine inlet temperature is limited to 1000°C to compensate for the lack of blade cooling in the turbine. The mass flow of air is varied to achieve this turbine inlet temperature. The heat from the exhaust flue gas stream is not recovered by a recuperator but by a bottoming steam cycle. Inputs to this block are shown in the Table 4.4

STEAM NETWORK

Waste heat from different parts of the model are recovered by producing steam and then expanding the steam in a steam turbine to produce power. This network is called the steam network and owing to its added complexity, is simulated in a separate model. Simple heaters or coolers are used in the main model wherever a heat demand or supply exists. The heat exchanger network as a part of the steam network are then modeld separately to reduce any added recycle loops within the model and thereby making it more stable. A submodel of the steam network modeled is shown in Appendix C. When the heat duties of each of these heaters or coolers are obtained by simulation, a pinch analysis is done to create this steam network. Summary of the pinch analysis done to build this steam network is shown in Table C.2 of Appendix C. Heat exchangers are then divided between a economiser, evaporator and a super-heater, by functionality.

Any internal heat demands such as high temperature steam for the gasifer and the hot air stream for the stripper column of the Gas Cleaning Unit are satisfied with a suitable heat supply. The excess available heat is used by the steam network to produce steam. Inputs to this model are shown in Table 4.5.

RESULTS

The models shown in Figure C.1 of Appendix C were simulated and optimized for the parameters discussed in the validation part (section 3.2) of the previous chapter. Two cases of operation were investigated as mentioned before: Gasification with and without an active CO_2 removal in-situ within the gasifer. The end results of the model for both cases are shown in Table 4.6 and Table 4.7. The Sankey diagram corresponding to each of this case is shown in Figure 4.1 and Figure 4.2.

Table 4.6: Results of simulation for the Case A: Conventional methanol synthesis route without CO_2 removal

Gasifier	
Biomass Input Flow Rate	0.653 kg/s
Calculated Biomass LHV	15.20 MJ/kg
Product Gas Yield from the Gasifier	0.604 kg/s
Product Gas Stoichiometric ratio	**2.10**
Product Gas LHV	15.32 MJ/kg
Gasification Temperature	860°C
Gasification Pressure	1 atm
Percentage of Char combusted	75 %
Carbon Conversion	100 %
Gas Cleaning Unit	
GCU Absorber Pressure	15 Bar
Syngas Yield	0.304 kg/s
Syngas LHV	25.29 MJ/kg
Tar Concentration	0.08 mg/Nm^3
Scrubbing Liquid loss	0.1 kg/s (2.3 MW)
Methanol Synthesis	
Methanol Synthesis Pressure	69 Bar
Flash gas Recycle Ratio	0.9
Methanol Yield	0.14 kg/s
Methanol Purity Achieved	99.6 mol %
Gas Turbine Unit	
Turbine Power produced	5.99 MW
Compressor power Consumed	3.98 MW
Net Shaft Power Produced	2 MW
Turbine Inlet Temperature	1004°C
Steam network	
Steam Pressure	25 Bar
Power Produced	3 MW
Cold Gas Efficiency	
Gasifier	86%
Gasifier + GCU	63 %
Methanol Synthesis	24.5 %
Overall Efficiency	
Net Power Consumed	6.4 MW
Net Power Produced	8.95 MW
Net Efficiency	**55%**

Table 4.7: Results of simulation for the Case A: Conventional methanol synthesis route with CO_2 removal

Gasifier	
Biomass Input Flow Rate	0.653 kg/s
Calculated Biomass LHV	15.20 MJ/kg
Product Gas Yield from the Gasifier	0.75 kg/s
Product Gas Stoichiometric ratio	**2.10**
Product Gas LHV	12.43 MJ/kg
Gasification Temperature	750 °C
Gasification Pressure	1 atm
Percentage of char combusted	62 %
Carbon Conversion	96.28 %
Gas Cleaning Unit	
GCU Absorber Pressure	15 Bar
Syngas Yield	0.35 kg/s
Syngas LHV	22.72 MJ/kg
Tar Concentration	0.02 mg/Nm^3
Scrubbing Liquid loss	0.1 kg/s (2.3 MW)
Methanol Synthesis	
Methanol Synthesis Pressure	69 Bar
Flash gas Recycle Ratio	0.9
Methanol Yield	0.15 kg/s
Methanol Purity Achieved	99.6 mol %
Gas Turbine Unit	
Turbine Power produced	5.86 MW
Compressor power Consumed	3.96 MW
Net Shaft Power Produced	1.9 MW
Turbine Inlet Temperature	1002°C
Steam network	
Steam Pressure	25 Bar
Power Produced	3.03 MW
Cold Gas Efficiency	
Gasifier	87.5 %
Gasifier + GCU	62.8 %
Methanol Synthesis	25.2 %
Overall Efficiency	
Net Power Consumed	6.9 MW
Net Power Produced	9 MW
Net Efficiency	**53.5 %**

Since the energy network within the complete setup is very intricate, the Sankey diagram was made simplified for better understanding. The gasifier and the shift reactor were combined as a single block. This is because of a large common bed material stream recycling between both the gasifier and the shift reactor, which makes the energy flows of the main product gas look very small. As explained in Section 3.2.2, the bio-diesel (Scrubbing liquid) wastage rate was one of the parameters optimized. Majority of this bio-diesel consumed is in the stripper. The hot air stream from the stripper strips most of the tars from the scrubbing liquid (bio-diesel) and a small fraction of the bio-diesel too. Although the energy content of this consumed bio-diesel is partially recovered in either the combustor of the gasifier or in the gas turbine unit, this loss of a high calorific bio-diesel poses a significant loss of economic value and efficiency of the system as evidently shown in the Sankey diagram. The cold gas efficiency calculated at different points along the model are also shown in Table 4.6 and Table 4.7. Power produced by the steam and gas turbine units are also shown. With these values, the net efficiency of the built case is calculated.

The aim of presenting two scenarios to a particular case is to help understand the importance of in-situ CO_2 removal within the gasifier (AER) and to understand its effect on the overall yield and efficiency of the case. By presenting results of simulations with a common input, comparing data is made much straightforward. This section discusses some of the key observations that can be made from these results.

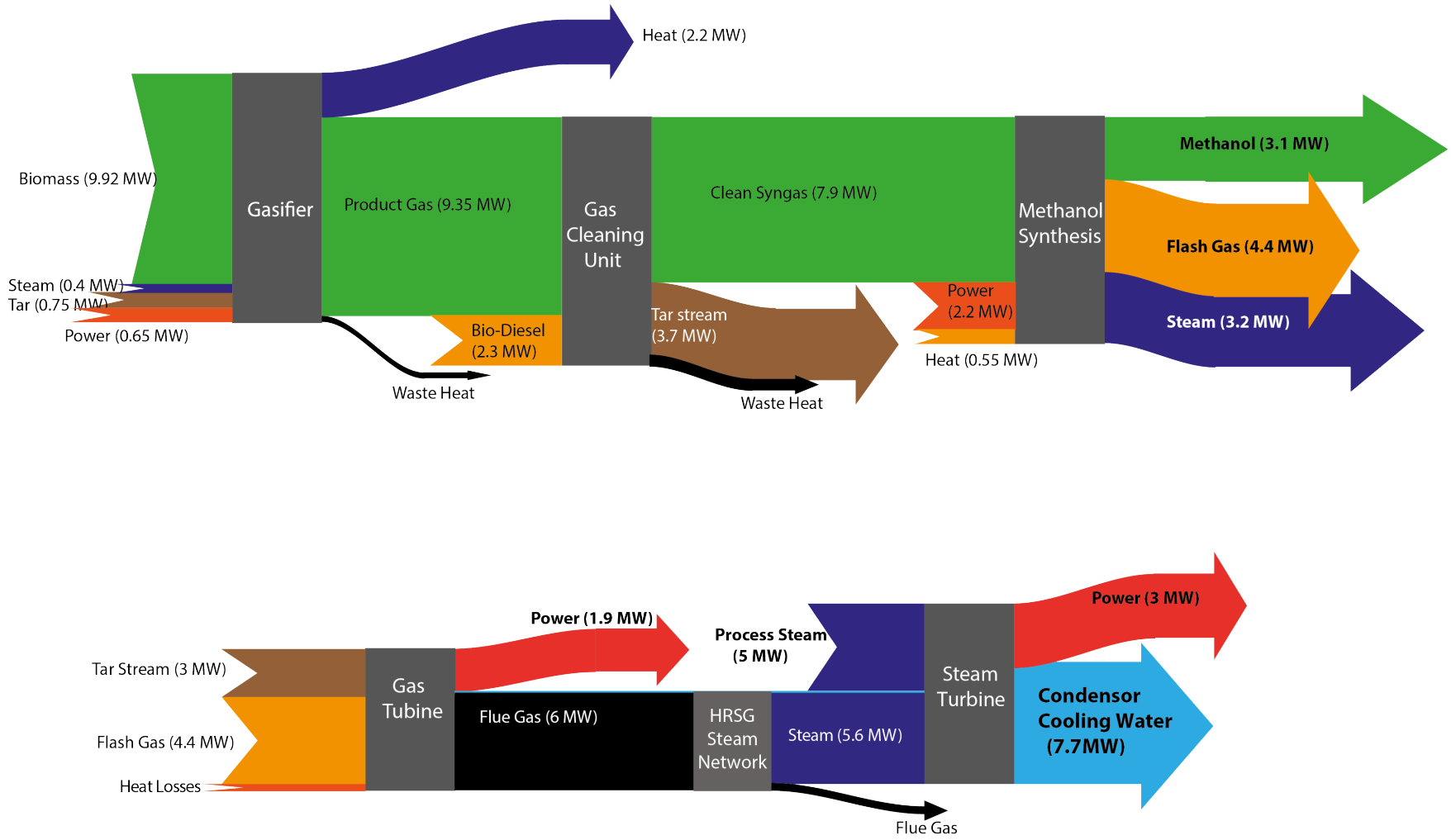

Figure 4.1: Sankey Plot for Case A - without in-situ CO_2 removal during gasification

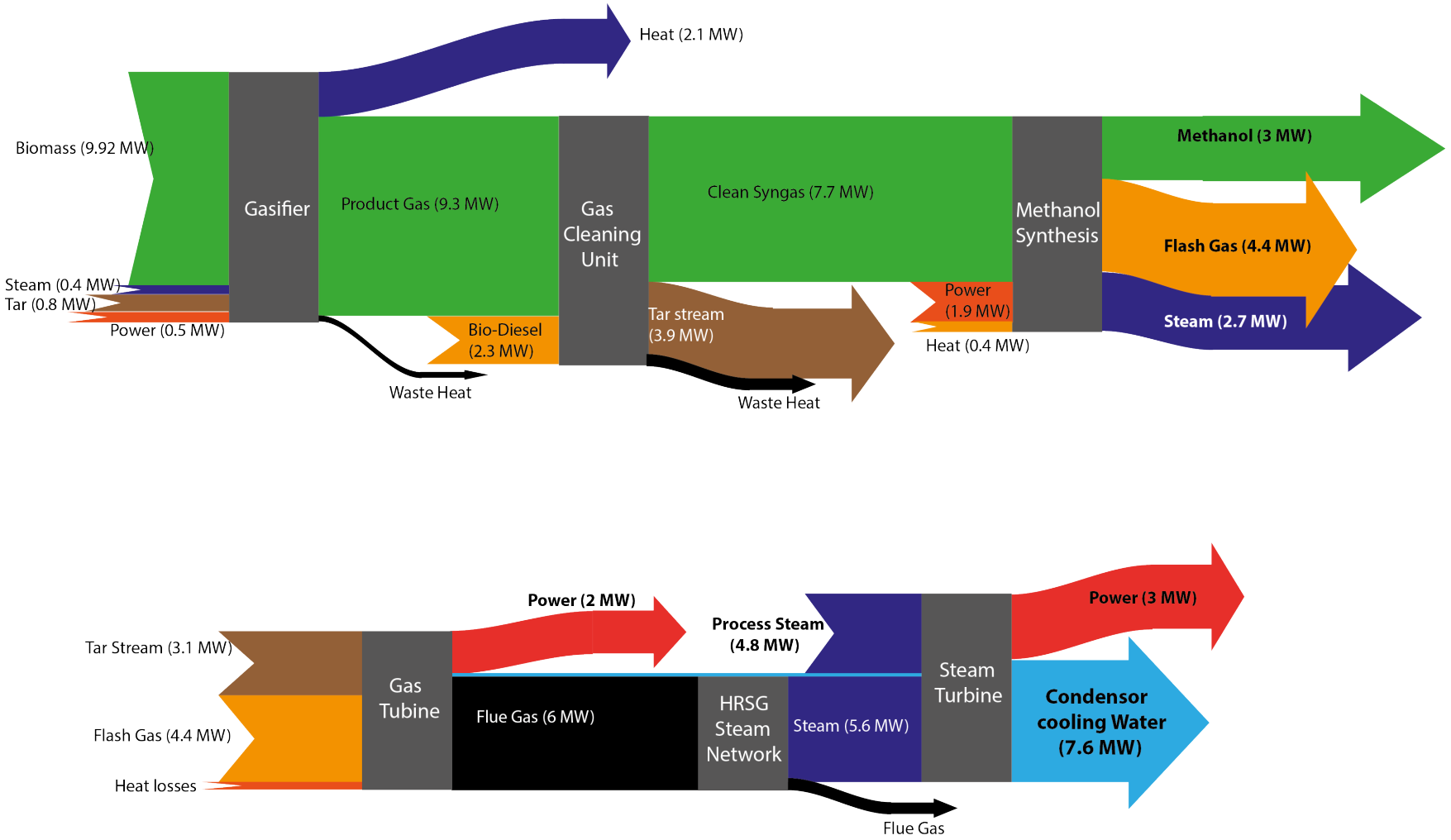

Figure 4.2: Sankey Plot for Case A - with in-situ CO_2 removal (AER) during gasification

OBSERVATIONS

The Cold gas efficiency of the gasifer is slightly higher with in-situ CO_2 removal. This can be attributed to two main factors: decreased fraction of char combusted due to lower gasification temperature and increased hydrogen fraction in the product gas. Gasification at 750°C results in a lower heat demand on the combustor, leading to a increased mass of char gasified. Removing CO_2 is proven to promote certain parallel reactions such as the water gas shift and other gasification reactions. This increased activity results in a relatively higher hydrogen fraction in the product gas (shown previously in Figure 3.14.

Carbon Conversion for both the scenarios is close to 1. Reducing the gasification temperature in the case of Absorption Enhanced Refroming (with in-situ CO_2 removal), the carbon conversion efficiency is expected to drop, as shown in Figure 2.5. The simulation results of this case do show a small drop in carbon conversion when dolomite is sued as a catalyst (96.3%). This can be attributed to the fraction of char that is combusted in both the cases. With majority of the char being combusted to generate enough heat to sustain gasification at such high temperatures, the mass of char present in the gasifier is usually completely gasified in the gasifier. This result was compared with reports from both ECN MILENA and the Gasifier at FICFB, Gussing [57, 63]. Although no evident data on this carbon conversion could be found in open literature, both these reports do mention a carbon conversion very close to unity being a major advantage of this allothermal gasification technology.

Bio-Diesel consumption, a significant efficiency loss in the Gas Cleaning Unit. Although the mass of bio-diesel lost is a very small fraction of the net mass of Bio-Diesel circulating in the Gas Cleaning Unit, its high calorific value makes it a very significant loss. This energy content of Bio-Diesel consumed can be observed much clearly in the Sankey plots.

Methanol Synthesis is a very energy intensive process. The main challenges with the methanol synthesis process were briefly discussed previously. Its poor single pass conversion would require a significantly large recycle fraction to increase the end methanol yield. This recycle would also cause a hydrogen rich flash gas stream that is not utilized. The hydrogen rich flash gas is very highly calorific and can be seen as the biggest outlet stream of this process in the Sankey plot. A more interesting observation is the methanol yield from both the scenarios considered. The end methanol yield is almost the same for both the simulations. This can have very interesting inferences on the presumed advantages of conventional high temperature gasification (Figure 2.5 shows gasification process benefits with increasing gasification temperature).

Auxiliary power and waste heat recovery make the methanol synthesis process practically viable. The Cold gas efficiency for both the scenarios for pure methanol production are very low. Only by incorporating a Gas Turbine and a bottoming steam cycle can make the overall efficiency of such a facility attractive. This can be very easily observed by the fraction of output methanol with input biomass feed in the Sankey diagram.

Potential for further optimization in the steam network is possible. Since the heat available among the different heat sources in the model is more concentrated on the lower temperatures (less than 230°C), using a two pressure steam network could convert more of the energy supplied to the steam network. As evident from the Sankey diagram, the energy content unitilized in the steam network is largely of hot water at saturation temperatures. This heat available can be put to better use by maybe using a second steam network of a lower pressure, say 5 bar.

4.2. CASE B : THE FREE ELECTRICITY CASE

The schematic built for this case is very similar to that of the previous case, the conventional methanol production process but with one significant addition. The objective of this case is to understand how the built model can be used for a practical case of utilizing a free hydrogen or free electricity source. To simulate this added source, a simple electrolysis process was modeled as a RYIELD reactor in the Aspen Plus® model. This study acknowledges that the energy demand of such an electrolysis process can not be considered to reflect reality by using such an approximation. Since the electrolysis module is not considered within the scope of this research, using a reactor to separate hydrogen and oxygen from water is just a figurative way of representing a electrolysis system. The schematic of the model developed is shown in Appendix C.

Table 4.8: Results of simulation for the Case B: The Free Electricity Case with CO_2 removal

Gasifier	
Biomass Input Flow Rate	0.653 kg/s
Calculated Biomass LHV	15.20 MJ/kg
Hydrogen Input to the Gasifier	0.03 kg/s (3.5 MW)
Product Gas Yield from the Gasifier	0.69 kg/s
Product Gas Stoichiometric ratio	**2.10**
Product Gas LHV	20.25 MJ/kg
Gasification Temperature	750°C
Gasification Pressure	1 atm
Percentage of Char combusted	38 %
Carbon Conversion	97 %
Gas Cleaning Unit	
GCU Absorber Pressure	15 Bar
Syngas Yield	0.55 kg/s
Syngas LHV	21.77 MJ/kg
Tar Concentration	0.05 mg/Nm^3
Scrubbing Liquid loss	0.1 kg/s (2.3 MW)
Methanol Synthesis	
Methanol Synthesis Pressure	69 Bar
Flash gas Recycle Ratio	0.9
Methanol Yield	0.27 kg/s
Methanol Purity Achieved	99.6 mol %
Gas Turbine Unit	
Turbine Power produced	6.7 MW
Compressor power Consumed	4.72 MW
Net Shaft Power Produced	2.23 MW
Turbine Inlet Temperature	1007°C
Steam network	25
Steam Pressure	25 Bar
Power Produced	3.8 MW

Cold Gas Efficiency	
Gasifier	94 %
Gasifier + GCU	79.2 %
Methanol Synthesis	36 %
Overall Efficiency	
Net Power Consumed	8.7 MW
Net Power Produced	10.8 MW
Net Efficiency	**59%**

Table 4.9: Results of simulation for the Case B: The Free Electricity Case without CO_2 removal

Gasifier	
Biomass Input Flow Rate	0.653 kg/s
Calculated Biomass LHV	15.20 MJ/kg
Hydrogen Input to the Gasifier	0.03 kg/s (4.4 MW)
Product Gas Yield from the Gasifier	0.74 kg/s
Product Gas Stoichiometric ratio	**2.10**
Product Gas LHV	20.12 MJ/kg
Gasification Temperature	860°C
Gasification Pressure	1 atm
Percentage of Char combusted	53.5 %
Carbon Conversion	100 %
Gas Cleaning Unit	
GCU Absorber Pressure	15 Bar
Syngas Yield	0.61 kg/s
Syngas LHV	21.77 MJ/kg
Tar Concentration	0.01 mg/Nm^3
Scrubbing Liquid loss	0.1 kg/s (2.3 MW)
Methanol Synthesis	
Methanol Synthesis Pressure	69 Bar
Flash gas Recycle Ratio	0.9
Methanol Yield	0.29 kg/s
Methanol Purity Achieved	99.6 mol %
Gas Turbine Unit	
Turbine Power produced	7.39 MW
Compressor power Consumed	5.01 MW
Net Shaft Power Produced	2.3 MW
Turbine Inlet Temperature	1004°C
Steam network	25
Steam Pressure	25 Bar
Power Produced	4.65 MW

Cold Gas Efficiency	
Gasifier	93.5%
Gasifier + GCU	80.5 %
Methanol Synthesis	36.1 %
Overall Efficiency	
Net Power Consumed	9.11 MW
Net Power Produced	12 MW
Net Efficiency	**61%**

The gas cleaning unit, methanol synthesis, gas turbine unit and the steam network remain unchanged from the inputs explained in the previous case. The key change however is in the gasifier part of the model. Since, there is a separate stream of hydrogen added to the product gas stream, the need for a water gas shift reactor is now eliminated. The other major change is that hot air stream for combustion in the combustor is now much enriched because of the pure oxygen stream from electrolysis. This addition of pure oxygen would decrease the mass of char required for gasification. The inputs for the gasifer for the model however remain unchanged from the previous case. Two scenarios were simulated, similar to the previous case, one with active CO_2 removal in-situ during gasification and the second was without this CO_2 removal. the major changes are in the gasification temperature used which is discussed more elaborately in the following part of this section.

RESULTS

With inputs and limits similar to the case A, simulations were performed and the results of these simulations are discussed in this section. The results of the simulations are shown in Table 4.6 and Table 4.8 corresponding to the case without and with CO_2 removal respectively. Similarly two Sankey plots were made to visualise the energy flow within the model and they are shown in the Figure 4.4 and Figure 4.3. Key observations and talking points from the recorded results are discussed in the next part of this section.

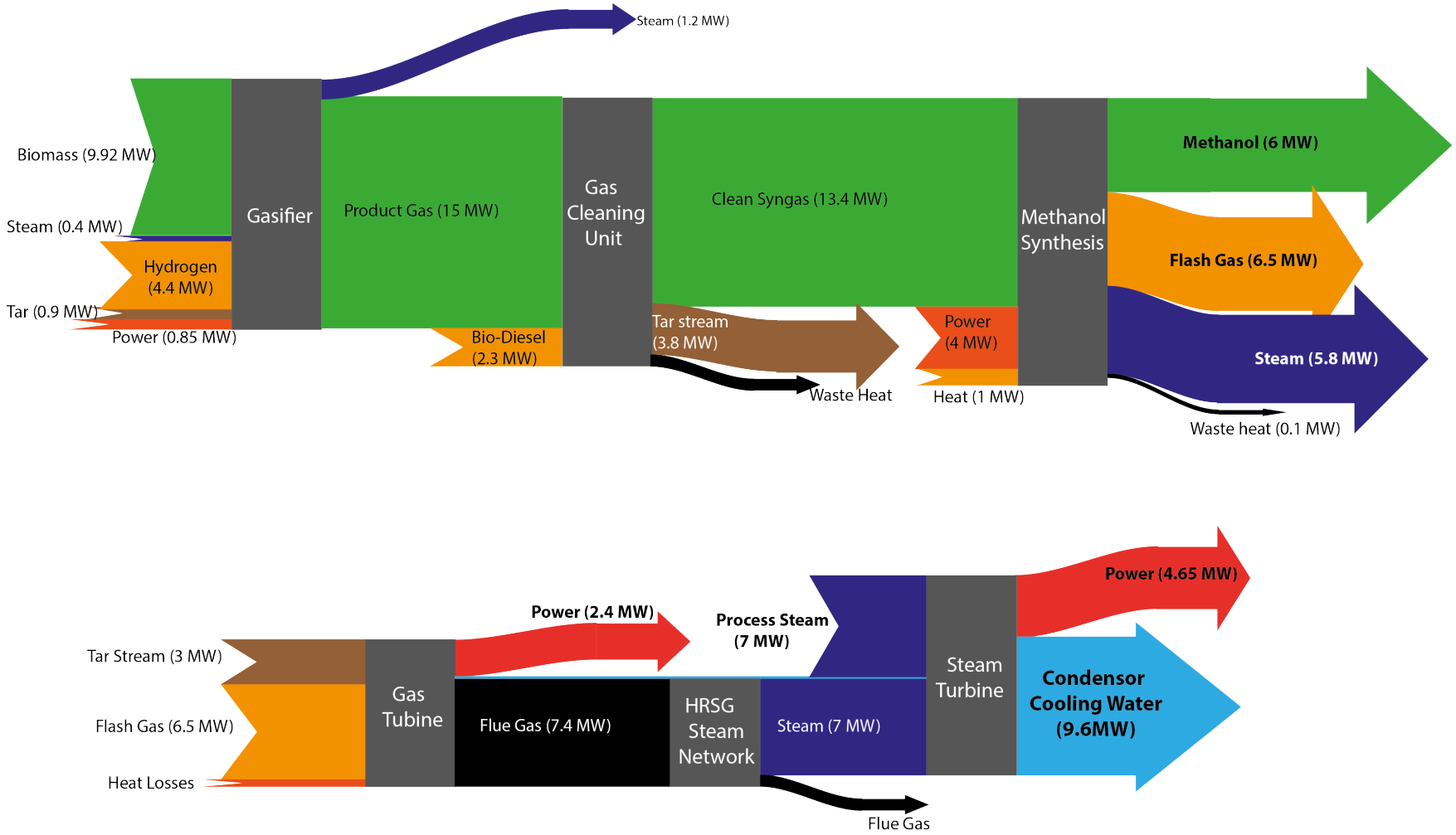

Figure 4.3: Sankey Plot for Case B - without in-situ CO_2 removal during gasification

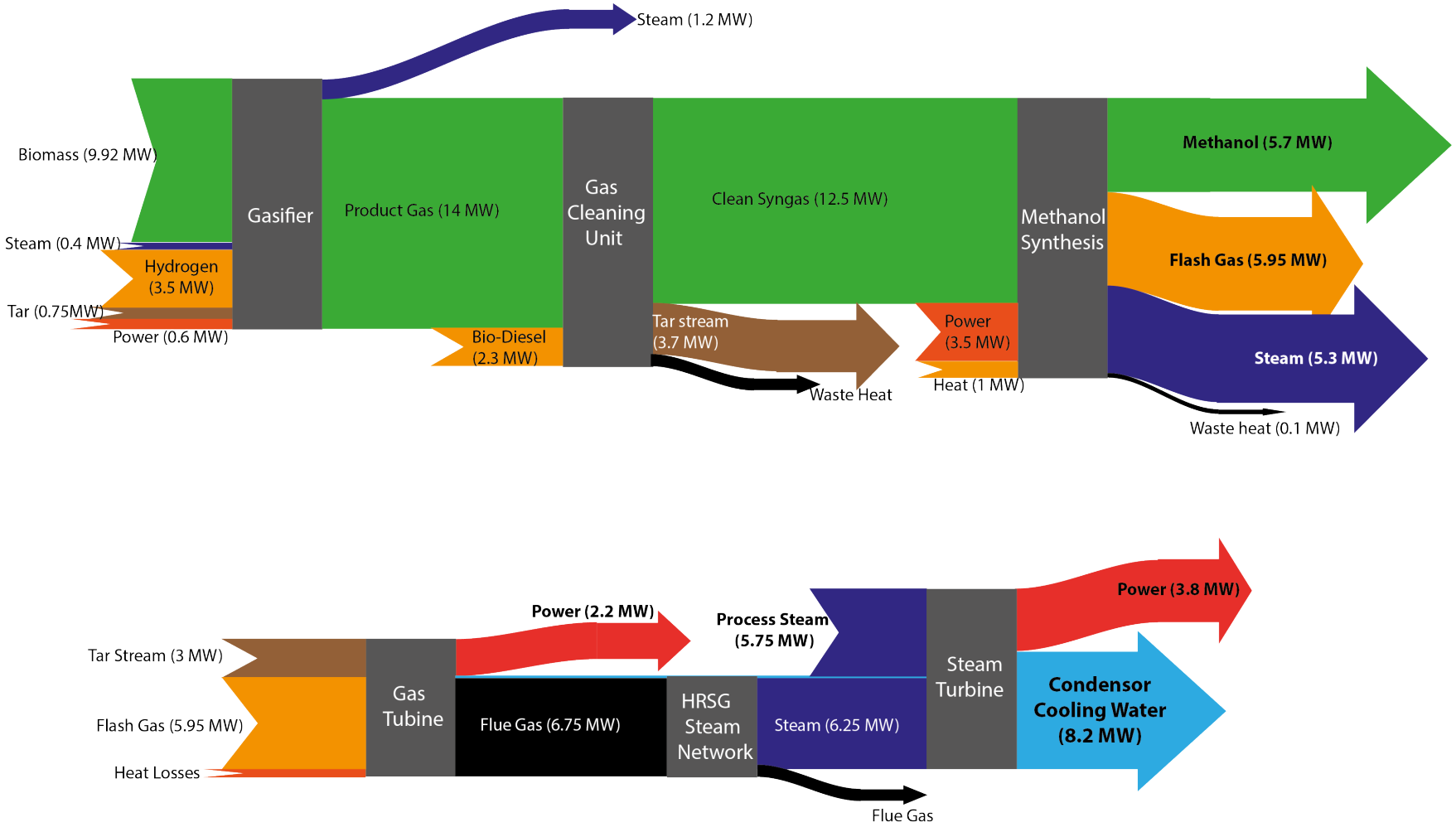

Figure 4.4: Sankey Plot for Case B - with in-situ CO_2 removal during gasification

OBSERVATIONS

Significantly reduced mass of char combusted. Mass of Char combusted in this case for both scenarios are significantly lower than the previous case. This can be mainly attributed to two factors: elimination of the water gas shift reactor and oxygen enriched combustion in the combustor. The heat demand of the water gas shift is mainly because the bed material needs to be cooled down to 450°C and then reheated again to gasification temperatures in the combustor. This cooling and reheating is very energy intensive and the results of this case prove its energy demand. The second factor is that, by using an enriched combustion in the combustor, the mass of air in the combustor is much reduced. This would reduce the amount of flue gas and hence increasing the efficiency of the combustor.

Efficiency of the gasification process is much higher compared to Case A. The addition of free hydrogen has eliminated the loss in the water gas shift reactor (compared to Case A) and this coupled with a very efficient combustion process, makes the product gas stream from the gasifier much more calorific than the previous case.

Effect of in-situ CO_2 removal is much less prominent in the gasifier. The advantages of in-situ CO_2 removal are well documented and were discussed previously in this study. A very interesting observation from the results of this case is that the gasifier efficiency more or less unchanged in both the cases. This could be attributed to the relatively reduced energy lost in the flue gas stream compared to the previous case. However, the effect of CO_2 removal is more prominent in the mass of hydrogen required by the gasifier to achieve stoichiometry for the methanol synthesis which signifies better H_2/CO ratio when dolomite is used as bed material.

A notable increase in both Cold Gas Efficiency and net efficiency can be observed compared to the previous case. The efficiency determined for the two scenarios in this case are notably higher than that of the previous case. This can be related to the increased gasifier efficiency that is cascaded onto the final methanol yield. This result goes on to emphasize how a relatively simple heat demand could affect the end methanol yield.

Significant energy losses warrant the need for further optimization, especially in the steam network and the Gas turbine Unit. Significant losses can be observed in steam network, the gas turbine and the methanol synthesis blocks. using a two or three stage steam network and further optimizing these blocks can increase the overall efficiency of the process.

4.3. CASES C & D: POWER GENERATION FROM BIOMASS GASIFICATION - IGCC

The third case considered was that of an IGCC - integrated Gasification Combined cycle. IGCC 's have long been implemented in commercial scales by numerous Siemens Gas Turbines and this simulation would help understand the advantages of a allothermal gasifier over a conventional IGCC with a air blown gasifier. The schematic of the model used is shown in Appendix C. Since the tar content from a typical allothermal gasifier is well within the requirements for combustion in a gas turbine, the need for a gas cleaning unit is eliminated. However, the particulate matter entrained with the product gas can be a problem in the gas turbine and hence a High Temperature Filter is used to remove the particulate matter in the product gas. One of the main assumptions used when designing the models in this study is that we assume no particulate matter to be entrained with the product stream. However, it is obviously not the realistic nature of how gasification works and this assumption was made mainly to simplify an already very complex model. Hence the high temperature filter shown in the flow sheet has no functional role in the model but just to show the chronology of such a filter system in the gasifier.

In the previous chapter, the boost in hydrogen flow in the product gas from the gasifier with dolomite was discussed (Figure 3.14). Hence, dolomite for its in-situ CO_2 removal ability was chosen as the bed material for this case. The other major inputs to the gasifier is same as the previous two cases. Since there is no Gas Cleaning Unit, there is no tar stream that is recycled back to the combustor as in the previous cases. As a result of this, the heat supplied by the recycled tar stream has to be compensated by increasing the mass of char combusted.

Table 4.10: Results of simulation for the Cases C and D: IGCC

	Conventional GT (Case C)	Inverted GT (Case D)
Gasifier		
Biomass Input Flow Rate	0.65 kg/s	
Calculated Input Biomass LHV (wet basis)	15.20 MJ/kg	
Product Gas Yield	0.62 kg/s	
Product gas LHV	15.22 MJ/kg	
Percentage of biomass combusted	20 %	
Gasification temperature	750°C	
Gasification Pressure	1 atm	
Energy supplied to produce steam	Recuperated internally	0.38 MW
Gas Turbine		
Pressure Ratio	20	3.76
Isentropic Efficiency	0.80	0.80
Turbine Inlet temperature	1004°C	1002°C
Turbine power produced	9.3 MW	3.1 MW
Compressor Power consumed	6.9 MW	1.58 MW
Net shaft power	2.35 MW	1.52 MW
Steam Cycle		
Steam pressure used	25 Bar	25 Bar
Power Produced	1.95 MW	2.8 MW
Net Efficiency of the Model	**43.3 %**	**41.75 %**

Case D represents power production from biomass gasification by means of an Inverted Brayton cycle. This is very similar to that of an IGCC but with an inverted Gas Turbine system in the place of a conventional gas Turbine unit. The main advantages (subsection 2.5.3) were in utilizing the thermal exergy in high temperature calorific fuel streams and extracting energy from these streams by combusting them and expanding them to sub-atmospheric pressures. The main strength of this technology is in its compactness in design and equipment required. However, since the combusted flue gas is expanded in a turbine to sub-atmospheric pressures, their pressure levels are usually not as high as conventional gas turbines and this can pose a stark disadvantage when compared to conventional gas turbines. However,previous literature on these IGT's do consider it more advantageous in micro scale gas turbines where the pressure ratios are limited to a a range between 4 - 8 [82]. A part reason behind simulating parallel simulations with a GT and an IGT is to understand how would these compare in a common but applied scenario as this.

Schematic of the model developed for the case D is shown in the Appendix C. The gasification conditions are maintained to be exactly the same in these two cases. The isentropic efficiency are assumed to be 0.8 for all the turbines and compressors in the both the cases C and D to aid easy comparison. Although, isentropic efficiency would realistically vary between the two cases based on their different scales. A steam cycle is used as a bottoming cycle in both the cases and the efficiency of the steam turbine is taken to be 0.8 for both the cases. Similar to the case C, a high temperature filter is used in the model to signal its need. The product gas stream is cooled down in a recuperator and the released heat is used to pre-heat air to the IGT. With a common gasification technology and inputs, the simulation results would help understand both these technologies by direct and easy comparison.

RESULTS AND OBSERVATIONS

The model showed in Appendix C were simulated and the results obtained are shown in the Table 4.10. A few straightforward observations from the attached results are discussed in this section.

Net shaft power from the IGT is much lower than the power output from the conventional Gas Turbine. This can be mainly attributed to the low pressure ratio of the IGT in case D in comparison with the conventional GT in Case C. Another cause for this low power output would be relatively lower isentropic efficiency when compared to the conventional Gas Turbine unit.

Net efficiency calculated for both the cases are much more comparable than the corresponding Gas Turbine efficiency. A lower turbine pressure ratio compared with a lower isentropic efficiency resulted in a larger heat transferred to the steam cycle in the IGT. This heat subsequently produced more steam than the conventional case yielding a higher power output from the steam turbine. This result signifies the need of a bottoming cycle or an appropriate heat demand to utilize the heat from the IGT. To reduce the compressor power, the flue gas from the turbine needs to be cooled as low as possible in an IGT. In other words, an inefficient recuperator between the turbine and compressor can have a drastic effect on the overall power output from the IGT. However, the net efficiency of the Case D is still lower than that of Case C.

4.4. DISCUSSION POINTS

EFFECT OF DOLOMITE

The scenarios simulated in the cases A and B were to understand the effect of dolomite on an already complex gasification process. The effect of dolomite on the composition of the product gas of an isolated gasifier was discussed previously in the Section Figure 3.2.1 and the results were plotted in Figure 3.14. However to predict the effect of this change in a compacted system such as methanol synthesis was still a uncertainty and a challenge. The results of this simulations now do shed better light on this uncertainty.

The most straightforward comparison that can be made between the Sankey plots in Figure 4.1 and Figure 4.2 is the overall methanol yield and the overall efficiency of the process. Cold gas efficiency of the gasifier is increased for the case with CO_2 removal compared to without CO_2 removal. This can be seen in the results of simulation of the first case (Table 4.6 and Table 4.7). This increased efficiency as a cascaded result can be seen to increase the end methanol yield. However, the net efficiency of the process is slightly lowered by CO_2 removal, mainly resulting from relatively lower power production. The major consequence of this result is that a relatively lower temperature gasification system can be more efficient than a high temperature gasification process by in-situ CO_2 removal. The new developments in gasification technology all seem to progress towards high temperature gasification at a temperature range between 800 - 900°C. This increase in gasification temperature does increase restrict the choice of gasifier design. Hence a lower temperature gasification process which can produce syngas of comparable or better quality would definitely aid the freedom of design of gasifiers and subsequent systems.

IDEAL OPERATING CONDITIONS OF THE GASIFIER

From the results of this study, favorable operating inputs for the gasifier can be roughly identified. The two input parameters with the biggest effect on the gasifier efficiency are the temperature of gasification and the Steam To Biomass Ratio (STBR). Increasing both have shown to increase the calorific value of the product gas by promoting its hydrogen fraction. However, a significant increase in the gasification temperature would need a larger portion of the biomass to be combusted, thereby reducing the net product gas yield. In the same manner, increasing the STBR would simply have no noticeable effect on the product gas composition, as evidenced from the water conversion plot shown in Figure 3.10b. Moreover, the energy required to heat this steam stream to gasification temperatures could hinder the overall energy efficiency of the gasifier.

The gasification temperature when dolomite is used as the bed material can be at a maximum of 750°C, if CO_2 is to be removed in-situ. For this case, we observe that the product gas can be as calorific as gasification at 850°C. At this temperature, from Figure 3.14 we observe that the hydrogen fraction of product gas remains relatively constant beyond a STBR of 0.55. Ideally the effects of AER at higher temperatures could give better insight whether this combination of higher gasification temperature and AER can possible negate the requirement of a water gas shift reactor. However, with a practical higher temperature constraint at 750°C for dolomite, the optimum conditions for operation of a gasifier of this nature could be fixed to be between a STBR of 0.5 - 0.8 and a gasification temperature of 750°C with in-situ CO_2 removal.

CHOICE OF SCRUBBING LIQUID IN THE GCU

This study chose Bio-diesel as the scrubbing liquid in the GCU, mainly because of its affinity to absorb tars that were modeled. However, with such a highly calorific scrubbing liquid, even the smallest loss makes its energy demand quite high. This can be easily observed in the Sankey plots where bio-diesel is the second heaviest input in terms of energy. Although this consumed bio-diesel is combusted in the gas turbine to produce energy, it is a significant loss nonetheless. Using a lesser volatile scrubbing liquid which can absorb

tars could mitigate this loss and thereby increasing the overall energy efficiency of the process. Using used vegetable oil could potentially be a replacement, because of its relatively low cost economic availability.

TAR STREAM RECYCLE

In the Sankey plots it can be observed that only a part of the tar stream is recycled back to the gasifier. It is very well possible that this tar stream can be completely recycled back to the gasifier, reducing the mass of char combusted. The FICFB gasifier does recycle the tars separated but the fraction that is recirculated is still unknown. Besides, the calorific value of the tar stream is mainly attributed to the fraction of bio-diesel that is stripped along with the tars. The technology and configuration of the gas cleaning unit majorly determines the flow and energy content of this tar stream. Hence, in this study, the fraction of tars were varied with a fixed char recycle fraction to best fit the product gas composition obtained from the FICFB gasifier.

METHANOL YIELD

The methanol yields from all the four simulations are poor. The cold gas efficiency of all the four cases is less than 36%, especially for the conventional methanol synthesis process (Case A) where the CGE drops to 25%. This low efficiency does call out the importance of a parallel heat recovery system such as the steam network and the gas turbine system. However, the overall efficiency of the system is now much lowered by the low cold gas efficiency for methanol production. Since the methanol yield is quite low, optimising the energy network (GT and steam network) would have a much lower impact on the overall efficiency when compared to the impact of increasing this methanol yield. From the sankey plots, it can be observed that even with a very optimistic recycle fraction (90%) in the methanol synthesis block, the amount of energy lost in the form of the stream of Flash Gas is very substantial. Although the mass flow of this flash Gas stream is very small compared to the recycled stream, the high hydrogen fraction in the stream increases the energy content of the flash gas stream. During the course of the methanol synthesis process, the stoichiometric ratio (Equation 2.6) increases, enriching the hydrogen fraction in the stream. To complete the study on why the conversion efficiency from biomass to methanol is low, the flow of carbon from the biomass was then mapped, as shown in Figure 4.5.

Since biomass is the only added source of carbon that converts to methanol, following the flow of carbon would present a different evaluation of the losses observed in the Sankey plots. The carbon flow plot shown is for the case A, Conventional Methanol synthesis process with in-situ CO_2 removal by dolomite in the gasifier. It can be observed that **only 16.5% of Carbon in the biomass is converted to methanol.**

The process of methanol synthesis is divided into different sub-processes and making the identification of carbon losses much easier. The pyrolysis converts the input biomass into volatile gases and char (and in theory into ash as well). A significant fraction of the char produced is then combusted in the combustor to sustain gasification as shown as the stream 'Char to Combustor'. The final product gas from the gasifier now contains only 69.25% of the carbon from the input biomass. Although, majorly unavoidable, the mass of carbon spent to combustion is still very significant. The product gas from the gasifier is then processed in the water gas shift reactor, increasing hydrogen fraction to achieve the required stoichiometry for methanol synthesis. This water gas shift reaction is promoted by removing CO_2 by dolomite. The removed CO_2 however does represent a loss of carbon mass from the system and this loss is shown to be 19.6%. In the next step, the Gas Cleaning Unit (GCU) removed the tars form the produced product gas which again is a loss of carbon mass from the process and this carbon mass lost in the tars is around 11.7%.

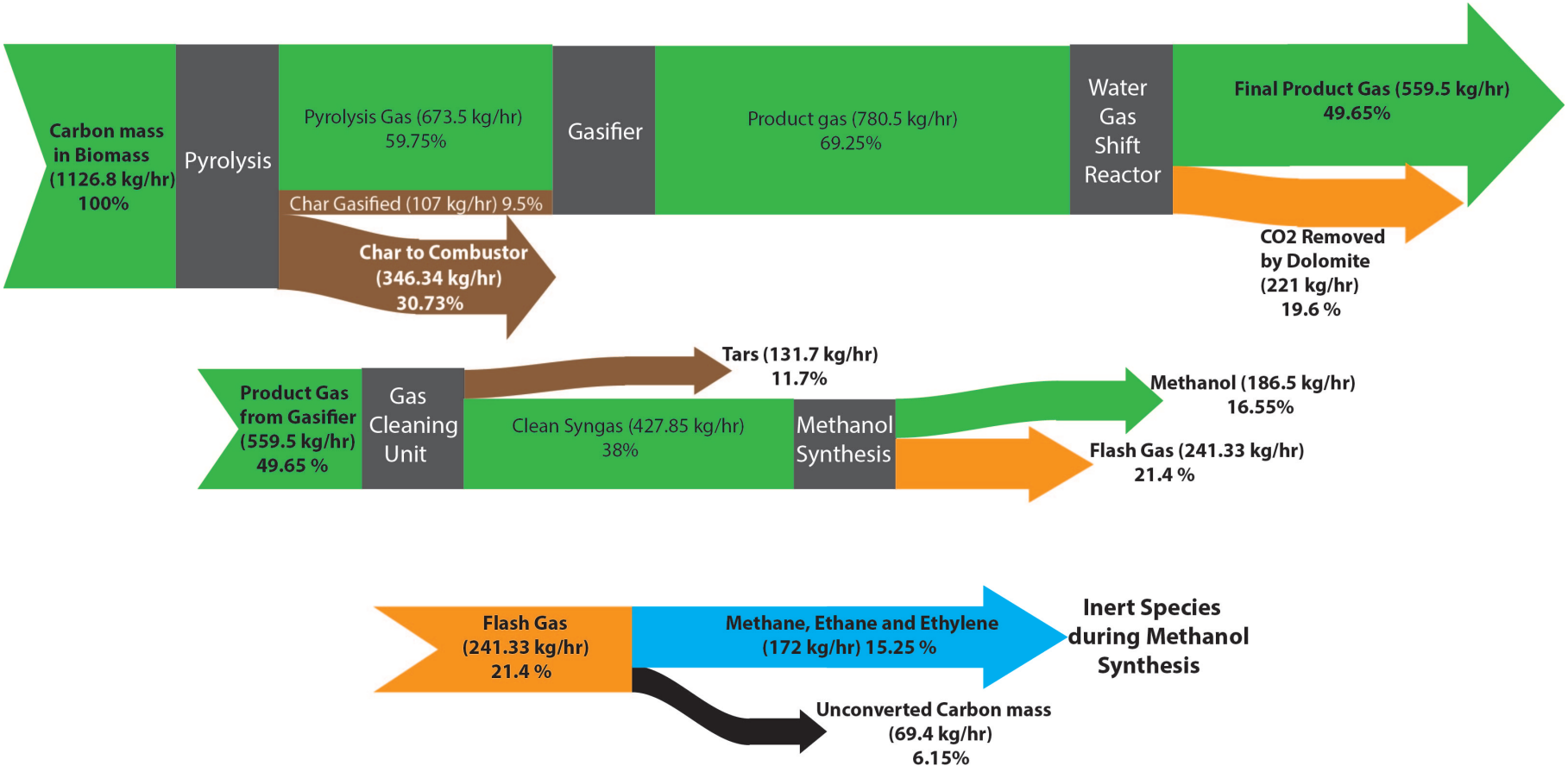

Figure 4.5: Carbon flow diagram for the Case A without in-situ CO_2 removal during gasification

Now only 38% of the carbon in the input biomass is input to the methanol synthesis block. The flash gas from the methanol synthesis block carries out a substantial 21.4% of carbon. This loss of carbon in the flash gas can be related to the energy lost in the flash gas stream in the Sankey plots. However, to completely understand and decide on the efficiency of the methanol synthesis block, the flash gas stream needs to be analyzed. Certain species originating from the pyrolysis of biomass are considered inert during the methanol synthesis process: Methane, Ethane, Ethene and the other tar species such as Benzene, Toluene, Phenol and Naphthalene. Since the tar species are detrimental to the catalysts used in the methanol synthesis process, these tars are removed a the gas cleaning unit. However, the gas cleaning unit is not designed to absorb the lighter hydrocarbons such as Methane, Ethane and Ethene and these lighter hydrocarbons are considered inert during the methanol synthesis. Hence the carbon mass in these three species represent a default a carbon loss that can not be converted into methanol. Hence, the flash gas stream can be split into to parts, the inert species and the unconverted carbon mass. From the results of the pyrolysis, the carbon fraction in both of these streams can be calculated. The actual amount of carbon lost in the flash gas which can be recovered by improving the methanol synthesis block is only 6.15%.

This analysis of carbon flow along with the Sankey plots for energy flow can provide a complete picture on the effectiveness of each of these blocks modeled in the model. The methanol synthesis reactor used in this simulation is a scaled down model of a commercial methanol synthesis plant. varying the configuration and size of the reactor may have a positive impact on the conversion efficiency of the methanol synthesis block. This was however beyond the scope of this study and all other parameters apart from this were optimized.

CHOICE OF GAS TURBINE TECHNOLOGY

Two different gas turbine technologies were compared in the case C and D of this study. By fixing the input variables in the gasifier, the comparison between the results of the two cases can be directly related to the gas turbine technology. The key factors of comparison were in the gas turbine efficiency and the overall efficiency of the system for both the cases. The inference from the results observed is that even at the Inverted gas turbine technology is not as efficient as the conventional gas turbine technology but the difference in efficiency between the two cases is not too large. The power produced is very dependant on the isentropic efficiency of the compressor and turbines in the gas turbine.

For a gas turbine system with a much smaller scale of power production, the isentropic efficiency tends to be low due to friction and heat loses. However, when the size of the gas turbine increases, the heat and friction loses become insignificant compared to the power produced, increasing its isentropic efficiency. For smaller cases, the isentropic efficeincy of the IGT would be higher than a GT due to the higher volumetric flow due to the sub-atmospheric operating pressure. Moreover, the power produced in the case of the IGT is majorly from the steam cycle. Hence, at lower scales, the IGT would be more efficient compared to the conventional gas turbine system. However, at higher scales, the disadvantage of lower pressure ratio of the IGT would make it less efficient than the conventional GT system.

One of the practical challenges of firing syngas in a gas turbine is problem of tar condensation in the moving parts of the gas Turbine system, especially in the compressor. This problem of condensation limits the inlet temperature of the syngas to the compressor. Since compressor work increases with increase in the inlet temperature of the syngas, work consumed for compression of syngas is usually not optimal. However, in the case of an Inverted Gas Turbine, this problem of tars is avoided as the first step is combustion. To draw exact conclusions between the suitability of either a conventional Gas Turbine system and a novel Inverted Gas Turbine system is very complicated by different technical, practical and also economical factors. However, the study does incline to a conclusion that Inverted Gas Turbine could me a more optimal choice at lower scales of power produced and conventional GT to be optimal at higher scales.

5

CONCLUSIONS

The base objective for this research was set out as to investigate biomass gasification and its practical importance. Since the syngas produced as a final product of gasification is only a starting step towards either fuel or power production, the research focused to investigate the integration of this gasification process with methanol synthesis. Following a detailed literature and technology study of different components required in the process of converting biomass into methanol and power, a single integrated model in Aspen Plus® was created. The model was divided into different functional blocks, which were then validated with their corresponding experimental data sourced from literature and thereby establishing the validity of the built model.

The practical purpose of this study was then extended to use the devloped model to predict, analyze and possibly improve different real life applications of utilizing biomass energy. Four different practical cases were then proposed, each considering different variations and improvements, whilst keeping the overall chronology of the process undisturbed. Variations ranging from dolomite to a new technology Inverted Gas Turbine technology were studied and simulated. The results of these simulations were then used to understand better the advantages and challenges of each of these cases and their variations. Although this study does acknowledge the number of practical assumptions and limitations considered when building this model, the results of the simulations do hold good for the purpose of understanding the inter-plays between different steps involved. To understand these inter-plays between different technologies and their functions thereby represent the underlying objective of this research.

At the beginning of this study, the objective of this research was consolidated into two key questions. This master thesis now concludes by answering these two questions.

Taking into consideration different experimental results of gasification studies, how accurately can this model predict the composition of the major product gas and operational conditions? The gasifier model developed is the bedrock of this study. Different allothermal gasifiers were studied and their developments investigated from published literature. The ECN Milena and the FICFB gasifier at Gussing were chosen as the most promising technologies and their experimental results were then collected. The gasifier model was then developed to reflect the FICFB gasification technology. The gasifier dimensions and operating conditions were designed to replicate the pilot plant of the FICFB gasifier and the results of the simulation and the collected data were then compared.

A number of output parameters were compared, ranging from the product gas composition to the tar concentration in the product gas. The results were plotted against recorded data and this comparison proves the accuracy of the built gasifier model to be within 3.5% for the product gas composition. The behaviour of the modeled gasifier was then validated with experiments conducted at the pilot plant of the FICFB gasifier. Sensitivity tests (Figures 3.8, 3.10b, 3.10a) done with the gasifier model prove that the gasifier model can replicate the behaviour of the actual pilot gasifier with very good accuracy. However, accuracy in predicting tar concentration is much more complicated since exact data on the bed material used in the pilot plant is still unknown. However, the built model can predict the tar concentration in the product gas stream with an accuracy of less than 0.5 g/Nm^3 for STBR's greater than 0.5. Moreover, the developed Aspen Plus® model

is quite sturdy and can easily be integrated with a downstream gas cleaning unit with a good level of accuracy.

With the discussed advantages of Absorption Enhanced Reforming (AER) on the gasification process, What are its effects on the overall process, producing methanol and power from biomass gasification? Upon choosing dolomite as the catalytic bed material to simulate the Absorption Enhanced Reforming principle in the modeled gasifier, the kinetics of sorption reaction was then validated with literature (Figure 3.13a). The effect of AER on the gasification process was then obtained and the simulated results were compared to the case without AER. The model developed validated the positive effect of dolomite, increasing the hydrogen composition in the product gas by 4% (Figure 3.14). Similarly, the effects of AER on the overall methanol synthesis process was then studied. Two simulations (Case A) were done, with and without AER to study the effect of AER. Although AER improved the cold gas efficiency of the gasifier (1.5%), the overall methanol yield for both the cases were considerably low. Upon further study, one of the main causes for this low methanol yield was identified as removal of CO_2 by dolomite in the water gas shift reactor (Figure 4.5). hence, despite the improvement of the gasification process, dolomite with this gasifier configuration (construction) is concluded to be detrimental to methanol yield when it is used as a sorbent/catalyst for the water gas shift reactor. However, this study does conclude by recommending the use of dolomite as the bed material only for the gasifier and using a separate catalyst that promotes water gas shift and doesn't remove CO_2 in the water gas shift reactor.

Could this model be used as a generic tool to compare the effect different choices in technology of these identified blocks on the performance of the overall process? Four practical cases of methanol and/or power production were discussed and simulated in the final part of the research. Individual blocks were first modeled and optimized by identifying different parameters. The optimized blocks were then integrated into a single model and the results of simulations were the used to draw a few conclusions. In all the models developed for the four cases, the base blocks remain the same. To couple each of these blocks differently and to generate a case by varying a parameter proves the versatility and the generic nature of the model.

Two different comparisons were studied: choice of a gas turbine technology and the choice of bed material in the gasifier. The effect of using dolomite over sand was simulated and the results were previously compared as the effect of Absorption Enhanced Reforming (AER). A promising Inverted Gas Turbine (IGT) technology was compared with a conventional Gas turbine system by simulating a IGCC case. The gasifier in the simulated IGCC was fixed, making comparison between the GT and IGT straightforward Table 4.10. The study discussed the effect of scale of power production on the comparison of the Gas Turbine technologies. The study concluded that the scale of power produced determined quantitatively the choice of Gas Turbine technology. Similarly, the model developed has been proven to be a capable tool to evaluate quantitatively different choices of technology in any of the identified blocks (gasifier, GCU, GT and methanol synthesis) within the process.

5.1. FURTHER RESEARCH

OPTIMIZATION

The modeled developed in this study was built on a Micro level approach. Optimization of individual blocks was done at a higher priority over optimizing the overall process. Each of the blocks identified and developed, the Gasifier, GCU, Methanol synthesis and the energy recovery blocks such as the steam network and the gas turbine block were optimizied by identifying variables within the block, in a near isolated fashion. Although certain key parameters that have a significant influence over the overall process were identified and optimized by performing several sensitivity tests, the scope and influence of these optimization steps are fairly limited. The next step that this research recommends is that a separate optimization algorithm such as Genetic or similar to be used to optimize a different design and operational variables to better optimize the process. The complexity in recycle and the inter dependant relationship between all the blocks could make this optimization process much challenging and hence is the reason why this Macro-level optimization was considered to be outside the scope of this study.

Similarly, one functional block which was not completely optimized is the Methanol synthesis block. The reactor dimensions were primarily scaled down data obtained from literature. However, choosing an optimum values for these physical parameters and data would involve a number of practical studies on technical

and economic feasibility. The considered values of the reactor design such as the reactor length, number of pipes and pipe diameter were varied to obtain a near ideal set of values but in reality, these obtained values may or may not reflect the optimal operating design of the reactor. **A more detailed analysis on these data used as inputs should be conducted to validate the obtained efficiency of the model.**

Performing such optimizations would require a better and a dedicated optimization algorithm such as a genetic or a sequential programmer, which would increase the complexity of the model manyfold. One possible measure to incorporate such an optimization scheme into an already complicated model would be to redesign the model with a much heavier dependence on Fortran. Since the key advantage of using Aspen Plus® is in obtaining property and interaction data between different species, creating an external Fortran program to generate and optimize results from the state points obtained from Aspen Plus® could reduce simulation time and increase accuracy of the model. However, doing so would require significant changes to the developed model and hence would be separate improvement step.

Since the model was developed for steady-state operating conditions, a major dependency on time has been eliminated. However, to understand the true complexities and the behaviour of such a system, a dynamic analysis of the developed model has to be performed. The existing model can be converted to be partially dynamic in operation as a first step but this would require additional physical data of the different blocks used. Hence, this study recommends combining this step with a Fortran based optimization sequence as the subsequent step to further this research.

PROCESS

Based on the results obtained from this study, the following can be recommended as future research pertaining the process,

- The carbon flow diagram, in Figure 4.5 showed the carbon loss due to sorption enhanced hydrogen enrichment in the water gas shift reactor by dolomite. Ideally, the carbon lost could have been converted to methanol in the subsequent stages. To quantitatively understand the actual loss of methanol yield due to dolomite, simulations using conventional water gas shift reactor with catalysts that promote hydrogen production by not removing CO_2 has to be done and studied.
- During the course of this study, we did come across literature on advanced catalysts which can be used as bed material (partly or completely) which can promote the tar reforming and hydrogen producing reactions with an activity greater than that of dolomite. This model can be used as a common tool to compare the effects of different bed materials. The most ideal scenario would be to achieve stoichiometry in the product gas composition at the gasifier exit so that the requirement of a separate water gas shift reactor could be negated.
- Scrubbing liquid consumption in the gas cleaning unit was the second heaviest energy input supplied to the system, as shown in the Sankey plots generated. Bio-Diesel was chosen as the scrubbing liquid mainly due to its better tar removal results from experiments. However, studying different scrubbing liquids with lesser volatility and economic value could greatly improve the overall efficiency of the system. Moreover, consuming Bio-Diesel roughly close to the same amount of methanol produced stains the sustainability in the process.
- The The flash gas stream from the methanol synthesis appears to be a large efficiency loss in the system. However, looking closely, the carbon flow diagram showed a significant fraction of this stream is the unconverted fraction of the inert methane, ethane and ethene species. Using a secondary reformer to crack and convert these inert species along with tars could increase the overall efficiency of the process.
- The reactor in the methanol synthesis block used in this study is a scaled down commercial reactor obtained from literature. Despite different sensitivity tests conducted to optimize the reactor dimensions, there is still room for further optimization as a reactor. Remodelling the reactor to suit the low scale of syngas flow from the gasifier in this study is hence recommended.
- A primary focus during the development of this model was to minimze the size of components designed. However, this was done understanding the trade-off between size and productivity. A economic analysis of the same model could help understand the validity of these choices. For example, the recycle ratio in the methanol synthesis block was limited to 0.9 since the throughput within the reactor

increased steeply upon increasing this recycle fraction. A economic study could prove the validity of this limit of 0.9.

- Inorganic elements in the biomass such as ash, nitrogen, sulfur and chlorine were not considered in this study. Including these elements would represent the reality of such a process. However, including these inorganic elements would raise the need for additional gas cleaning equipment to remove trace H_2S and other products formed during gasification. This added modeling is recommended as an extension of this existing model.

BIBLIOGRAPHY

[1] L. A. Davis, *Climate agreement,* Engineering **2**, 387 (2016).

[2] P. B. R. D. L. M. e. B. Metz, O.R. Davidson, *Climate Change 2007: Mitigation. Contribution of Working Group III to the Fourth Assessment Report of the Intergovernmental Panel on Climate Change* (Cambridge University Press, Cambridge, United Kingdom and New York, NY, USA., 2007).

[3] BP, *Statistical review of world energy 2017,* http://www.bp.com/en/global/corporate/energy-economics/statistical-review-of-world-energy.html, accessed: 16-09-2017.

[4] J. N. H. C. G. B. Jan Ros, Jos Olivier, *Sustainability of biomass in a bio-based economy* (PBL Netherlands Environmental Assessment Agency, 2012).

[5] U. S. E. protection Agency, *Sources of greenhouse gas emissions,* https://www.epa.gov/ghgemissions/sources-greenhouse-gas-emissions, accessed: 16-09-2017.

[6] P. M. Herder and R. M. Stikkelman, *Methanol-based industrial cluster design: A study of design options and the design process,* Industrial & Engineering Chemistry Research **43**, 3879 (2004), http://dx.doi.org/10.1021/ie030655j .

[7] P. Basu, *Biomass gasification and pyrolysis: practical design and theory* (Academic press, 2010).

[8] *Process: The potential for biomass in the energy mix,* Filtration & Separation **43**, 28 (2006).

[9] J. Goldemberg, *Ethanol for a sustainable energy future,* Science **315**, 808 (2007), http://science.sciencemag.org/content/315/5813/808.full.pdf .

[10] F. Cherubini, G. Jungmeier, M. Wellisch, T. Willke, I. Skiadas, R. Van Ree, and E. de Jong, *Toward a common classification approach for biorefinery systems,* Biofuels, Bioproducts and Biorefining **3**, 534 (2009).

[11] A. M. Wibisono, *Master thesis: Circulating fluidized bed of biomass gasification: Product compound prediction by application of a constrained equilibrium model,* (2016).

[12] J. Bourgois and R. Guyonnet, *Characterization and analysis of torrefied wood,* Wood Science and Technology **22**, 143 (1988).

[13] S. Heidenreich, M. Müller, and P. U. Foscolo, *Advanced Biomass Gasification: New Concepts for Efficiency Increase and Product Flexibility* (Academic Press, 2016).

[14] A. Gómez-Barea and B. Leckner, *Modeling of biomass gasification in fluidized bed,* Progress in Energy and Combustion Science **36**, 444 (2010).

[15] X. Meng, *Biomass-gasification: The understanding of sulfur, tar, and char reaction in fluidized bed gasifiers (tu delft),* .

[16] P. Basu, *Chapter 7 - gasification theory,* in *Biomass Gasification, Pyrolysis and Torrefaction (Second Edition)*, edited by P. Basu (Academic Press, Boston, 2013) second edition ed., pp. 199 – 248.

[17] I. Olofsson, A. Nordin, and U. Söderlind, *Initial Review and Evaluation of Process Technologies and Systems Suitable for Cost-Efficient Medium-Scale Gasification for Biomass to Liquid Fuels*, Tech. Rep. 05-02 (Mid Sweden University, Department of Engineering, Physics and Mathematics, 2005).

[18] S. Anis and Z. A. Zainal, *Tar reduction in biomass producer gas via mechanical, catalytic and thermal methods: A review,* Renewable and Sustainable Energy Reviews **15**, 2355 (2011).

[19] L. Devi, K. J. Ptasinski, and F. J. J. G. Janssen, *A review of the primary measures for tar elimination in biomass gasification processes : Devi, L. et al. Biomass and Bioenergy, 2003, 24, (2), 125–140,* Fuel and Energy Abstracts **44**, 125 (2003).

[20] C. E. D. of University of Michigan, *Encyclopedia of chemical engineering equipment - fluidized bed reactor,* (2014).

[21] C. Van der Meijden and van der MEIJDEN, *ECN Energy Research of the Netherlands*, December (2010) p. 206.

[22] N. Panayiotis, *Master thesis: Removal, utilization and separation of tars form syngas,* (2016).

[23] W. A. Punjak and F. Shadman, *Aluminosilicate sorbents for control of alkali vapors during coal combustion and gasification,* Energy & Fuels **2**, 702 (1988).

[24] B. Dou, W. Shen, J. Gao, and X. Sha, *Adsorption of alkali metal vapor from high-temperature coal-derived gas by solid sorbents,* Fuel Processing Technology **82**, 51 (2003).

[25] S. R. Rieger M, Mönter D, *No Title,* in *High temperature gas cleaning Volume II* (Karlsruhe: Institut für Mechanische Verfahrenstechnik und Mechanik Universität, Karlsruhe, 1999) p. 760–71.

[26] D. E. M. P. Bachovchin DM, Alvin MA, *A study of alkali in pressurized gasification system*, Tech. Rep. (Westinghouse Research and Development Center, Chemical Sciences Division, Pittsburgh, 1986).

[27] K. J. Wolf, M. Müller, K. Hilpert, and L. Singheiser, *Alkali sorption in second-generation pressurized fluidized-bed combustion,* Energy and Fuels **18**, 1841 (2004).

[28] M. Diaz-Somoano and M. R. Martínez-Tarazona, *Retention of zinc compounds in solid sorbents during hot gas cleaning processes,* Energy and Fuels **19**, 442 (2005).

[29] M. Riess and M. Müller, *High temperature sorption of arsenic in gasification atmosphere,* Energy and Fuels **25**, 1438 (2011).

[30] O. P. Neeft JPA, Knoef HAM, *Behaviour of tar in biomass gasification systems : tar related problems and their solutions*, Tech. Rep. (Energy from waste and biomass(EWAB), November Report No: 9919, 1999).

[31] P. Bergman, S. van Paasen, and H. Boerrigter, *The novel "OLGA" technology for complete tar removal from biomass producer gas,* Pyrolysis and Gasification of Biomass and Waste , 10 (2002).

[32] T. Bui, R. Loof, and S. C. Bhattacharya, *Multi-stage reactor for thermal gasification of wood,* Energy **19**, 397 (1994).

[33] T. A. Milne, R. J. Evans, and N. Abatzaglou, *Biomass Gasifier"Tars": Their Nature, Formation, and Conversion*, Tech. Rep. (National Renewable Energy Laboratory, Golden, CO (US), 1998).

[34] P. Hasler, R. Bühler, and T. Nussbaumer, *Evaluation of gas cleaning technologies for biomass gasification,* in *Biomass for Energy and Industry Conference* (1998).

[35] H. Hofbauer, R. Rauch, and K. Ripfel-Nitsche, *Report on gas cleaning for synthesis applications–work package 2e:„gas treatment",* Wien (Österreich) (2007).

[36] P. Hasler and T. Nussbaumer, *Gas cleaning for ic engine applications from fixed bed biomass gasification,* Biomass and Bioenergy **16**, 385 (1999).

[37] H. Hofbauer, *Biomass gasification for electricity and fuels, large scale,* in *Encyclopedia of Sustainability Science and Technology*, edited by R. A. Meyers (Springer New York, New York, NY, 2017) pp. 1–24.

[38] K. Zhang, H. T. Li, Z. S. Wu, and T. Mi, *The Thermal Cracking Experiment Research of Tar Model Compound,* 2009 International Conference on Energy and Environment Technology , 655 (2009).

[39] C. M. Kinoshita, Y. Wang, and J. Zhou, *Tar formation under different biomass gasification conditions,* Journal of Analytical and Applied Pyrolysis **29**, 169 (1994).

[40] Q. Yu, C. Brage, G. Chen, and K. Sjöström, *Temperature impact on the formation of tar from biomass pyrolysis in a free-fall reactor,* Journal of Analytical and Applied Pyrolysis **40-41**, 481 (1997).

[41] J. Zhou, S. M. Masutani, D. M. Ishimura, S. Q. Turn, and C. M. Kinoshita, *Release of fuel-bound nitrogen during biomass gasification,* Industrial and Engineering Chemistry Research **39**, 626 (2000).

[42] J. Fjellerup, B. Gøbel, J. Ahrenfeldt, and U. Henriksen, *Formation , Decomposition and Cracking of Biomass Tars in Gasification*, April (2005) pp. 1–60.

[43] I. Narvaez, A. Orıo, M. P. Aznar, and J. Corella, *Biomass Gasification with Air in an Atmospheric Bubbling Fluidized Bed . Effect of Six Operational Variables on the Quality of,* Ind. Eng. Chem. Res. **35**, 2110 (1996).

[44] P. Aznar, M. A. Caballero, J. Gil, and J. A. Martı, *99/01160 Commercial steam reforming catalysts to improve biomass gasification with steam-oxygen mixtures. 2. Catalytic tar removal,* Fuel and Energy Abstracts **40**, 119 (1999).

[45] J. Gil, M. P. Aznar, M. A. Caballero, E. Francés, and J. Corella, *Biomass gasification in fluidized bed at pilot scale with steam- oxygen mixtures. product distribution for very different operating conditions,* Energy & Fuels **11**, 1109 (1997).

[46] V. Minkova, S. P. Marinov, R. Zanzi, E. Björnbom, T. Budinova, M. Stefanova, and L. Lakov, *Thermochemical treatment of biomass in a flow of steam or in a mixture of steam and carbon dioxide,* Fuel processing technology **62**, 45 (2000).

[47] M. Siedlecki, W. De Jong, and A. H. Verkooijen, *Fluidized bed gasification as a mature and reliable technology for the production of bio-syngas and applied in the production of liquid transportation fuels—a review,* Energies **4**, 389 (2011).

[48] F. Walawender WP, Ganesan S, *Steam gasification of manure in fluid bed. Influence of limestone as bed additive.* Symposium papers on Energy from Biomass and Wastes **517-27** (1981).

[49] J. Delgado, M. P. Aznar, and J. Corella, *Calcined Dolomite, Magnesite, and Calcite for Cleaning Hot Gas from a Fluidized Bed Biomass Gasifier with Steam: Life and Usefulness,* Industrial & Engineering Chemistry Research **35**, 3637 (1996).

[50] J. Corella, M. Aznar, J. Gil, and M. Caballero, *Biomass gasification in Iuidised bed: where to locate the dolomite to improve gasi cation?* Energy and Fuels **13**, 1122 (1999).

[51] W. Wang, N. Padban, Z. Ye, A. Andersson, and I. Bjerle, *Kinetics of Ammonia Decomposition in Hot Gas Cleaning,* Industrial & Engineering Chemistry Research **38**, 4175 (1999).

[52] B. M. Baker EG, Mudge LK, *Methanol and ammonia from biomass,* Chemical Engineering Progress **80(12)**, 43 (1984).

[53] Z. Abu El-Rub, E. a. Bramer, G. Brem, and et al., *Review of Catalysts for Tar Elimination in Biomass Gasification Processes,* Industrial & Engineering Chemistry Research **45**, 75 (2004).

[54] E. G. Baker, L. K. Mudge, and M. D. Brown, *Steam Gasification of Biomass with Nickel Secondary Catalysts,* Industrial & Engineering Chemistry Research **26**, 1335 (1987).

[55] S. K. Chembukulam, A. S. Dandge, N. L. Kovllur, and R. K. Seshaglri, *I–l,* **719**, 714 (1981).

[56] Z. A. El-Rub, E. Bramer, and G. Brem, *Experimental comparison of biomass chars with other catalysts for tar reduction,* Fuel **87**, 2243 (2008).

[57] H. Hofbauer, R. Rauch, G. Loeffler, S. Kaiser, E. Fercher, and H. Tremmel, *Six years experience with the FICFB-gasification process,* 12th European Conference and Technology Exhibition on Biomass for Energy, Industry and Climate Protection , 982–985 (2002).

[58] H. Hofbauer, E. Fercher, T. Fleck, R. Rauch, and G. Veronik, *Two years experience with the FICFB-gasification process,* 10th European Conference and Technology Exhibition, Wurzburg , 3 (1998).

[59] H. Hofbauer and R. Rauch, *Stoichiometric Water Consumption of Steam Gasification by the FICFB-Gasification Process,* Progress in Thermochemical Biomass Conversion , 199 (2008).

[60] S. Koppatz, C. Pfeifer, R. Rauch, H. Hofbauer, T. Marquard-Moellenstedt, and M. Specht, *H2 rich product gas by steam gasification of biomass with in situ co2 absorption in a dual fluidized bed system of 8 mw fuel input,* Fuel Processing Technology **90**, 914 (2009).

[61] N. Poboss, K. Swiecki, A. Charitos, C. Hawthorne, M. Zieba, and G. Scheffknecht, *Experimental investigation of the absorption enhanced reforming of biomass in a 20 kwth dual fluidized bed system,* International Journal of Thermodynamics **15**, 53 (2012).

[62] N. H. Florin and A. T. Harris, *Hydrogen production from biomass coupled with carbon dioxide capture: the implications of thermodynamic equilibrium,* International Journal of Hydrogen Energy **32**, 4119 (2007).

[63] C. M. V. D. Meijden, H. J. Veringa, a. V. D. Drift, and B. J. Vreugdenhil, *The 800 kWth allothermal biomass gasifier MILENA,* , 2 (2008).

[64] H. Leibold, A. Hornung, and H. Seifert, *HTHP syngas cleaning concept of two stage biomass gasification for FT synthesis,* Powder Technology **180**, 265 (2008).

[65] H. Boerrigter, S. Van Paasen, P. Bergman, J. Könemann, R. Emmen, and A. Wijnands, *Olga tar removal technology,* Energy research Centre of the Netherlands, ECN-C–05-009 (2005).

[66] J. D. Seader, E. J. Henley, and D. K. Roper, *Separation process principles,* (1998).

[67] S. Lee, *Methanol synthesis technology* (CRC Press, 1989).

[68] H.-W. Lim, M.-J. Park, S.-H. Kang, H.-J. Chae, J. W. Bae, and K.-W. Jun, *Modeling of the kinetics for methanol synthesis using cu/zno/al2o3/zro2 catalyst: Influence of carbon dioxide during hydrogenation,* Industrial & Engineering Chemistry Research **48**, 10448 (2009), http://dx.doi.org/10.1021/ie901081f .

[69] S. Lee, *Reaction mechanisms in liquid-phase methanol synthesis*, Tech. Rep. (Electric Power Research Inst., Palo Alto, CA (USA); Akron Univ., OH (USA). Dept. of Chemical Engineering, 1990).

[70] A. Cybulski, *Liquid-phase methanol synthesis: catalysts, mechanism, kinetics, chemical equilibria, vapor-liquid equilibria, and modeling—a review,* Catalysis Reviews—Science and Engineering **36**, 557 (1994).

[71] L. Chen, Q. Jiang, Z. Song, and D. Posarac, *Optimization of methanol yield from a lurgi reactor,* Chemical engineering & technology **34**, 817 (2011).

[72] T. Gibbons and I. G. Wright, *A review of Materials for gas turbines firing syngas fuels*, Tech. Rep. (Oak Ridge National Laboratory (ORNL), 2009).

[73] V. Poloczek and H. Hermsmeyer, *Modern Gas Turbines with High Fuel Flexibility,* POWER-GEN Asia (2008).

[74] M. J. A. Tijmensen, A. P. C. Faaij, C. N. Hamelinck, and M. R. M. Van Hardeveld, *Exploration of the possibilities for production of Fischer Tropsch liquids and power via biomass gasification,* Biomass and Bioenergy **23**, 129 (2002).

[75] H. Li, H. Hong, H. Jin, and R. Cai, *Analysis of a feasible polygeneration system for power and methanol production taking natural gas and biomass as materials,* Applied Energy **87**, 2846 (2010).

[76] I. M. Smith, *Gas turbine technology for syngas/hydrogen in coal-based IGCC* (IEA Clean Coal Centre, 2009).

[77] S. Gadde, J. Wu, A. Gulati, G. Mcquiggan, B. Koestlin, and B. Prade, *Syngas capable combustion systems development for advanced gas turbines,* Proceedings of ASME Turbo Expo 2006 , 1 (2006).

[78] M. Moliere, *Hydrogen-fueled Gas Turbines: Status and Prospects,* (Presentation at 2nd CAME-GT Conference,, Bled, Slovenia., 2004).

[79] M. C. Lee, S. B. Seo, J. H. Chung, S. M. Kim, Y. J. Joo, and D. H. Ahn, *Gas turbine combustion performance test of hydrogen and carbon monoxide synthetic gas,* Fuel **89**, 1485 (2010).

[80] E. O. Oluyede and J. N. Phillips, *Gt2007-27385 Fundamental Impact of Firing Syngas in Gas Turbines,* Most , 1 (2007).

[81] M. S. Johnson, *Prediction of gas turbine on-and off-design performance when firing coal-derived syngas,* Journal of engineering for gas turbines and power **114**, 380 (1992).

[82] M. Henke and T. Monz, *Inverted Brayton Cycle With Exhaust Gas Recirculation — A Numerical Investigation,* **135**, 1 (2017).

[83] M. Bianchi, G. Negri di Montenegro, A. Peretto, and P. Spina, *A feasibility study of inverted brayton cycle for gas turbine repowering,* Journal of Engineering for Gas Turbines and Power(Transactions of the ASME) **127**, 599 (2005).

[84] L. Abdelouahed, O. Authier, G. Mauviel, J. P. Corriou, G. Verdier, and A. Dufour, *Detailed Modeling of Biomass Gasi fi cation in Dual Fluidized Bed Reactors under Aspen Plus,* (2012).

[85] S. Srinivas, R. P. Field, and H. J. Herzog, *Modeling Tar Handling Options in Biomass Gasification,* (2013).

[86] E. Mostafavi, M. H. Sedghkerdar, and N. Mahinpey, *Thermodynamic and kinetic study of co2 capture with calcium based sorbents: experiments and modeling,* Industrial & Engineering Chemistry Research **52**, 4725 (2013).

[87] A. Dufour, P. Girods, E. Masson, Y. Rogaume, and A. Zoulalian, *Synthesis gas production by biomass pyrolysis: effect of reactor temperature on product distribution,* international journal of hydrogen energy **34**, 1726 (2009).

[88] N. H. Florin and A. T. Harris, *Enhanced hydrogen production from biomass with in situ carbon dioxide capture using calcium oxide sorbents,* **63**, 287 (2008).

[89] G. Bassil, I. Mokbel, R. A. Naccoul, J. Stephan, J. Jose, and C. Goutaudier, *Tar removal from biosyngas in the biomass gasification process.(liquid+ liquid) equilibrium {water+ solvent (paraxylene and methyl hexadecanoate)+ model molecules of tar (benzene, toluene, phenol)}*, The Journal of Chemical Thermodynamics **48**, 123 (2012).

[90] K. V. Bussche and G. Froment, *A steady-state kinetic model for methanol synthesis and the water gas shift reaction on a commercial cu/zno/al 2 o 3 catalyst,* Journal of Catalysis **161**, 1 (1996).

[91] P. Sun, J. R. Grace, C. J. Lim, and E. J. Anthony, *Determination of intrinsic rate constants of the cao–co2 reaction,* Chemical Engineering Science **63**, 47 (2008).

[92] G. Graaf, J. Winkelman, E. Stamhuis, and A. Beenackers, *Kinetics of the three phase methanol synthesis,* Chemical Engineering Science **43**, 2161 (1988).

[93] W. L. Luyben, *Design and control of a methanol reactor/column process,* Industrial & Engineering Chemistry Research **49**, 6150 (2010).

[94] C. Charlton, *Germany pays people to use electricity: Excess energy created by wind and solar power meant consumers made a profit as prices were driven so low they went negative,* http://www.dailymail.co.uk/news/article-3584461/Germany-PAYS-people-use-electricity-Excess-energy-created-wind-solar\-power-meant-consumers-profit-prices-driven-low-went-NEGATIVE.html, accessed: 11-05-2017.

[95] I. Petersen and J. Werther, *Experimental investigation and modeling of gasification of sewage sludge in the circulating fluidized bed,* **44**, 717 (2005).

[96] Y. Wang and C. Kinoshita, *Kinetic model of biomass gasification,* Solar energy **51**, 19 (1993).

[97] A. Dufour, A. Celzard, B. Ouartassi, F. Broust, V. Fierro, and A. Zoulalian, *Effect of micropores diffusion on kinetics of ch 4 decomposition over a wood-derived carbon catalyst,* Applied Catalysis A: General **360**, 120 (2009).

[98] Wang, L. Jiang, Cai, Pan, Zhao, W. Huang, Xie, Li, Sun, and B. Zhong, *Surface structure sensitivity of the watergas shift reaction on cu(hkl) surfaces: a theoretical study,* The Journal of Physical Chemistry B **107**, 557 (2003), http://dx.doi.org/10.1021/jp0215567 .

[99] Y. Su, Y. Luo, Y. Chen, W. Wu, and Y. Zhang, *Experimental and numerical investigation of tar destruction under partial oxidation environment,* Fuel Processing Technology **92**, 1513 (2011).

A

ASPEN PLUS® MODEL DESCRIPTION

The tables A.1 and A.2 explains the function of different blocks in the developed aspen model.

Table A.1: Description of the different Aspen Plus® modules used in this study - 1

Module Name	Scheme	Unit operation	Operating Parameters	Comments
Mixer	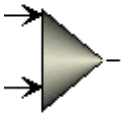	Flow Mixer	Mixes one or more streams together	
Yield Reactor (RYIELD)	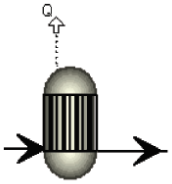	Reactor	Adiabatic Reactor with Output Temperature calculated by Enthalpy balance.	The Pyrolysis reaction is simulated in RYIELD Reactor called PYRGAS. The mass yields are defined in a FORTRAN file as a function of the bed material Temperature. This reactor is set to adiabatic by defining the Net Duty of the reactor as Zero.
Separation Column	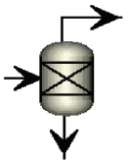	Separation	Separates the input stream between two or more streams with the input of separation degree or fraction.	Primarily used for gas-solid separation in the process model. Only exception where a separator block is used for a gas - gas separation is to separate inorganic gases from the process gases in the block INORSEP
RPlug (Plug Flow Rector)		Reactor	Plug flow reactor used to simulate the free-board of the gasifier and the methanol synthesis reactions.	Kinetics of different homogeneous and heterogeneous reactions are used to simulate different zones of the gasifier and the complete methanol synthesis process.
RCSTR	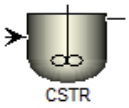	Constantly Stirred Tank Reactor (CSTR)	CSTR is used to simulate mainly the three phase reactions of the gasifier and the Water Gas Shift reactor	The heterogeneous reactions of gasification and the Water Gas Shift reactor are simulated in a CSTR with previously defined reaction kinetics. Primarily operated as Adiabatic with no pressure loss.
Stoichiometric Reactor	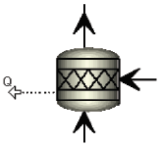	Reactor	Used to simulate reactions with known stoichiometry and conversion extent	Primarily used to simulate combustion reactions of the gasifier and the Gas Turbine unit. The RSTOIC module can generate its own combustion equations depending on the reactants supplied.
FSPLIT	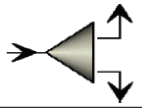	Flow divider	Used to split a stream into two or more streams.	The FSPLIT module is not capable of altering the mole fraction of the split streams but only the fraction split.
RADFRAC	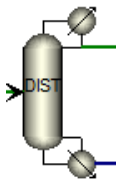	Distillation Column	Rigorous fractionation (RadFrac), is a multistage separation module used to simulate liquid - gas separation methods such as Absorption, Stripping and distillation.	Primarily considered adiabatic in the Gas Cleaning Unit, the RadFrac columns Absorber and Collector simulate the absorption and stripping processes. In the Methanol synthesis block, RadFrac unit DIST is used to simulate the methanol - water distillation separation process.

Table A.2: Description of the different Aspen Plus® modules used in this study - 2

Module Name	**Scheme**	**Unit operation**	**Operating Parameters**	**Comments**
Flash	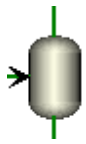	Flash Separator	Used to separate gas and liquid from a stream.	The Flash module is used to remove the condensate from a mixed stream in the Gas Cleaning Unit and the methanol synthesis blocks.
Heater	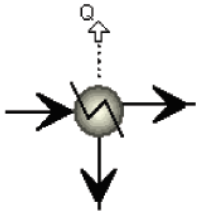	Heater /Cooler	Temperature increase or the outlet temperature or the vapor fraction of the stream can be specified to heat or cool the stream.	
Heat Exchanger	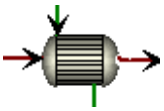	Heat Exchanger	Different modes of operation such as Shell and Tube or Plate type exchangers can be chosen	The heat exchanger module used in this model are always of the shortcut mode of Shell and Tube. By specifying the pinch / outlet temperature, the TQ curves and the outlet temperature of the other stream is calculated by Aspen plus.
Pump	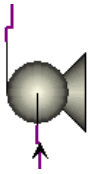	Pump	used to increase pressure of liquid streams. Mainly water in the steam network and oil pressure in the Gas Cleaning Unit.	
Compressor / Turbine	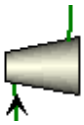	Compressor / Turbine	Can function either as a turbine or a compressor. Used to increase or decrease pressure of gas/mixed streams.	Isentropic Efficiency of the compressors and turbines are defined based on the mass flow rate of the stream compressed/expanded.

B

Reaction Kinetics

B.1. Gasifier

Kinetics for set 1

The first set of gasification reactions chosen as a set is shown in Table B.1. The corresponding reaction kinetics used is referred to as set 1 and is shown in the tables, Table B.2 and Table B.3. Table B.3 represents the tar gasification reactions and Table B.2 represents the other main gasification reactions simulated. The reaction numbers are numbered with a suffix 'R' and the corresponding reaction kinetics can be found starting with a suffix 'K' with the same number.

Table B.1: List of Gasification Reactions simulated in the reaction **set 1**

Reaction Name	**Reaction Type**	**Reaction Expression**
Pyrolysis	R1	$\text{Biomass} \longrightarrow \text{Volatiles(VM)} + \text{Char} + a_1C_6H_6 + a_2C_6H_6O + a_3C_7H_8 + a_4c_{10}H_8 + a_5H_2O$ $\text{VM} \longrightarrow b_1CO + b_2CO_2 + b_3H_2 + b_4CH_4 + b_5N_2 + b_6C_2H_4 + b_7C_2H_6$
Char Steam Reforming	R2	$C + 1.2H_2O \longrightarrow 0.8CO + 0.2CO_2 + 1.2H_2$
Char Oxidation	R3	$\alpha C + O_2 \longrightarrow 2(\alpha-1)CO + (2-\alpha)CO_2$
Boudouard Reaction	R4	$C + CO_2 \longrightarrow 2CO$
Water Gas Shift	R5	$CO + H_2O \longleftrightarrow CO_2 + H_2$
Methane Steam Reforming	R6	$CH_4 + H_2O \longleftrightarrow CO + 3H_2$
Naphthalene	R7	$C_{10}H_8 \longrightarrow 9C + \frac{1}{6}C_6H_6 + \frac{7}{2}H_2$
Toluene	R8	$C_7H_8 + H_2 \longrightarrow C_6H_6 + CH_4$
Benzene	R9	$C_6H_6 + H_2O \longrightarrow 3C + 2CH_4 + CO$
Phenol	R10	$C_6H_6O \longrightarrow CO + 0.4C_{10}H_8 + 0.15C_6H_6 + 0.1CH_4 + 0.75H_2$

Table B.2: Kinetics (**set 1**) used for the main gasification reactions used in the developed Aspen Plus model

	Reaction	Reaction Kinetics	Reactor name	Source
K1	Pyrolysis	Correlations in Table 3.3	PYRGAS	[84]
K2	Char Steam Reforming	$r_{(2)} = \frac{k_{(2)} c_{H_2O}}{1 + K^{(2)}_{k-H_2O} c_{H_2O} + K^{(2)}_{k-H_2} c_{H_2} + K^{(2)}_{k-CO} c_{CO}} f_{(2)}$ $f_{(2)} = 0.5$ $k_{(2)} = 2.39 * 10^2 (m^3/s \cdot mol)\ \exp(-\frac{129{,}000\,(J/mol)}{RT}) \frac{\rho_{char}}{M_C} (1-X)$ $K^{(2)}_{k-H_2O} = 3.16 * 10^{-2} (m^3/mol)\ \exp(-\frac{30{,}100\,(J/mol)}{RT})$ $K^{(2)}_{k-H_2} = 5.36 * 10^{-3} (m^3/mol)\ \exp(-\frac{59{,}800\,(J/mol)}{RT})$ $K^{(2)}_{k-CO} = 8.25 * 10^{-5} (m^3/mol)\ \exp(-\frac{96{,}100\,(J/mol)}{RT})$ X = 0.5	PLUG	[95]
K3	Char Oxidation	$r_{(3)} = 1.426 * 10^5 (kmol/m^3 \cdot s)\ \exp(-\frac{59.9\,(kJ/mol)}{RT}) c_{O_2} f_{(3)}$ $f_{(3)} = 3$	PLUG	[95]
K4	Boudouard Reaction	$r_{(4)} = \frac{k_{(4)} c_{CO_2}}{1 + K^{(4)}_{k-CO_2} c_{CO_2} + K^{(4)}_{k-CO} c_{CO}} f_{(4)}$ $f_{(4)} = 1$ $k_{(4)} = 4.89 * 10^7 (m^3/s \cdot mol)\ \exp(-\frac{268{,}000\,(J/mol)}{RT}) \frac{\rho_{char}}{M_C} (1-X)$ $K^{(4)}_{k-CO_2} = 6.60 * 10^{-2} (m^3/mol)$ $K^{(4)}_{k-CO} = 0.12 (m^3/mol)\ \exp(-\frac{268{,}000\,(J/mol)}{RT})$ X = 0.35	CSTR	[95]
K5	Water Gas Shift	$r_{(5)} = k_{(5)} (c_{CO} c_{H_2O} - \frac{c_{CO_2} c_{H_2}}{K_{(5)eq}}) f_{(5)}$ $f_{(5)} = 0.1$ $k_{(5)} = 2.778 (m^3/mol \cdot s)\ \exp(-\frac{180{,}032\,(J/mol)}{RT})$ $K_{(7)_{eq}} = 0.022\ \exp(\frac{3.473 * 10^4\,(J/mol)}{RT})$	PLUG	[95]
K6	Methane Steam Reforming	$r_{(6)} = 3.015 * 10^6 (kmol/m^3 \cdot s)\ \exp(-\frac{127.71\,(kJ/mol)}{RT}) c_{H_2O} c_{CH_4}$	PLUG	[96]

Table B.3: Reaction Kinetics for the tar reducing reactions in the gasifier for the reaction kinetics **set 1**. The tar reduction reactions mentioned in this table are with Char as a catalyst. Reaction rate mentioned is in $kmol/m^3.s$ and the activation energy is is the units of kg/kmol.

	Reaction	Reaction Kinetics	Reactor name	Source
K7	Napthalene	$r_{(7)} = 21.11\ \exp(-\frac{61{,}000}{RT}) \frac{m_{char}}{V_R} c_{C_{10}H_8}$	PLUG	[56, 84]
K8	Toluene	$r_{(8)} = 21.11\ \exp(-\frac{61{,}000}{RT}) \frac{m_{char}}{V_R} c_{C_7H_8}$	PLUG	[56, 84]
K9	Benzene	$r_{(9)} = 21.11\ \exp(-\frac{61{,}000}{RT}) \frac{m_{char}}{V_R} c_{C_6H_6}$	PLUG	[56, 84]
K10	Phenol	$r_{(10)} = 95{,}978\ \exp(-\frac{79{,}000}{RT}) \frac{m_{char}}{V_R} c_{C_6H_6O}$	PLUG	[56, 84]
K11	Methane	$r_{(11)} = 10^{-2}\ \exp(-\frac{263{,}000}{RT}) \frac{m_{char}}{V_R} P_{CH_4}$	PLUG	[84, 97]

KINETICS FOR SET 2

The first set of gasification reactions chosen as a set is shown in Table B.4. The corresponding reaction kinetics used is referred to as set 1 and is shown in the tables, Table B.5 and Table B.6. Table B.6 represents the tar gasification reactions and Table B.5 represents the other main gasification reactions simulated. The reaction numbers are numbered with a suffix 'R' and the corresponding reaction kinetics can be found starting with a suffix 'K' with the same number.

Table B.4: List of Gasification Reactions simulated in the reaction **set 2**

Reaction Name	**Reaction Type**	**Reaction Expression**
Pyrolysis	R1	$\text{Biomass} \longrightarrow \text{Volatiles(VM)} + \text{Char} + a_1C_6H_6 + a_2C_6H_6O + a_3C_7H_8 + a_4c_{10}H_8 + a_5H_2O$ $\text{VM} \longrightarrow b_1CO + b_2CO_2 + b_3H_2 + b_4CH_4 + b_5N_2 + b_6C_2H_4 + b_7C_2H_6$
Char Oxidation	R3	$\alpha C + O_2 \longrightarrow 2(\alpha-1)CO + (2-\alpha)CO_2$
Boudouard Reaction	R4	$C + CO_2 \longrightarrow 2CO$
Water Gas Shift	R12	$CO + H_2O \longleftrightarrow CO_2 + H_2$
Char Steam Reforming	R13	$C + H_2O \longrightarrow CO + H_2$
Methane Steam Reforming	R14	$CH_4 + H_2O \longleftrightarrow CO + 3H_2$
Benzene Steam Reforming	R15	$C_6H_6 + 2H_2O \longrightarrow 1.5C + 2.5CH_4 + 2CO$
Phenol Thermal Cracking	R16	$C_6H_6O \longrightarrow CO + 0.4C_{10}H_8 + 0.15C_6H_6 + 0.1CH_4 + 0.75H_2$
Phenol Steam Reforming	R17	$C_6H_6O + 3H_2O \longrightarrow 2CO + CO_2 + 0.05C + 2.95CH_4 + 0.1H_2$
Toluene Steam Reforming	R18	$2C_7H_8 + 21H_2O \longrightarrow 7CO_2 + 29H_2 + 7CO$
Toluene Hydrodealkylation	R19	$C_7H_8 + H_2 \longrightarrow C_6H_6 + CH_4$
Naphthalene Steam Reforming	R20	$C_{10}H_8 + 4H_2O \longrightarrow C_6H_6 + 4CO + 5H_2$
Naphthalene Thermal Cracking	R21	$C_{10}H_8 \longrightarrow 7.38C + 0.275C_6H_6 + 0.97CH_4 + 1.235H_2$

Table B.5: Kinetics (**set 2**) used for the main gasification reactions used in the developed Aspen Plus model

	Reaction	Reaction Kinetics	Reactor name	Source
K1	Pyrolysis	Correlations in Table 3.3	PYRGAS	[84]
K3	Char Oxidation	$r_{(3)} = 1.426 * 10^5 (\text{kmol/m}^3 \cdot \text{s}) \exp(-\frac{59.9(\text{kJ/mol})}{\text{RT}}) c_{O_2} f_{(3)}$ $f_{(3)} = 3$	PLUG	[95]
K4	Boudouard Reaction	$r_{(4)} = \frac{k_{(4)} c_{CO_2}}{1+K^{(4)}_{k-CO_2} c_{CO_2} + K^{(4)}_{k-CO} c_{CO}} f_{(4)}$ $f_{(4)} = 1$ $k_{(4)} = 4.89 * 10^7 (\text{m}^3/\text{s} \cdot \text{mol}) \exp(-\frac{268{,}000(\text{J/mol})}{\text{RT}}) \frac{\rho_{char}}{M_C} (1-\text{X})$ $K^{(4)}_{k-CO_2} = 6.60 * 10^{-2} (\text{m}^3/\text{mol})$ $K^{(4)}_{k-CO} = 0.12 (\text{m}^3/\text{mol}) \exp(-\frac{268{,}000(\text{J/mol})}{\text{RT}})$ X = 0.35	CSTR	[95]
K12	Water Gas Shift	$r_{(12)} = 5.2 * 10^5 (\text{kmol/m}^3 \cdot \text{s}) \exp(-\frac{102{,}400(\text{kJ/mol}))}{\text{RT}}) c_{H_2O} . c_{CO}$	PLUG	[98]
K13	Char Steam Reforming	$r_{(13)} = 3.6 * 10^{12} (\text{kmol/m}^3 \cdot \text{s}) \exp(-\frac{3.1 * 10^8 (\text{J/kmol})}{\text{RT}}) c_C . c_{H_2O}$	PLUG	[99]
K14	Methane Steam Reforming	$r_{(14)} = 1044.44 (\text{kmol/m}^3 \cdot \text{s}) \exp(-\frac{62 * 10^6 (\text{J/kmol})}{\text{RT}}) c m_{CH_4}$	PLUG	[44]

Table B.6: Reaction Kinetics for the tar reducing reactions in the gasifier for the reaction kinetics **set 2**

	Reaction	Reaction Kinetics	Reactor name	Source
K15	Benzene Steam Reforming	$r_{(15)} = 1602.78(\text{kmol/m}^3\cdot\text{s})\ \exp(-\frac{58*10^6(\text{J/kmol})}{RT})cm_{C_6H_6}$	PLUG	[44]
K16	Phenol Thermal Cracking	$r_{(16)} = 1*10^7(\text{kmol/m}^3\cdot\text{s})\ \exp(-\frac{1*10^8(\text{J/kmol})}{RT})c_{C_6H_6O}$	PLUG	[99]
K17	Phenol Steam Reforming	$r_{(17)} = 1327.78(\text{kmol/m}^3\cdot\text{s})\ \exp(-\frac{58*10^6(\text{J/kmol})}{RT})cm_{C_6H_6O}$	PLUG	[44]
K18	Toluene Steam Reforming	$r_{(18)} = 1358.33(\text{kmol/m}^3\cdot\text{s})\ \exp(-\frac{58*10^6(\text{J/kmol})}{RT})cm_{C_7H_8}$	PLUG	[44]
K19	Toluene Hydrodealkylation	$r_{(19)} = 3.3*10^5(\text{kmol/m}^3\cdot\text{s})\ \exp(-\frac{2.47*10^8(\text{J/kmol})}{RT})c_{C_7H_8}.c_{H_2}^{0.5}$	PLUG	[99]
K20	Naphthalene Steam Reforming	$r_{(20)} = 977.78(\text{kmol/m}^3\cdot\text{s})\ \exp(-\frac{58*10^6(\text{J/kmol})}{RT})cm_{C_10H_8}$	PLUG	[44]
K21	Naphthalene Thermal Cracking	$r_{(21)} = 3.39*10^14(\text{kmol/m}^3\cdot\text{s})\ \exp(-\frac{3.5*10^8(\text{J/kmol})}{RT})c_{C_10H_8}^{1.6}.c_{H_2}^{-0.5}$	PLUG	[99]

B.2. DOLOMITE

Table B.7: Reaction Kinetics for carbonation reaction of Dolomite both in the Gasifier and the Water Gas Shift reactor

	Reaction	Reaction Kinetics	Reactor name	Source
K22a	CO_2 Sorption	$r_{(22a)} = 1.04 * 10^{-6}(\text{kmol/m}^2\cdot\text{s})\ \exp(-\frac{24(\text{kJ/mol})}{RT})$	CSTR, CST-SORP	Ping Sun et al. [91]
K22b	CO_2 Sorption	$r_{(22b)} = 2.45 * 10^{-10}(\text{kmol/m}^2\cdot\text{s})\ \exp(\frac{25.71(\text{kJ/mol})}{RT})$	CSTR, CST-SORP	Mostafavi et al. [86]

B.3. METHANOL SYNTHESIS

The methanol synthesis process can be modelled by two principle reactions, the CO_2 hydrogenation and the Water Gas Shift reaction (WGS). The kinetic model used is sourced from Bussche and Froment [90]. The two principle reaction and their corresponding reaction kinetics are shown below.

$$CO_2 + 3H_2 \longleftrightarrow CH_3OH + H_2O \tag{B.1}$$

$$CO + H_2O \longleftrightarrow CO_2 + H_2 \tag{B.2}$$

$$r_{\text{MeOH}} = k_{\text{MEOH}} \frac{\left(P_{CO_2} P_{H_2}\right) - \left(1/K_{p1}\right)\left(P_{CH_3OH} P_{H_2O} / P_{H_2}^2\right)}{\left(1 + K_a\left(P_{H_2O}/P_{H_2}\right) + K_b\sqrt{P_{H_2}} + K_c P_{H_2O}\right)^3} \quad [90] \tag{B.3}$$

$$r_{\text{RWGS}} = k_{\text{RWGS}} \frac{P_{CO_2} - \left(1/K_{p2}\right)\left(P_{CO} P_{H_2O} / P_{H_2}\right)}{\left(1 + K_a\left(P_{H_2O}/P_{H_2}\right) + K_b\sqrt{P_{H_2}} + K_c P_{H_2O}\right)} \quad [90] \tag{B.4}$$

where,
r_i = reaction rate
k_i = Kinetic factor
P_i = Partial pressure
K_{pi} = equilibrium constant
$K_{a/b/c}$ = adsorption constant

The values for the adsorption constants and kinetic factors were obtained from Bussche and Froment[90]. Since the values of these constants as reported by Bussche and Froment are in the units of Bar, mol, s and kg , the expressions for the constants need to be changed to suit the units used in Aspen Plus (kg, s, Pascal and kmol). Moreover, the kinetic pre-factor and the constants needs to be changed to the form shown in Equation B.5 and Equation B.6. The adjusted reaction kinetic pre-factor and the equilibrium constants are shown in the Table B.8. The reaction rate is now changed to the units of kmol.m^{-3}.s^{-1}.

$$K_i = K_{i,o}\ exp(-\frac{E_i}{RT}) \tag{B.5}$$

$$ln\ K_i = A_i + \frac{B_i}{T} \tag{B.6}$$

Table B.8: Values of Reaction kinetics for the Methanol synthesis process. The values of kinetic factors and constants are modified to suit the form of representation showed in Equation B.5 and Equation B.6. Values shown are direct inputs for the developed Aspen Plus model.

Variable	$k_{i,o}$	E_i
K_{MeOH}	$1.07\,\mathrm{X}\,10^{-13}\ kmolkg_{cat}^{-1}s^{-1}Pa^{-2}$	-36 696 $kJkmol^{-1}$
K_{RWGS}	$1.22\,\mathrm{X}\,10^{2}\ kmolkg_{cat}^{-1}s^{-1}Pa^{-1}$	94 765 $kJkmol^{-1}$

Variable	A_i	B_i
$\ln \frac{1}{K_{p,1}}$	47.415	-7059.73
$\ln \frac{1}{K_{p,2}}$	-4.672	4773.26
$\ln K_a$	8.1471	0
$\ln K_b$	-6.4522	2068.44
$\ln K_c$	-34.9526	14 928.92

C

Simulation Results

C.1. Gasifier

C.1.1. Pyrolysis results

Mass yield obtained from the correlations mentioned in Table 3.3 are shown in

Table C.1: Mass Yields from Pyrolysis

Methane	0,062
Hydrogen	0,020
Carbon Monoxide	0,319
Carbon Dioxide	0,092
Ethylene	0,034
Ethane	0,002
Benzene	0,019
Toluene	0,028
Phenol	0,001
Napthalene	0,004
Water/Steam	0,236
Char (Carbon)	0,182

C.2. Steam Network

C.2.1. Steam network Pinch Analysis results

Table C.2: Pinch Analysis for developing the steam network for Case A

HX	Heat	High T (°C)	Low T (°C)	Designated usage
COOL1	0,414 MW	709,56	549,499	HX-SG: Steam for gasification
	0,65MW	549,499	110	HX-AFS2: Economiser
COOL2	1,15 MW	528,052	110	Economiser + Hot Air
COOL-MET	0,97 MW	476,14	234	Evaporator
COOL-FLA	1,06 MW	242,466	40	Economiser
COOL-H2O	2 MW	223,853	223,853	Evaporator
HX-FUEL	0,15 MW	163,94	30	Economiser
Stream: COLD-FG	0,22 MW	240,968	100	Economiser
Stream: FG-HOT				
SUPERHEA	1,04 MW	570,238	472,602	Superheater
HX-EVA	2,060 MW	472,602	228,853	Evaporator
HX-EC1	2,07 MW	228,853	34,7845	Economiser

C.3. ASPEN PLUS SCHEMATICS AND STREAM SUMMARY FOR THE FOUR CASES

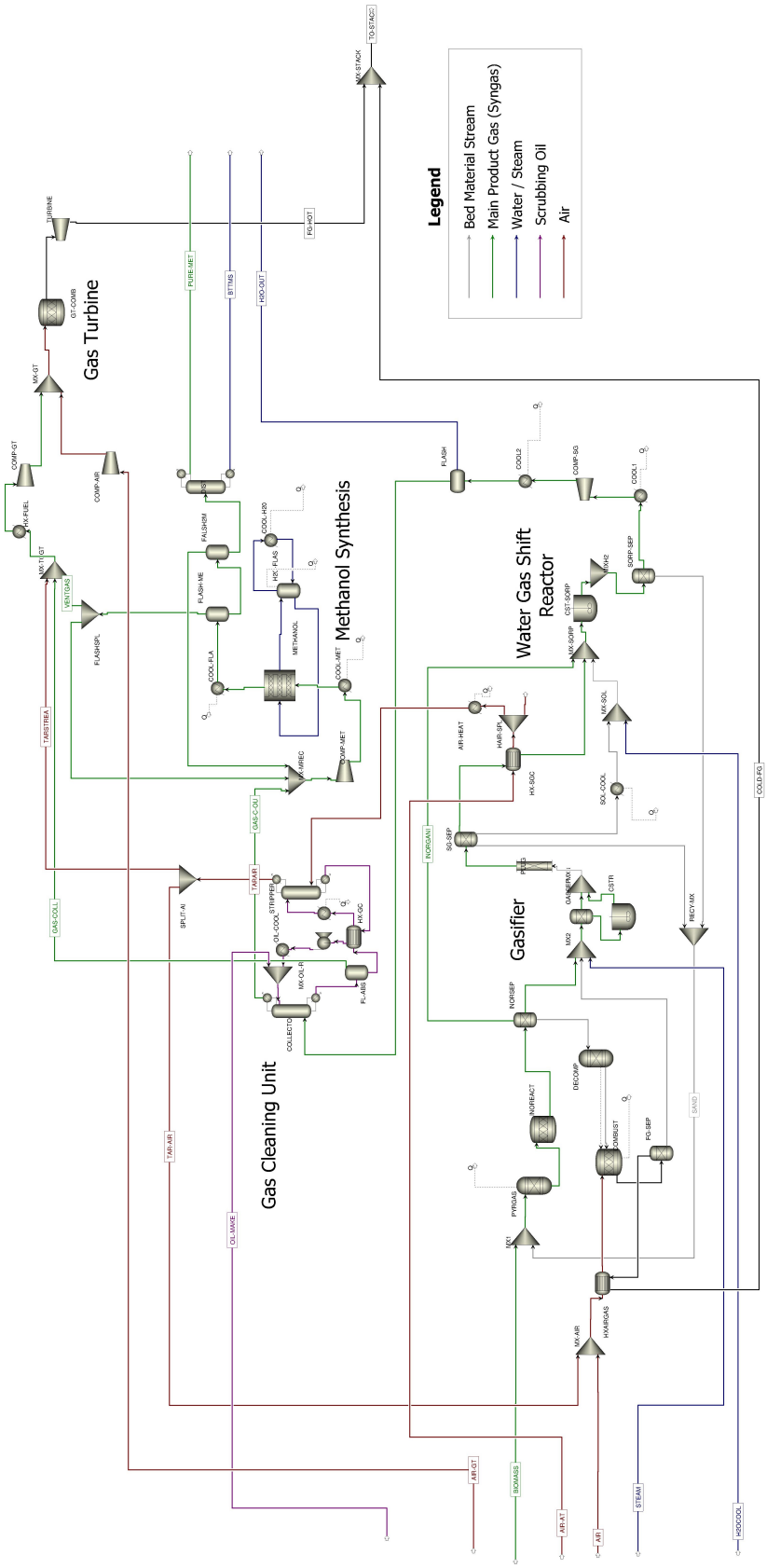

Figure C.1: Aspen Model flow-sheet for the Case A: Conventional Methanol Synthesis Process

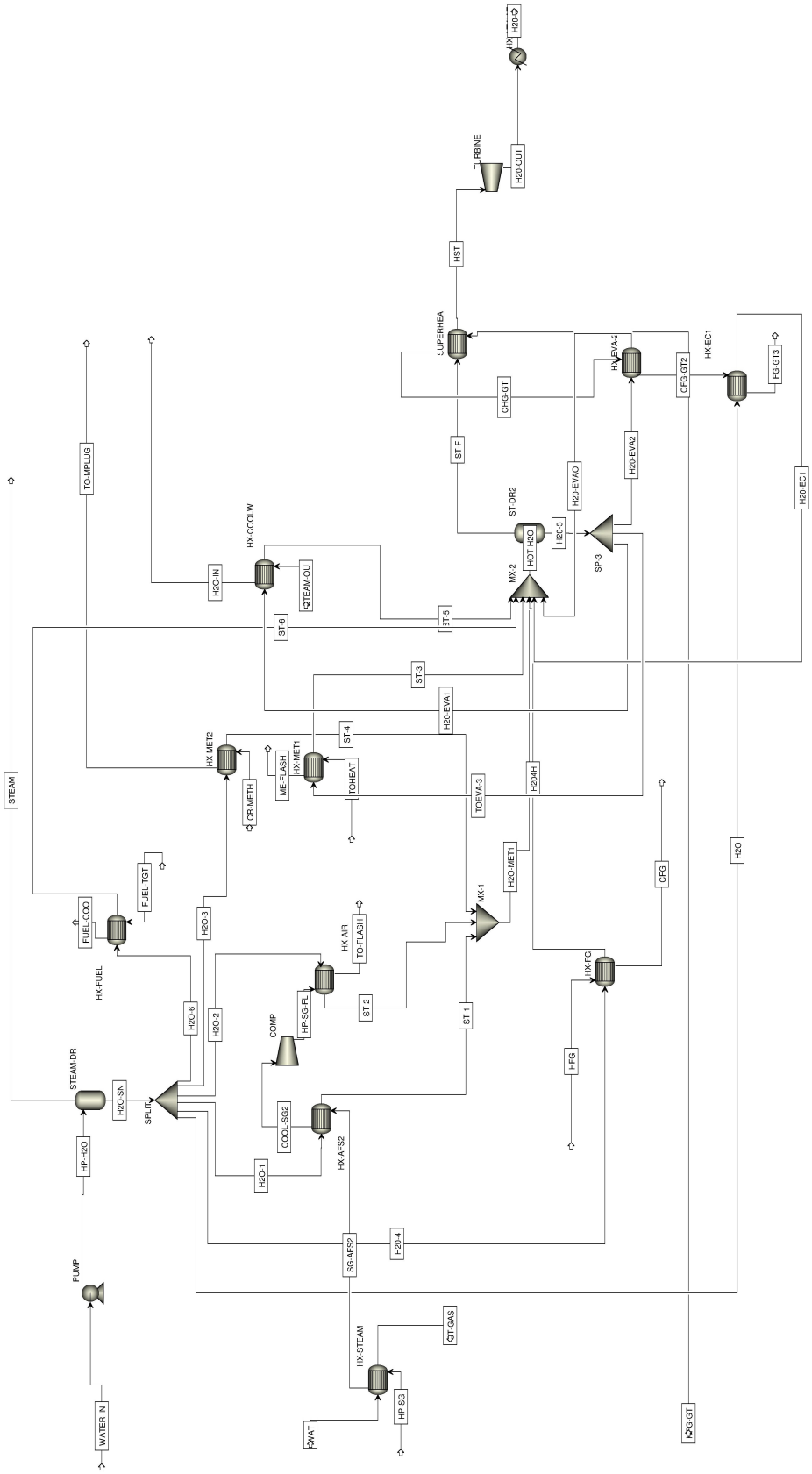

Figure C.2: Aspen Model flow-sheet of the Steam Network for Case A: Conventional Methanol Synthesis Process

Table C.3: Stream summary for the case A: Conventional Methanol Synthesis Process, without in-situ CO_2 removal during gasification

	Units	AIR	TAR-AIR	STEAM	H2OCOOL	SYNGAS	COLD-FG	TO-FLASH	GAS-C-OU	GAS-COLL	TARAIR	OIL-MAKE	VENTGAS	BTTMS	PURE-MET	AIR-GT	FG-HOT
From			SPLIT-AI			SG-SEP	HXAIRGAS	COOL2	COLLECTO	FL-ABS	STRIPPER		FLASHSPL	DIST	DIST		TURBINE
To		MX-AIR	MX-AIR	MX2	MX-SOL	HX-SGC	MX-STACK	FLASH	MX-MREC	MX-TOGT	SPLIT-AI	MX-OIL-R	MX-TOGT			COMP-AIR	MX-STACK
Substream: ALL																	
Mass Flow	KG/HR	4680	644,0494	413,741	540	2444,377	6455,078	2174,194	1123,893	84,29174	2995,589	384,5612	486,7232	139,5891	497,3636	37800	40722,55
Substream: MIXED																	
Phase:		Vapor	Vapor	Vapor	Liquid	Vapor	Vapor	Vapor	Vapor	Vapor	Vapor	Liquid	Vapor	Liquid	Liquid	Vapor	Vapor
Component Mass Flow																	
CARBON MONOXIDE	KG/HR	0	0,05	0	0	821,21	0	407,13	398,36	7,00	0,25	0	36,57	0	0	0	0,00
CARBON DIOXIDE	KG/HR	0	1,00	0	0	503,23	2301,80	343,65	312,28	24,24	4,67	0	186,59	0	2,40	0	2110,87
HYDROGEN	KG/HR	0	0,00	0	0	79,15	0	108,95	108,56	0,33	0	0	39,56	0	0	0	0
WATER/STEAM	KG/HR	0	9,92	413,74	540,00	691,35	119,81	965,03	84,61	38,65	46,13	0	0,30	134,58	0,13	0	1271,28
NITROGEN	KG/HR	3589,95	403,26	0	0	0	3993,21	0	1,28	0	1875,64	0	1,28	0	0	28995,74	30469,39
METHANE	KG/HR	0	0,03	0	0	142,72	0	142,72	139,32	3,16	0,15	0	139,30	0	0,02	0	0
ETHYLENE	KG/HR	0	0,15	0	0	80,57	0	80,57	75,05	4,71	0,71	0	74,87	0	0,17	0	0
ETHANE	KG/HR	0	0,01	0	0	4,30	0	4,30	3,95	0,29	0,05	0	3,94	0	0,01	0	0
BENZENE	KG/HR	0	8,75	0	0	44,27	0	44,27	0	3,40	40,68	0	0	0	0	0	0
TOLUENE	KG/HR	0	13,41	0	0	66,31	0	66,31	0	2,48	62,37	0	0	0	0	0	0
PHENOL	KG/HR	0	0	0	0	0	0	0	0	0	0	0	0	0	0	0	0
NAPHTHALENE	KG/HR	0	2,35	0	0	11,26	0	11,26	0	0,02	10,95	0	0	0	0	0	0
OXYGEN	KG/HR	1090,05	122,43	0	0	0	40,26	0	0,45	0	569,46	0	0,45	0	0	8804,26	6871,01
CARBON (CHAR)	KG/HR	0	0	0	0	0	0	0	0	0	0	0	0	0	0	0	0
METHYL-PALMITATE	KG/HR	0	23,17	0	0	0	0	0	0,02	0,01	107,78	107,80	0	0	0	0	0
METHYL-OLEATE	KG/HR	0	51,54	0	0	0	0	0	0,02	0,01	239,75	239,77	0	0	0	0	0
METHYL-STEARATE	KG/HR	0	7,95	0	0	0	0	0	0	0	36,98	36,99	0	0	0	0	0
METHANOL	KG/HR	0	0	0	0	0	0	0	0	0	0	0	3,87	5,00	494,63	0	0
Mole Flow	KMOL/HR	162,22	19,37	22,97	29,97	131,68	202,76	143,24	91,42	3,55	90,08	1,33	36,85	7,63	15,51	1310,21	1420,93
Mass Flow	KG/HR	4680,00	644,05	413,74	540,00	2444,38	6455,08	2174,19	1123,89	84,29	2995,59	384,56	486,72	139,59	497,36	37800,00	40722,55
Volume Flow	CUM/HR	3967,45	755,55	1786,51	0,54	12304,89	8559,42	334,99	185,24	104,45	3513,03	0,49	14,76	0,15	0,64	32044,79	99005,19
Temperature	C	25,00	202,18	675,00	25,00	865,19	241,16	155,66	92,41	85,00	202,01	80,00	50,80	96,33	41,40	25,00	575,53
Pressure	BAR	1,01	1,01	1,01	1,01	1,01	1,01	15,00	15,00	1,01	1,01	20,00	66,70	1,01	1,01	1,01	1,01
Vapor Fraction		1	1	1	0	1	1	1	1	1	1	0	1	0	0	1	1
Liquid Fraction		0	0	0	1	0	0	0	0	0	0	1	0	1	1	0	0
Mass Enthalpy	KJ/KG	-0,28	-279,23	-12098,44	-15972,07	-5379,24	-3215,95	-8033,39	-5182,52	-8983,14	-279,23	-2497,06	-4809,26	-15259,09	-7398,13	-0,28	-283,08
Enthalpy Flow	MW	0,00	-0,05	-1,39	-2,40	-3,65	-5,77	-4,85	-1,62	-0,21	-0,23	-0,27	-0,65	-0,59	-1,02	0,00	-3,20
Mass Entropy	KJ/KG-K	0,15	-0,12	-0,15	-9,32	3,33	0,73	-0,94	-0,24	-0,57	-0,12	-5,93	-3,24	-8,06	-7,31	0,15	1,27
Mass Density	KG/CUM	1,18	0,85	0,23	993,96	0,20	0,75	6,49	6,07	0,81	0,85	790,30	32,97	911,81	773,62	1,18	0,41
Average Molecular Weight		28,85	33,26	18,02	18,02	18,56	31,84	15,18	12,29	23,72	33,26	288,88	13,21	18,30	32,07	28,85	28,66

Table C.4: Stream summary for the case A: Conventional Methanol Synthesis Process, with in-situ CO_2 removal during gasification

	Units	AIR	TAR-AIR	STEAM	H2OCOOL	SYNGAS	COLD-FG	TO-FLASH	GAS-C-OU	GAS-COLL	TARAIR	OIL-MAKE	VENTGAS	BTTMS	PURE-MET	AIR-GT	FG-HOT
From			SPLIT			SG-SEP	HXAIRGAS	COOL2	COLLECTO	FL-ABS	STRIPPER		FLASHSPL	DIST	DIST		TURBINE
To		MX-AIR	MX-AIR	MX2	MX-SOL	HX-SGC		FLASH	END-MX		SPLIT	MX-OIL-R	MX-TOGT			COMP-AIR	MX-STACK
Substream: ALL																	
Mass Flow	KG/HR	4680	748,59	413,74	1080	2263,33	6569,43	2705,16	1252,16	99,63	2994,37	386,85	526,20	193,81	531,72	37440	40311,64
Substream: MIXED																	
Phase:		Vapor	Vapor	Vapor	Liquid	Vapor	Vapor	Vapor	Vapor	Vapor	Vapor	Liquid	Vapor	Liquid	Liquid	Vapor	Vapor
Component Mass Flow																	
CARBON MONOXIDE	KG/HR	0	0,06	0	0	898,34	0	375,31	366,83	6,41	0,22	0	43,48	0	0	0	0
CARBON DIOXIDE	KG/HR	0	1,69	0	0	333,03	2322,86	516,64	468,53	36,44	6,76	0	234,30	0	2,31	0	2031,40
HYDROGEN	KG/HR	0	0	0	0	90,43	0	128,07	127,60	0,38	0	0	49,15	0	0,00	0	0
WATER/STEAM	KG/HR	0	12,72	413,74	1080,00	628,39	139,39	1371,99	94,14	44,23	50,90	0	0,39	188,47	0,19	0	1294,22
METHANE	KG/HR	0	0,03	0	0	121,65	0	121,65	118,75	2,68	0,13	0	118,71	0	0,01	0	0
ETHYLENE	KG/HR	0	0,14	0	0	66,97	0	66,97	62,37	3,91	0,56	0	62,24	0	0,11	0	0
ETHANE	KG/HR	0	0,04	0	0	13,05	0	13,05	11,99	0,89	0,16	0	11,98	0	0,02	0	0
BENZENE	KG/HR	0	5,29	0	0	23,14	0	23,14	0	1,84	21,17	0	0	0	0	0	0
TOLUENE	KG/HR	0	16,99	0	0	72,92	0	72,92	0	2,82	67,96	0	0	0	0	0	0
PHENOL	KG/HR	0	0	0	0	0,02	0	0,02	0	0	0	0	0	0	0	0	0
NAPHTHALENE	KG/HR	0	3,70	0	0	15,39	0	15,39	0	0,02	14,81	0	0	0	0	0	0
OXYGEN	KG/HR	1090,05	142,35	0	0	0	48,38	0	0,50	0	569,41	0	0,50	0	0	8720,41	6858,40
METHYL-PALMITATE	KG/HR	0	27,10	0	0	0	0	0	0,02	0	108,40	108,43	0	0	0	0	0
METHYL-OLEATE	KG/HR	0	60,30	0	0	0	0	0	0,02	0,01	241,19	241,22	0	0	0,01	0	0
METHYL-STEARATE	KG/HR	0	9,30	0	0	0	0	0	0	0	37,21	37,21	0	0	0	0	0
METHANOL	KG/HR	0	0	0	0	0	0	0	0	0	0	0	4,03	5,34	529,08	0	0
Mass Flow	KG/HR	4680,00	748,59	413,74	1080,00	2263,34	6569,44	2705,17	1252,17	99,63	2994,38	386,85	526,20	193,81	531,73	37440,00	40311,64
Volume Flow	CUM/HR	3967,45	880,21	1266,93	1,09	10973,58	8295,79	416,58	207,40	120,25	3519,67	0,49	16,65	0,21	0,69	31739,60	96976,59
Temperature	C	25,00	202,29	400,00	25,00	747,33	215,33	161,25	92,41	85,00	202,12	80,00	49,30	97,33	45,57	25,00	565,89
Pressure	BAR	1,01	1,01	1,01	1,01	1,01	1,01	15,00	15,00	1,01	1,01	20,00	66,70	1,01	1,01	1,01	1,01
Vapor Fraction		1,00	1,00	1,00	0,00	1,00	1,00	1,00	1,00	1,00	1,00	0,00	1,00	0,00	0,00	1,00	1,00
Liquid Fraction		0,00	0,00	0,00	1,00	0,00	0,00	0,00	0,00	0,00	0,00	1,00	0,00	1,00	1,00	0,00	0,00
Mass Enthalpy	KJ/KG	-0,28	-312,96	-12692,45	-15972,07	-5236,33	-3251,66	-8928,11	-5712,15	-9435,48	-312,96	-2497,04	-5217,02	-15324,35	-7386,30	-0,28	-292,83
Enthalpy Flow	MW	0,00	-0,07	-1,46	-4,79	-3,29	-5,93	-6,71	-1,99	-0,26	-0,26	-0,27	-0,76	-0,83	-1,09	0,00	-3,28
Mass Entropy	KJ/KG-K	0,15	-0,12	-0,89	-9,32	3,42	0,67	-1,13	-0,32	-0,53	-0,12	-5,93	-3,03	-8,07	-7,27	0,15	1,26
Mass Density	KG/CUM	1,18	0,85	0,33	993,96	0,21	0,79	6,49	6,04	0,83	0,85	790,31	31,61	913,14	768,49	1,18	0,42
Average Molecular Weight		28,85	33,19	18,02	18,02	17,28	31,75	15,33	12,23	24,35	33,19	288,89	12,68	18,24	32,07	28,85	28,63

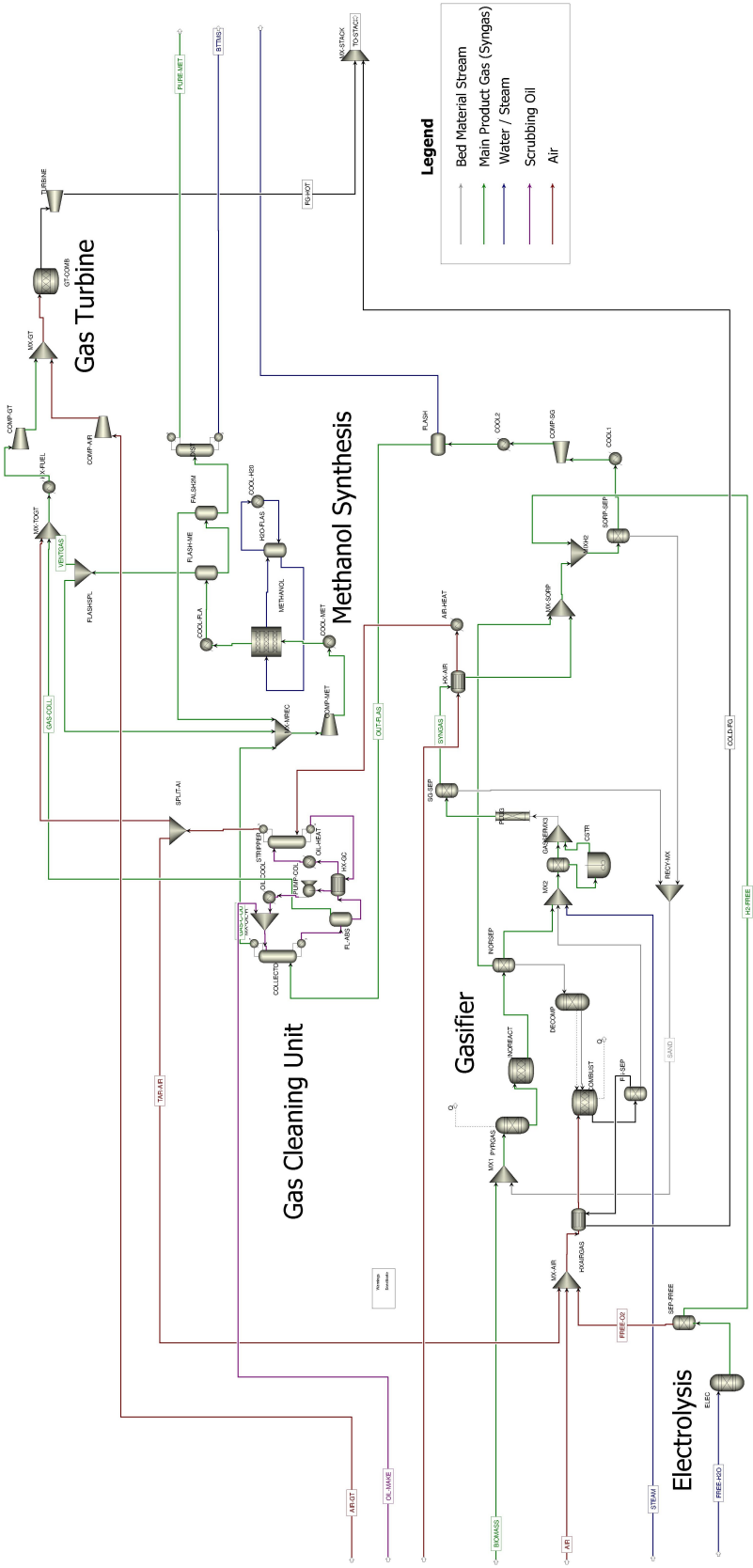

Figure C.3: Aspen Model flow-sheet for the Case B: The Free Electricity case

Table C.5: Stream summary for the case B: The Free Electricity Case, with in-situ CO_2 removal during gasification

	Units	AIR	TAR-AIR	STEAM	SYNGAS	COLD-FG	TO-FLASH	GAS-C-OU	GAS-COLL	TARAIR	OIL-MAKE	VENTGAS	BTTMS	PURE-MET	AIR-GT	FG-HOT
From			SPLIT-AI		SG-SEP	HXAIRGAS	COOL2	COLLECTO	FL-ABS	STRIPPER		FLASHSPL	DIST	DIST		TURBINE
To		MX-AIR	MX-AIR	MX2	HX-AIR	MX-STACK	FLASH	MX-MREC	MX-TOGT	SPLIT-AI	MX-OIL-R	MX-TOGT			COMP-AIR	MX-STACK
Substream: ALL																
Mass Flow	KG/HR	0	748,18	413,74	2375,07	1970,51	2479,89	1972,99	60,30	2992,71	382,84	776,39	217,25	979,61	44640,00	47721,23
Substream: MIXED																
Phase:		Vapor	Vapor	Vapor	Vapor	Vapor	Vapor	Vapor	Vapor	Vapor	Liquid	Vapor	Liquid	Liquid	Vapor	Vapor
Component Mass Flow																
CARBON MONOXIDE	KG/HR	0	0,11	0	1018,53	0	1018,53	1007,81	9,52	0,45	0	134,74	0	0,01	0	0
CARBON DIOXIDE	KG/HR	0	0,78	0	341,22	1259,70	341,22	325,13	12,47	3,13	0	339,47	0	5,64	0	2328,24
HYDROGEN	KG/HR	0	0	0	98,10	0	202,92	202,57	0,34	0	0	79,61	0	0	0	0
WATER/STEAM	KG/HR	0	11,53	413,74	579,62	138,90	579,62	222,05	29,68	46,10	0	0,46	213,30	0,21	0	1584,58
METHANE	KG/HR	0	0,03	0	132,24	0	132,24	130,54	1,59	0,10	0	130,52	0	0,02	0	0
ETHYLENE	KG/HR	0	0,11	0	74,97	0	74,97	72,21	2,29	0,45	0	71,99	0	0,22	0	0
ETHANE	KG/HR	0	0,02	0	11,43	0	11,43	10,93	0,41	0,10	0	10,89	0	0,04	0	0
BENZENE	KG/HR	0	6,90	0	29,40	0	29,40	0	1,78	27,60	0	0	0	0	0	0
TOLUENE	KG/HR	0	17,97	0	74,41	0	74,41	0	2,21	71,87	0	0	0	0	0	0
PHENOL	KG/HR	0	0	0	0,01	0	0,01	0	0	0,01	0	0	0	0	0	0
NAPTHA	KG/HR	0	3,76	0	15,12	0	15,12	0	0,02	15,02	0	0	0	0	0	0
OXYGEN	KG/HR	0	142,37	0	0	103,00	0	0,44	0	569,47	0	0,44	0	0	10397,41	8157,82
METHYL-PALMITATE	KG/HR	0	26,83	0	0	0	0	0,03	0	107,31	107,35	0	0	0	0	0
METHYL-OLEATE	KG/HR	0	59,66	0	0	0	0	0,04	0	238,63	238,67	0	0,04	0	0	0
METHYL-STEARATE	KG/HR	0	9,20	0	0	0	0	0,01	0	36,81	36,82	0	0	0	0	0
METHANOL	KG/HR	0	0	0	0	0	0	0	0	0	0	7,02	3,91	973	0	0
Mass Flow	KG/HR	0	748,18	413,74	2375,07	1970,51	2479,89	1972,99	60,30	2992,71	382,84	776,39	217,25	979,61	44640,00	47721,23
Volume Flow	CUM/HR	0	877,65	1266,93	11692,43	2707,81	420,48	341,16	78,72	3509,43	0,48	25,48	0,24	1,26	37843,37	115148,00
Temperature	C	25	202,10	400,00	762,31	313,05	128,05	94,72	85,00	201,94	80,00	47,62	97,62	40,91	25,00	567,49
Pressure	BAR	1,013	1,013	1,013	1,013	1,013	15,000	15,000	1,013	1,013	20,000	66,700	1,013	1,013	1,013	1,013
Vapor Fraction			1	1	1	1	1	1	1	1	0	1	0	0	1	1
Liquid Fraction			0	0	0	0	0	0	0	0	1	0	1	1	0	0
Mass Enthalpy	KJ/KG	0	-275,42	-12692,45	-4851,09	-6358,18	-5913,32	-5073,59	-9002,94	-275,40	-2497,09	-5266,63	-15400,19	-7401,59	-0,28	-290,86
Enthalpy Flow	MW	0	-0,06	-1,46	-3,20	-3,48	-4,07	-2,78	-0,15	-0,23	-0,27	-1,14	-0,93	-2,01	0,00	-3,86
Mass Entropy	KJ/KG-K		-0,12	-0,89	3,62	0,85	0,11	0,41	-0,33	-0,12	-5,93	-2,46	-8,08	-7,30	0,15	1,26
Mass Density	KG/CUM		0,85	0,33	0,20	0,73	5,90	5,78	0,77	0,85	790,30	30,47	915,51	774,42	1,18	0,41
Average Molecular Weight		28,8504	33,25	18,02	17,27	35,01	13,08	11,79	22,51	33,25	288,88	12,25	18,16	32,08	28,85	28,60

Table C.6: Stream summary for the case B: The Free Electricity Case, without in-situ CO_2 removal during gasification

	Units	AIR	TAR-AIR	FREE-H2O	H2-FREE	STEAM	SYNGAS	COLD-FG	TO-FLASH	GAS-C-OU	GAS-COLL	TARAIR	OIL-MAKE	VENTGAS	BTTMS	PURE-MET	AIR-GT	FG-HOT
From			SPLIT-AI		SEP-FREE		SG-SEP	HXAIRGAS	COOL2	COLLECTO	FL-ABS	STRIPPER		FLASHSPL	DIST	DIST		TURBINE
To		MX-AIR	MX-AIR	ELEC	MIXH2	MX2	HX-AIR	MX-STACK	FLASH	END-MX	MX-TOGT	SPLIT-AI	MX-OIL-R	MX-TOGT			COMP-AIR	MX-STACK
Substream: ALL																		
Mass Flow	KG/HR	0,0	749,2	1171,0	131,0	413,7	2535,2	2019,0	2666,2	2216,6	66,6	2996,8	384,1	898,2	285,1	1033,1	47340,0	50552,4
Substream: MIXED																		
Phase:		Missing	Vapor	Liquid	Vapor	Vapor	Vapor	Vapor	Vapor	Vapor	Vapor	Vapor	Liquid	Vapor	Liquid	Liquid	Vapor	Vapor
Component Mass Flow																		
CARBON MONOXIDE	KG/HR	0	0,10	0	0	0	1021,78	0	1021,78	1012,02	8,83	0,40	0	149,61	0	0,01	0	0
CARBON DIOXIDE	KG/HR	0	1,07	0	0	0	523,51	1210,94	523,51	500,95	17,76	4,28	0	423,56	0	5,57	0	2479,16
HYDROGEN	KG/HR	0	0,00	0	131,03	0	95,25	0	226,28	225,91	0,35	0	0	91,92	0	0	0	0
WATER/STEAM	KG/HR	0	11,48	1170,99	0	413,74	545,00	139,46	545,00	252,42	30,82	45,90	0	0,59	280,92	0,28	0	1717,79
NITROGEN	KG/HR	0	468,91	0	0	0	0	468,91	0	1,28	0	1875,64	0	1,28	0	0	36313,71	37721,71
METHANE	KG/HR	0	0,02	0	0	0	142,77	0	142,77	141,08	1,59	0,10	0	141,06	0	0,02	0	0
ETHYLENE	KG/HR	0	0,11	0	0	0	80,70	0	80,70	77,96	2,29	0,43	0	77,78	0	0,18	0	0
ETHANE	KG/HR	0	0,01	0	0	0	4,59	0	4,59	4,40	0,15	0,04	0	4,39	0	0,01	0	0
BENZENE	KG/HR	0	10,22	0	0	0	43,63	0	43,63	0	2,73	40,87	0	0	0	0	0	0
TOLUENE	KG/HR	0	16,09	0	0	0	66,62	0	66,62	0	2,05	64,36	0	0	0	0	0	0
PHENOL	KG/HR	0	0	0	0	0	0	0	0,00	0	0	0	0	0	0	0	0	0
NAPTHA	KG/HR	0	2,82	0	0	0	11,35	0	11,35	0	0,01	11,29	0	0	0	0	0	0
OXYGEN	KG/HR	0	142,36	0	0	0	0	199,69	0	0,45	0	569,46	0	0,45	0	0	11026,29	8633,76
METHYL-PALMITATE	KG/HR	0	26,91	0	0	0	0	0	0	0,04	0	107,66	107,70	0	0	0	0	0
METHYL-OLEATE	KG/HR	0	59,86	0	0	0	0	0	0	0,04	0	239,44	239,49	0	0,04	0	0	0
METHYL-STEARATE	KG/HR	0	9,23	0	0	0	0	0	0	0,01	0	36,94	36,95	0	0	0	0	0
METHANOL	KG/HR	0	0	0	0	0	0	0	0	0	0	0	0	7,59	4,12	1027,06	0	0
Mole Flow	KMOL/HR	0	22,52	65,00	65,00	22,97	139,17	58,24	204,17	185,37	2,84	90,07	1,33	72,60	15,72	32,20	1640,88	1768,06
Mass Flow	KG/HR	0	749,20	1170,99	131,03	413,74	2535,19	2019,00	2666,22	2216,57	66,60	2996,79	384,13	898,23	285,08	1033,13	47340,00	50552,42
Volume Flow	CUM/HR	0	878,45	1,28	1991,10	1266,93	12929,50	2626,41	448,36	378,24	83,61	3512,63	0,49	29,18	0,31	1,34	40132,29	122189,00
Temperature	C	25,00	202,15	100,00	100,00	400,00	858,53	276,49	123,70	94,97	85,00	201,99	80,00	47,57	98,05	43,30	25,00	568,62
Pressure	BAR	1,013	1,013	1,013	1,013	1,013	1,013	1,013	15,000	15,000	1,013	1,013	20,000	66,700	1,013	1,013	1,013	1,013
Vapor Fraction			1,00	0,00	1,00	1,00	1,00	1,00	1,00	1,00	1,00	1,00	0,00	1,00	0,00	0,00	1,00	1,00
Liquid Fraction			0,00	1,00	0,00	0,00	0,00	0,00	0,00	0,00	0,00	0,00	1,00	0,00	1,00	1,00	0,00	0,00
Mass Enthalpy	KJ/KG	0,00	-276,18	-15631,17	1078,46	-12692,45	-4753,09	-6027,56	-5939,39	-5407,09	-9021,39	-276,18	-2497,07	-5478,20	-15428,03	-7394,73	-0,28	-301,82
Enthalpy Flow	MW	0,00	-0,06	-5,08	0,04	-1,46	-3,35	-3,38	-4,40	-3,33	-0,17	-0,23	-0,27	-1,37	-1,22	-2,12	0,00	-4,24
Mass Entropy	KJ/KG-K		-0,12	-8,30	3,22	-0,89	3,71	0,80	0,09	0,30	-0,32	-0,12	-5,93	-2,36	-8,09	-7,29	0,15	1,26
Mass Density	KG/CUM		0,85	918,29	0,07	0,33	0,20	0,77	5,95	5,86	0,80	0,85	790,30	30,78	916,09	771,48	1,18	0,41
Average Molecular Weight		28,85	33,27	18,02	2,02	18,02	18,22	34,67	13,06	11,96	23,41	33,27	288,88	12,37	18,13	32,08	28,85	28,59

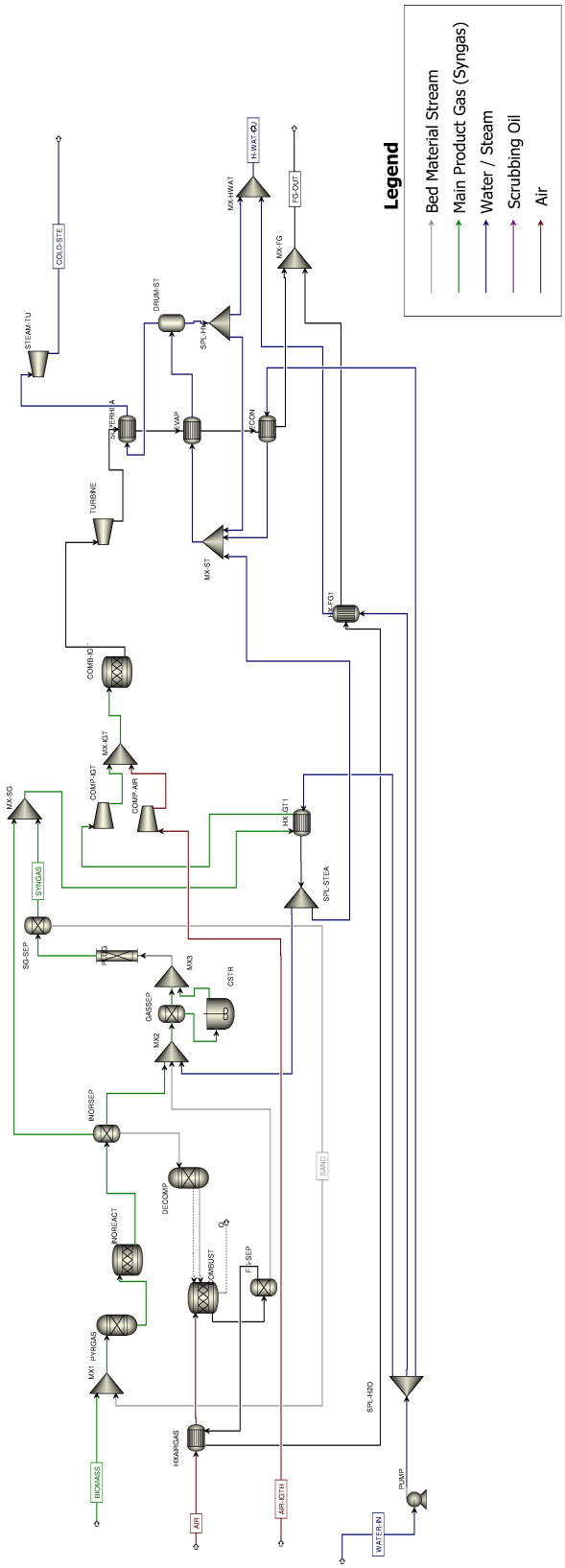

Figure C.4: Aspen Plus schematic of Case C: Conventional IGCC

Table C.7: Stream Results for the Case C: Conventional IGCC

	Units	AIR	STEAM	WATER-IN	AIR-IGTH	SYNGAS	FG-OUT	H-WATER
From			**SPL-STEA**			**SG-SEP**	**MX-FG**	**SPL-HW**
To		**HXAIRGAS**	**MX2**	**PUMP**	**COMP-AIR**	**MX-SG**		**MX-HWAT**
Substream: ALL								
Mass Flow	KG/HR	4320	413,741	9000	50400	2237,709	57485,6	1267,428
Substream: MIXED								
Phase:		Vapor	Vapor	Liquid	Vapor	Vapor	Vapor	Liquid
Component Mass Flow								
CARBON MONOXIDE	KG/HR	0	0	0	0	860,29	0	0
CARBON DIOXIDE	KG/HR	0	0	0	0	337,78	4076,88	0
HYDROGEN	KG/HR	0	0	0	0	87,37	0	0
WATER/STEAM	KG/HR	0	413,74	9000	0	629,79	1889,01	1267,43
NITROGEN	KG/HR	3313,80	0	0	38660,98	0	41974,78	0
METHANE	KG/HR	0	0	0	0	126,29	0	0
ETHYLENE	KG/HR	0	0	0	0	71,58	0	0
ETHANE	KG/HR	0	0	0	0	10,96	0	0
BENZENE	KG/HR	0	0	0	0	28,02	0	0
TOLUENE	KG/HR	0	0	0	0	71,14	0	0
PHENOL	KG/HR	0	0	0	0	0,00	0	0
NAPHTHALENE	KG/HR	0	0	0	0	14,47	0	0
OXYGEN	KG/HR	1006,20	0	0	11739,02	0	9544,93	0
METHYL-PALMITATE	KG/HR	0	0	0	0	0	0	0
METHYL-OLEATE	KG/HR	0	0	0	0	0	0	0
METHYL-STEARATE	KG/HR	0	0	0	0	0	0	0
METHANOL	KG/HR	0	0	0	0	0	0	0
Mole Flow	KMOL/HR	149,74	22,97	499,58	1746,94	128,72	1994,16	70,35
Mass Flow	KG/HR	4320,00	413,74	9000,00	50400,00	2237,71	57485,60	1267,43
Volume Flow	CUM/HR	3662,26	72,79	9,05	42715,84	10938,04	61050,36	1,64
Temperature	C	25,00	688,72	25,00	25,00	761,98	99,96	223,85
Pressure	BAR	1,013	25	1,013	1,013	1,013	1,013	25
Vapor Fraction		1	1	0	1	1	1	0
Liquid Fraction		0	0	1	0	0	0	1
Mass Enthalpy	KJ/KG	-0,28	-12086,60	-15972,07	-0,28	-5240,03	-997,66	-15024,38
Enthalpy Flow	MW	0,00	-1,39	-39,93	0,00	-3,26	-15,93	-5,29
Mass Entropy	KJ/KG-K	0,15	-1,61	-9,32	0,15	3,39	0,39	-6,91
Mass Density	KG/CUM	1,18	5,68	993,96	1,18	0,20	0,94	771,10
Average Molecular Weight		28,85	18,02	18,02	28,85	17,38	28,83	18,02

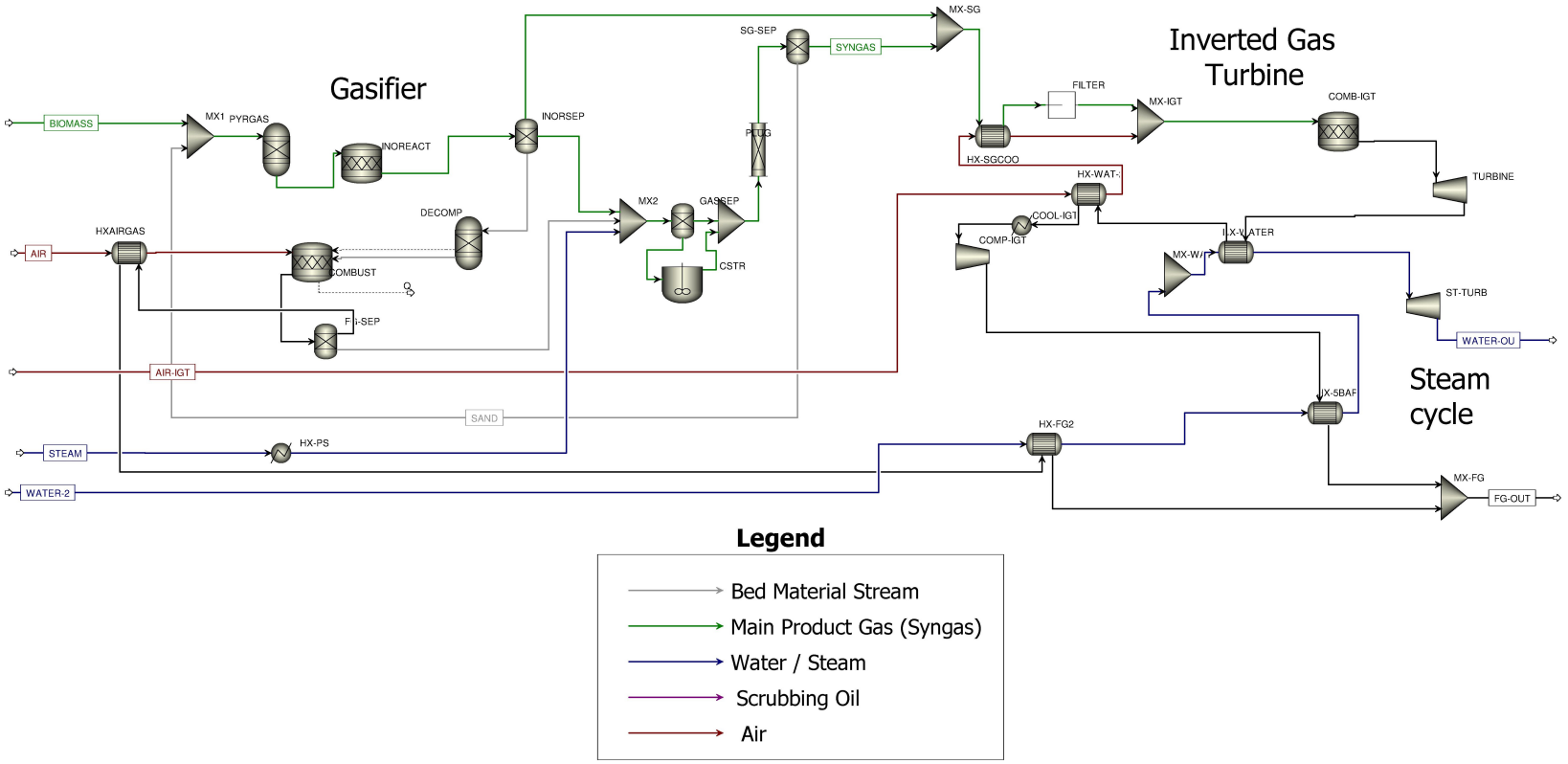

Figure C.5: Aspen Plus schematic of Case D: IGCC with an Inverted Gas Turbine

Table C.8: Stream summary for the Case D: IGCC with an Inverted Gas Turbine

	Units	AIR	AIR-IGT	STEAM	WATER-2	SYNGAS	Turbine Inlet	Compressor Inlet	FG-OUT
From						**SG-SEP**	**COMB-IGT**	**COOL-IGT**	MX-FG
To		**HXAIRGAS**	**HX-WAT-2**	**HX-PS**	**HX-FG2**	**MX-SG**	**TURBINE**	**COMP-IGT**	
Substream: ALL									
Mass Flow	KG/HR	4248	32760	413,7408	8820	2238,314	34998,31	34998,31	39774,29
Substream: MIXED									
Phase:		Vapor	Vapor	Liquid	Liquid	Vapor	Vapor	Vapor	Vapor
Component Mass Flow									
CARBON MONOXIDE	KG/HR	0	0	0	0	869,54	0	0	0
CARBON DIOXIDE	KG/HR	0	0	0	0	333,18	2661,31	2661,31	4080,44
HYDROGEN	KG/HR	0	0	0	0	87,88	0	0	0
WATER/STEAM	KG/HR	0	0	413,74	8820,00	632,95	1885,16	1885,16	1885,16
NITROGEN	KG/HR	3258,57	25880,40	0	0	0	25880,40	25880,40	29138,97
METHANE	KG/HR	0	0	0	0	122,67	0	0	0
ETHYLENE	KG/HR	0	0	0	0	68,41	0	0	0
ETHANE	KG/HR	0	0	0	0	12,12	0	0	0
BENZENE	KG/HR	0	0	0	0	24,93	0	0	0
TOLUENE	KG/HR	0	0	0	0	71,69	0	0	0
PHENOL	KG/HR	0	0	0	0	0,00	0	0	0
NAPHTHALENE	KG/HR	0	0	0	0	14,93	0	0	0
OXYGEN	KG/HR	989,43	6879,60	0	0	0	4571,44	4571,44	4669,72
METHYL-PALMITATE	KG/HR	0	0	0	0	0	0	0	0
METHYL-OLEATE	KG/HR	0	0	0	0	0	0	0	0
METHYL-STEARATE	KG/HR	0	0	0	0	0	0	0	0
METHANOL	KG/HR	0	0	0	0	0	0	0	0
Mass Flow	KG/HR	4248,00	32760,00	413,74	8820,00	2238,31	34998,31	34998,31	39774,29
Volume Flow	CUM/HR	3601,22	27854,10	0,42	8,87	10816,66	128714,00	101747,00	42352,61
Temperature	C	25	25	25	25	747,9248	999,6565	25	99,99947
Pressure	BAR	1,013	1,013	1,013	25	1,013	1,013	0,3	1,013
Vapor Fraction		1	1	0	0	1	1	1	1
Liquid Fraction		0	0	1	1	0	0	0	0
Mass Enthalpy	KJ/KG	-0,28	-0,28	-15972,07	-15969,80	-5287,84	-266,99	-1403,07	-1474,99
Enthalpy Flow	MW	0,00	0,00	-1,84	-39,13	-3,29	-2,60	-13,64	-16,30
Mass Entropy	KJ/KG-K	0,15	0,14	-9,32	-9,33	3,37	1,76	0,47	0,36
Mass Density	KG/CUM	1,18	1,18	993,96	993,96	0,21	0,27	0,34	0,94
Average Molecular Weight		28,85	28,77	18,02	18,02	17,35	28,41	28,41	28,75

D

A Non-Conventional solid approach to Char in Aspen Plus

During the development of the Aspen plus model for all the cases considered in this study, char was always simplified by assuming it to be pure carbon (carbon graphite). This assumption is not completely inaccurate as char by mass is composed mainly of carbon. However, like biomass, char does contain a fraction of hydrogen and oxygen in its ultimate analysis. In Aspen Plus, these streams of undefined and variable elemental composition such as the biomass and char stream are modelled as a *Non-Conventional* stream. By declaring these streams as Non-Conventional, it is then possible to input (Biomass) or compute (Char) the composition of these streams.

Considering char as pure carbon is a very common assumption observed in majority of the literature studied during the course of this study. In other words, literature that do not consider char as pure carbon are very scarce. Considering char as a non-conventional substance does make the model more realistic and hence a separate study was done to validate the reaction kinetics of char gasification published by [84] considering char not as pure carbon. The schematic of the model used for this validation remains same as the model for the other cases, shown in Figure 3.3. The reaction kinetics are the same as mentioned in Table B.2 and Table B.3 but with one change. The char gasification reaction was replaced with the one shown in Equation D.1 and its subsequent reaction kinetic shown in Equation D.2. Since no literature on the reaction kinetics of the Boudouard reaction with char not as pure carbon couldn't be found, this reaction was ignored.

$$C_xH_yO_z + (x-y)H_2O \longrightarrow xCO + (x-z+y/2)\,H_2 \tag{D.1}$$

$$r_{(13)} = 4.8 * 10^4 (kmol/m^3.s)\ exp(-\frac{211{,}000(kJ/kmol)}{RT}) P_{H_2O}^{0.51} \tag{D.2}$$

The Aspen Plus model was then simulated under the assumptions mentioned before and the results were then generated. The effect of the Steam To Biomass Ratio (STBR) on the product gas composition was the key comparison between the previous simulation result (with char as pure carbon) and this simulation. The results are plotted in Figure D.1. The simulation results were plotted against experimental results from the FICFB gasifer at Gussing [59].

Similar to the previous simulations, gasification is simulated by three reactors: the pyrolysis reactor (RYIELD), the heterogeneous reaction zone (RCSTR) and the free-board (RPLUG). The most significant change is that the composition of the char stream is computed by a fortran program. The correlations shown in Table 3.3 were used to calculate the mass yields of the pyrolysis block. The composition of the char stream was then calculated by performing a mole balance between the biomass input and the pyrolysis yield stream. Composition of the char stream computed is shown in Table D.1.

Observations

The char composition predicted by the model does agree with the experiments of [87]. The effect of changing char from a pure substance to a non conventional solid of varying composition can be observed to be quite

Table D.1: Computed mass composition of Char calculated as a Non - Conventional Solid

Carbon	93.37 %
Hydrogen	1.98 %
Oxygen	4.64 %

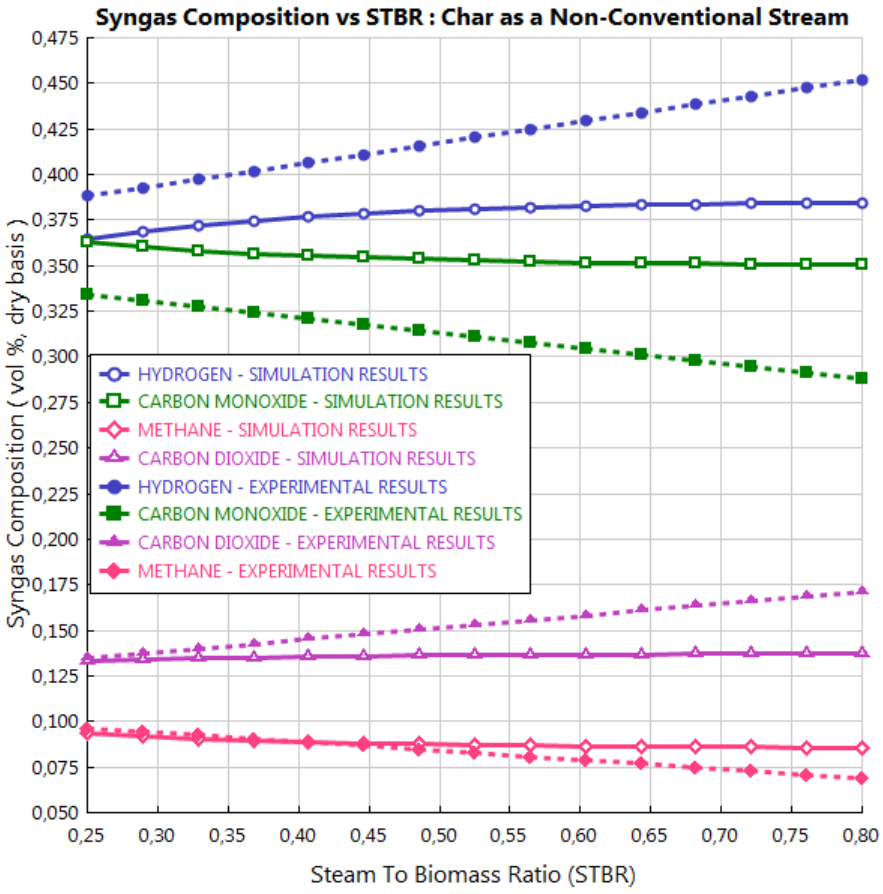

Figure D.1: Effect of Steam-To-Biomass-Ratio on the syngas composition when Char is considered as a Non-Conventional Solid and not as pure carbon during simulation

significant. The accuracy of the developed Aspen Plus model has significantly dropped from the previous results (Figure 3.8). A significant observation is that the model has relatively lost its ability to predict the trend of the variation in composition with increasing STBR that was observed very clearly in the previously results. All elemental composition, H_2, CO, CO_2 and CH_4 reach a state close to equilibrium, losing accuracy with increasing values of STBR.

INFERENCES

Although the predicted composition of char does agree with data found in literature, the difference in the simulated syngas composition and the studied experimental results is much too significant. This difference in accuracy, compared to the simulation results of using Carbon graphite as char does illustrate the dearth of kinetic models available in literature. Moreover, the importance of Boudouard reaction in the gasification process is not considered which could limit the potential importance of this approach. This study can hence be concluded that char can be accurately simplified during simulation as pure carbon graphite.

E

Investigating Inverted Brayton Cycle as an Efficient alternative for Coolers

The Inverted Brayton Cycle concept discussed in Section 2.5.3 was primarily used in this study as an alternative to the conventional Gas Turbine system to produce power from combusting product gas from the gasifier. However, a very important advantage of this Inverted Brayton Cycle (IBC) concept is its versatility in producing power from high temperature streams by expanding the stream to sub-atmospheric pressures. In other words, the inverted Brayton Cycle can in theory produce power without combustion in streams with sufficiently high temperatures.

Two particular sources for power production by cooling have been identified in the existing model. The product gas stream from the gasifier needs to be cooled to the required downstream filter or Water Gas Shift reactor (450°C). Similarly the flue gas stream from the combustor of the gasifier carries a significant thermal exergy which needs to be extracted to increase the overall efficiency of the process. These are the two streams identified (as shown in Figure E.1) and a two separate simulations was performed for each source and the results of these simulations are discussed in this chapter.

A key challenge with designing such a system is the heat losses in the moving parts of the IBC, the compressor and the turbine. This heat losses commonly cause an increase in entropy of the working fluid and can be quantified as in the isentropic efficiency of the component. Heat losses from the turbine and compressor can be understood as a function of the power produced as consumed as higher power turbines/compressors are relatively larger in size, reducing the impact of heat lost compared to the power produced/consumed. This is also the reason why micro turbines and compressors usually have lower isentropic efficiency than larger turbines and compressors. An advantage of working with sub-atmospheric pressures is that the specific volume of the working fluid is higher. This higher volumetric flow increases the size of the turbine/compressor which in turn increases the isentropic efficiency compared to pressurized operation. Since the gasifier considered in this study is of a pilot scale, the isentropic efficiency practically achievable are much lower than 1. this chapter aims to study the impact of using such a inverted Brayton Cycle system for cooling high temperature streams at different scales of operation, simulated by varying the isentropic efficiency of the turbines and compressors.

E.1. IGT for Product gas cooling

The syngas stream from the gasifier needs to be cooled down from 860°C to around 450°C and this heat released can be used to produce power by using the Inverted Brayton Cycle concept. A model was developed and simulated in Aspen Plus® (Figure E.2) for the product gas flow from gasifier at 860°C. The isentropic efficiency of the turbine and the compressor was varied from a realistic value of 0.65 to an ideal value 1 and the results obtained from simulation were then plotted in the Figure E.3. The flow rate and composition were

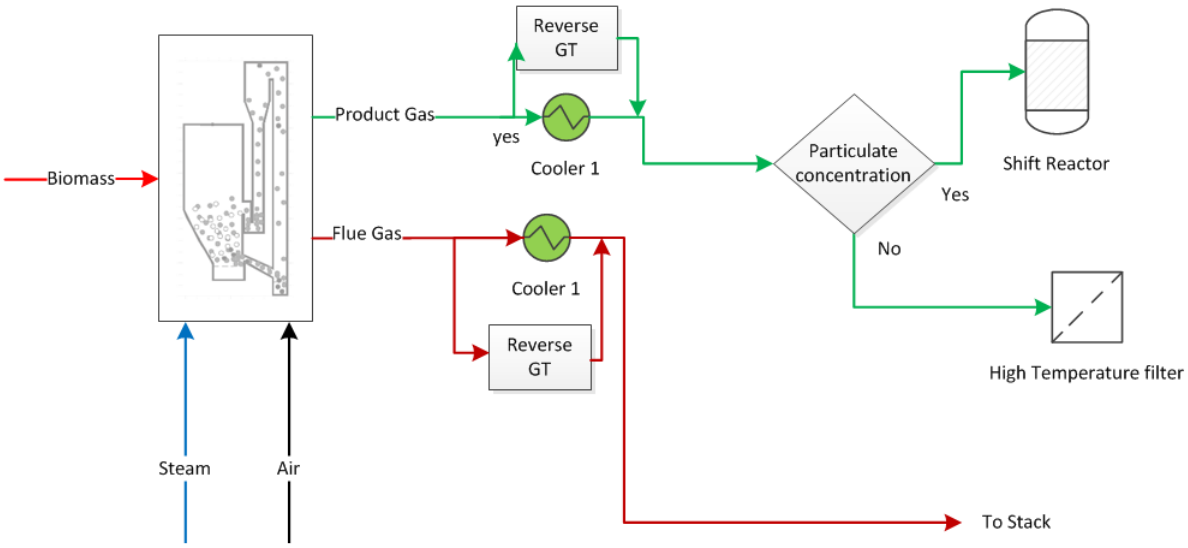

Figure E.1: Functional Schematic of the use of Inverted Brayton Cycle as a cooler during gasification

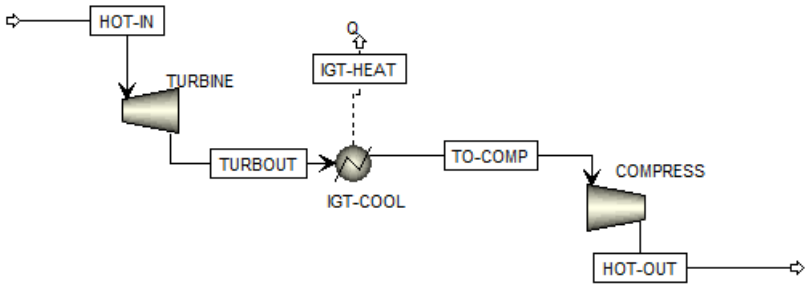

Figure E.2: Aspen Plus® Schematic of an IBC system as a cooler

obtained from the results of Case A, without in-situ CO_2 removal shown in Table C.3.

DISCUSSION

Net shaft power produced, obtained from simulation is negative at lower isentropic efficiency of the turbine and compressor. An isentropic efficiency of 0.65 represents a more realistic scenario for the scale of gasification considered in this study. However, when the isentropic efficiency increases, the net shaft power becomes positive, indicating technical feasibility at higher scales of operation. The results of the simulation dies indicate that the IGT system is infeasible below an isentropic efficiency of 77% and this isentropic efficiency of 77% would represent higher gasification scales than what is considered in this study. Since the input and output temperatures of the product gas stream are fixed at 860°C and 450°C respectively, the net amount of energy extracted stays constant at 0.635 MW, which can be computed as the sum of net shaft power and the heat extracted by the recuperator IGT-COOL.

E.2. IGT FOR FLUE GAS COOLING

The Aspen plus® model for simulating flue gas cooling in an IGT is the same as the previous case, shown in Figure E.2. The flue gas from the combustor of the gasifier has a significant thermal exergy which needs to be extracted to increase the energy efficiency of the gasification process. The flue gas stream is cooled from combustion temperatures of 875°C to the required stack temperature and the heat extracted from this stream is used to produce both power and heat in the IBC system modeled. Since the exit temperature is much lower

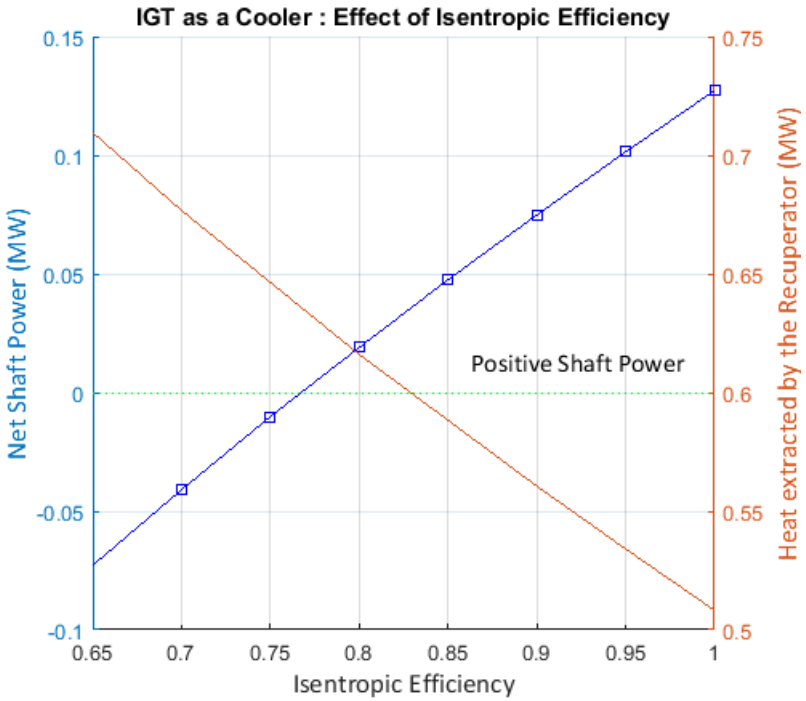

Figure E.3: Simulation results of producing work and heat from an IBC system cooling syngas stream from the gasifier

than the previously discussed syngas cooling case, the power and heat produced are expected to be relatively higher. The model was simulated with the flue gas mass results from the simulation of Case A, without in-situ CO_2 removal shown in Table C.3. The obtained simulation results are shown in Figure E.4. The isentropic efficiency was varied from 0.65 to 1 and its effect on the results of the IGT system was studied.

DISCUSSION

The effect of lower exit temperature of the flue gas stream can be seen in the positive net shaft power produced by the system even at ow isentropic efficiency. The flue gas stream was cooled down to 30°C in the recuperator IGT-COOL before subsequent compression to atmospheric pressure. The trend of increasing shaft power with isentropic efficiency can be observed, similar to the case of syngas cooling. The net energy output of the IGT system can be seen to increasing with the isentropic efficiency and hence this system of IGT for cooling the syngas stream can be seen to be quite effective. Air supplied to the combustor can be pre-heated with the energy extracted from the recuperator which could possibly reduce the amount of char combusted. It can hence be concluded that the IGT can be an attractive option to produce power to satisfy localized power demands. Moreover, Using an IGT for the flue gas cooling looks much more attractive than the product gas stream at any scale.

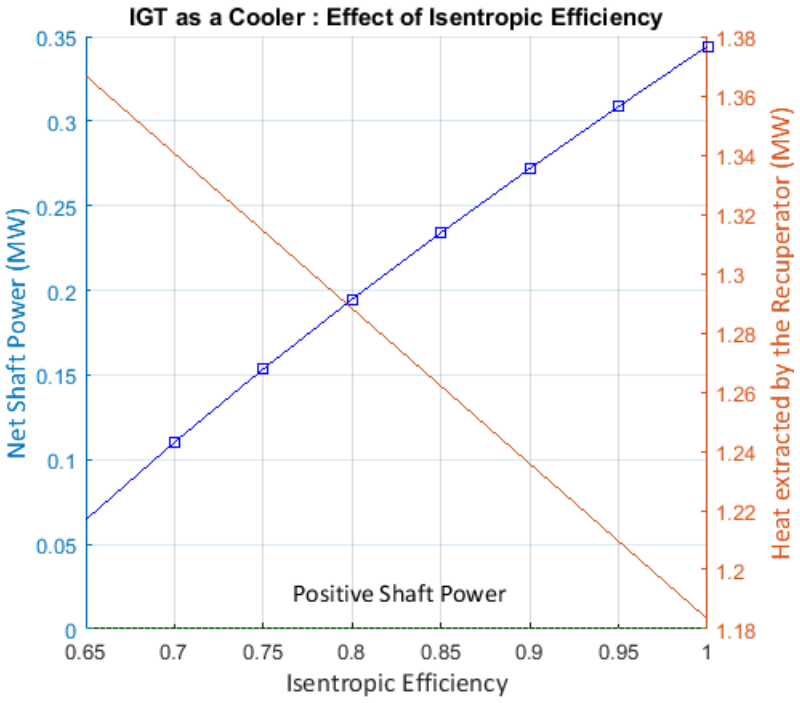

Figure E.4: Simulation results of producing work and heat from an IBC system cooling flue gas stream from the combustor of the gasifier system

F

DOLOMITE - CATALYST FOR HYDROGEN ENRICHMENT

Dolomite has been extensively studied in this study to remove CO_2 in-situ during gasification and also to promote water gas shift reaction to increase hydrogen fraction in the product gas. The water gas shift reactor in Figure 3.4 is primarily used for this purpose. By removing CO_2 in the water gas shift reactor, hydrogen production is promoted by shifting the equilibrium towards reducing CO in the product mixture according to the Equation B.2. Although, quite innovative and potentially attractive towards achieving a process without dedicated catalysts for a water gas shift reactor, this usage of dolomite does carry some serious challenges. As shown from Figure 4.5, removing CO_2 from the water gas shift reactor causes a loss of around 20% of carbon from the biomass which resulted in a very low methanol efficiency.

However, Dolomite could prove a very good solution for applications requiring a very enriched hydrogen fraction in the produced product gas. This chapter discusses in brief how the dolomite in the system can be potentially used to increase the hydrogen fraction of the product gas produced from the gasifier.

The schematic used for this study remains the same as shown in Figure 3.3 followed by the schematic shown in Figure 3.4. Hydrogen fraction can be increased by three easy ways, first by increasing the gasification temperature and the STBR,second by increasing the residence time in the water gas shift reactor and third, by increasing the fraction of dolomite sent to the water gas shift reactor. The first method is very straightforward. Increase in hydrogen fraction with increasing STBR was discussed in detail in the previous sections, shown in the Figure 3.8. The second method, increasing the residence time within the water gas shift reactor provides more time for the sorption reaction and the water gas shift reaction, increasing the fraction of hydrogen. This can be seen very easily from the study of dolomite, shown in Figure 3.13b. The third method is relatively more complicated, by increasing the fraction of dolomite sent to the water gas shift reactor, the amount of char required to maintain the gasification temperature at 860°C increases as the temperature of water gas shift reactor is much lower (450°C) than the gasifier.

As a first stage study, the second method was primarily simulated and the final composition of the product syngas was studied. The residence time was varied from 5 to 40 seconds and the change in product gas composition is plotted in Figure F.1. It can be observed that the initial sharp increase of hydrogen fraction slowly plateaus with increasing residence time. This can be explained by the decreasing fraction of CO. Decreasing CO fraction coupled with a very large concentration of H_2 slows down the water gas shift reaction resulting a very slow increase in higher residence times. Methane fraction remains constant as the temperature of water gas shift reactor is much too less for the cracking reactions to occur.

Hydrogen fraction reaches 80% (volume basis) at a residence time of 40 seconds. The produced product gas is essentially free of CO_2 (<1%) and minimal CO fraction (3%). This product gas is hence hydrogen enriched and this process of using dolomite could be very attractive for applications that demand such high composition of hydrogen. A secondary high temperature reactor after the gasifier to crack methane and tars could enhance the hydrogen fraction of the product gas even further, closer to even 90 - 95%.

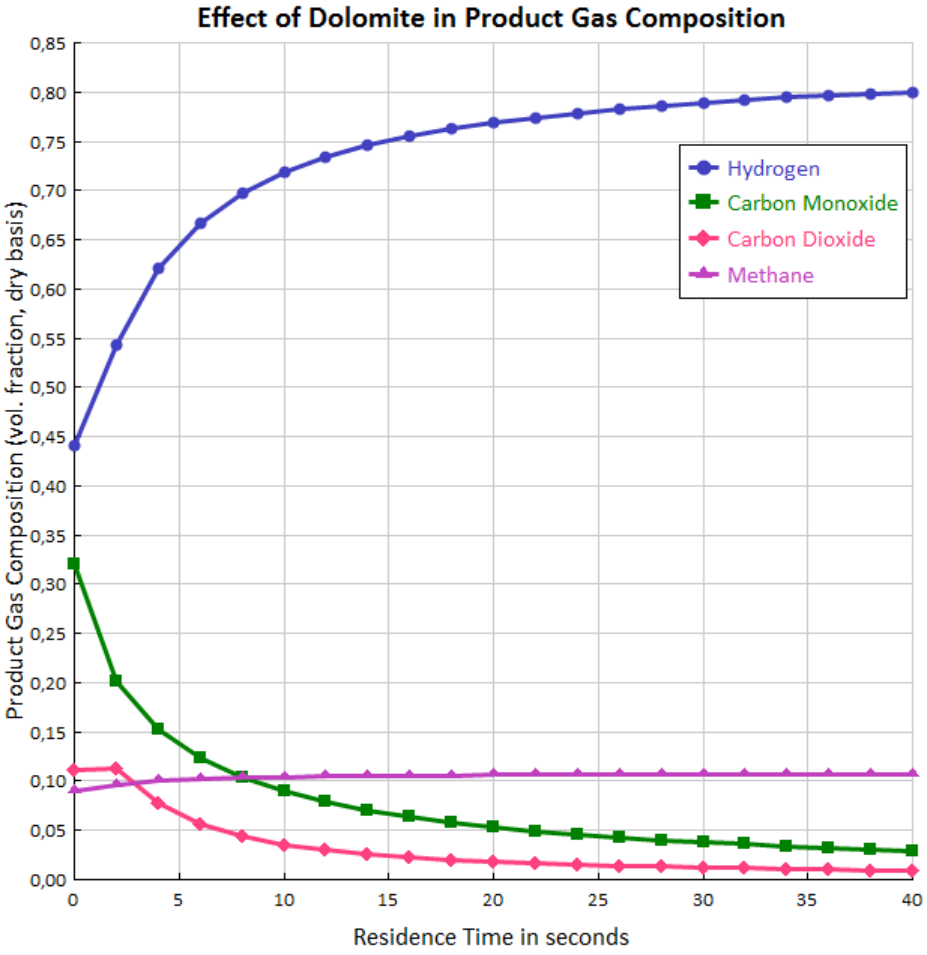

Figure F.1: Simulation results of using dolomite for hydrogen enrichment in product gas from gasification